Key Enabling Mechanisms for Mission-Critical Internet of Things

by **Muhammad Ahmad Raza**

Thesis submitted in fulfilment of the requirements for the degree of
Doctor of Philosophy

Principal Supervisor: Prof. Mehran Abolhasan
Co-supervisors: A/Prof. Justin Lipman and Dr. Negin Shariati

School of Electrical and Data Engineering
Faculty of Engineering and IT
University of Technology Sydney
September 20, 2023

Certificate of Authorship / Originality

I, Muhammad Ahmad Raza, declare that this thesis is submitted in fulfilment of the requirements for the award of Doctor of Philosophy, in the School of Electrical and Data Engineering at the University of Technology Sydney.

This thesis is wholly my own work unless otherwise referenced or acknowledged. In addition, I certify that all information sources and literature used are indicated in the thesis. This document has not been submitted for qualifications at any other academic institution.

This research is supported by the Australian Government Research Training Program.

Signature: Production Note: Signature removed prior to publication.

Date: September 20, 2023

Abstract

Internet-of-Things (IoT) networks are composed of devices generating varying amounts of data with diverse quality of service (QoS) requirements. Mission-critical IoT networks aim to support applications requiring ultra-reliability and low-latency communication interfaces. Fulfilling the application-specific QoS requirements becomes challenging when network parameters change dynamically in IoT networks having limited radio resources. The efficient use of available time and frequency resources in these networks relies on choosing a network access mechanism, which controls channel access when devices communicate over shared channels. The centralized network access schemes cause additional latency due to the involvement of feedback and control signaling overheads. Therefore, device-level learning-based distributed network access mechanisms are essential for designing wireless networks supporting mission-critical IoT applications. To design such distributed network access schemes, statistical learning and multi-agent multi-armed bandit (MAB) learning are promising tools that address decision-making problems in dynamic environments.

This thesis aims to design distributed network access schemes for IoT networks in which massive devices generate delay-sensitive and delay-tolerant data and communicate over shared radio resources. Firstly, we enable the end devices in multi-channel slotted ALOHA-based networks to predict the retransmission limit according to a given latency-reliability criterion. Secondly, we propose a statistical learning-based grant-free network access mechanism for delay-sensitive IoT applications. The proposed mechanism employs a static resource allocation strategy, enabling end devices to use their transmission history to predict different network parameters. Thirdly, to improve the utilization of available radio resources, we design an adaptive network access mechanism operating in a semi-distributed manner.

Under this mechanism, we propose a novel grant-free access scheme using a statistical learning approach that enables IoT entities to perform delay-sensitive and delay-tolerant transmissions over dynamically partitioned resources in a prioritized manner.

Finally, we propose a multi-agent MAB learning-based grant-free access mechanism for ultra-dense IoT networks, where multiple base stations serve a large number of delay-sensitive and delay-tolerant devices. The proposed mechanism enables the devices to improve their base-station (BS) selection over time to maximize the number of devices connecting to each BS when they meet a prescribed latency-reliability criterion.

This thesis demonstrates that the distributed network access approach can efficiently manage delay-sensitive and delay-tolerant transmissions over shared radio resources in a dynamic environment. Moreover, this thesis opens new research directions in designing device-level learning-assisted wireless networks to support heterogeneous IoT applications.

Dedication

For my parents!

Acknowledgements

Firstly, I'm very thankful to my supervisor, Prof. Mehran Abolhasan, for supporting my application to pursue a Ph.D. at the University of Technology Sydney (UTS), Australia. I'm also very thankful to UTS for offering me the UTS International Research Scholarship and UTS President's research scholarship to support my Ph.D. at UTS.

I'm very grateful to Prof. Mehran for his supervision, guidance, help, and support throughout my Ph.D. Moreover, I'm also very thankful to my co-supervisors, A/Prof. Justin Lipman and Dr. Negin Shariati for their help and support. I'm very grateful to Dr. Wei Ni, from the Commonwealth Scientific and Industrial Research Organization, Australia, for his guidance throughout my Ph.D. I'm also very thankful to Prof. Abbas Jamalipour, from the University of Sydney, Australia, for his guidance and constructive feedback on my research work. Indeed, the help they provided played an essential role in completing this thesis.

I thank the examination panels for giving constructive comments on my candidature stage assessments. I also appreciate the help and support provided by the research and administrative staff of the School of Electrical and Data Engineering at UTS.

Finally, I thank my family in Pakistan for their encouragement and support in pursuing my Ph.D. abroad.

Muhammad Ahmad Raza

September 20, 2023

Sydney, Australia

Contents

List of Figures

List of Tables

List of Algorithms

Table of Notations

Notations used in Chapter-4	
Notation	**Definition**
$A_{m,n}$	Outcome of a transmission
$\alpha_{m,n}$	Probability of collision in a frame
$\widehat{\alpha}_n$	Prediction of $\alpha_{m,n}, \forall m$
$\epsilon_r^{(i)}$	Reliability constraint of i^{th}-group
$\mathbb{G}$	Number of groups
$\mathbf{H}$	Transmissions history matrix for network exploration
K	Number of orthogonal channels in each frame
$K_{m,n}$	Number of idle channels in n^{th} frame of m^{th} round
$L_{max}^{(i)}$	Group specific maximum affordable latency
L	Random component of the latency
$M^{(i)}$	Number of active IoT devices in i^{th}-group
M	Total number of active IoT devices
$M_{m,n}$	Number of active devices in a frame
$\widehat{M_n}$	Prediction of $M_{m,n}, \forall m$
$\text{MSE}_{S_{av}}$	MSE in prediction of S_{av}
MSE_P	MSE in prediction of P_s
MSE_μ	MSE in prediction of μ_L
N	Number of frames in one round
$\Pr(.)$	Probability measure
P_{s_m}	Probability of success in m^{th} round
P_s	Average probability of success per round
$\widehat{P}_s$	Prediction of P_s
$R^{(i)}$	Reliability constrained number of rounds for i^{th}-group

$R_{max}^{(i)}$	Rounds according to affordable latency for i^{th}-group
$\widehat{R}$	Optimal number of rounds for network exploration
R	Number of rounds
S_{av}	Average number of successful devices in one round
$\widehat{S}_{av}$	Prediction of S_{av}
μ_L	Average (re)transmissions for a successful transmission
$\widehat{\mu}_L$	Prediction of μ_L
ζ_S	MSE constraint to predict S_{av}
ζ_P	MSE constraint to predict P_{s_m} $\forall m$
ζ_μ	MSE constraint to predict μ_L

Table 1: List of notations used in chapter-4

Notations used in Chapter-5	
Notation	**Definition**
$\mathcal{C}_{m,n}^{(ds)}$	Subset of $\mathcal{C}$ for delay-sensitive transmissions
$\widehat{\mathcal{C}}_{m,n}^{(ds)}$	Device-level prediction of $\mathcal{C}_{m,n}^{(ds)}$ $\forall m$
$\mathcal{C}_{m,n}^{(dt)}$	Subset of $\mathcal{C}$ for delay-tolerant transmissions
$\widehat{\mathcal{C}}_{m,n}^{(dt)}$	Device-level prediction of $\mathcal{C}_{m,n}^{(dt)}$ $\forall m$
$K_{m,n}$	Number of channels available for delay-sensitive transmissions
$\widehat{K}_n$	Device-level prediction of $K_{m,n}$ $\forall m$
$\mathcal{L}_{\max}$	Application specific latency bound
M	Number of active devices
$\widehat{M}$	Device-level prediction of active devices
N	Number of slots per round
$\mathcal{S}_{\text{ds}}^{(\text{DRA})}$	Average successful delay-sensitive transmissions per round
$\mathcal{S}_{\text{dt}}^{(\text{DRA})}$	Average successful delay-tolreant transmissions per round
$V_{m,n}$	Number of devices transmitting delay-sensitive data
$W_{m,n}$	Number of devices transmitting delay-tolerant data
$\alpha_{m,n}$	Probability of collision for delay-sensitive transmission in the SRA scheme
$\beta_{m,n}$	Probability of collision for delay-sensitive transmission in the DRA scheme
$\gamma_{m,n}$	Probability of collision for delay-tolerant transmission in the DRA scheme
$\eta^{(\text{SRA})}$	Channel utilization in the SRA scheme
$\widehat{\eta}^{(\text{SRA})}$	Device-level prediction of $\eta^{(\text{SRA})}$
$\eta^{(\text{DRA})}$	Channel utilization in the DRA scheme
$\widehat{\eta}^{(\text{DRA})}$	Device-level prediction of $\eta^{(\text{DRA})}$
$\mu_{\text{ds}}^{(\text{SRA})}$	Average latency in the SRA scheme
$\widehat{\mu}_{\text{ds}}^{(\text{SRA})}$	Device-level prediction of $\mu_{\text{ds}}^{(\text{SRA})}$
$\mu_{\text{ds}}^{(\text{DRA})}$	Average latency in the DRA scheme
$\widehat{\mu}_{\text{ds}}^{(\text{DRA})}$	Device-level prediction of $\mu_{\text{ds}}^{(\text{DRA})}$

Table 2: List of notations used in chapter-5

Notations used in Chapter-6	
Notation	**Definition**
$A_{i,m,1}$	Outcome of a transmission from an intended device during the DDE phase
$A_{i,t,m,1}$	Outcome of a transmission from an intended device during the MAB learning-based data transmission phase
$\mathcal{B}$	Base stations' index set
B	Number of base stations
D	Excessive network load
$\mathcal{L}_{\max}$	Maximum number of (re)transmissions allowed
M_{ds}	Number of delay-sensitive devices
M_{dt}	Number of delay-tolerant devices
M^*	Number of devices in MAB-GFA-based data transmission phase
$M_{i,t}$	Number of devices connected with BS-i in epoch-t
K_i	Number of orthogonal channels allocated to BS-i
$\mathcal{P}_{\text{out}}$	Outage probability
$T_{\max}$	Number of epochs per window
T_{con}	Number of epochs to reach the stable state
$T_{\text{con}}^{(\text{CMAC})}$	Number of epochs to reach stable state under CMAC
$X_{i,0}^{(d)}$	Binary decision of the d^{th} device from BS-i in epoch-t
ϕ_i	Probability that a device selects BS-i
$Y_{i,t}^{(d)}$	Binary reward of the d^{th} device from BS-i in epoch-t
α_n	Average collision probability in the n^{th} slot of a round
β_0^*	Device's elimination probability
$\beta_{i,t-1}$	Exploration probability in epoch-t
Δ_t	Number of devices performing exploration in epoch-t
δ_t	Desired probability threshold for the distributed device elimination phase
η_t	Normalized average load meeting the prescribed latency-reliability criterion
ϵ_r	Reliability constraint

ζ_i	Number of devices supported by BS-i
$\zeta_{\max}$	Maximum network load support
$\mu_{T_{\text{con}}}$	Expected number of epochs required to reach the stable state
$\mu_{T_{\text{con}}}^{(\text{CMAC})}$	Expected number of epochs to reach the stable state under CMAC

Table 3: List of notations used in chapter-6

Chapter 1

Introduction

1.1 Background

Internet of Things (IoT) networks are composed of a large number of connected devices which generate and exchange data in varying amounts. The latency experienced by data packets in IoT networks comprises deterministic and random components, while reliability is defined as the probability of meeting a latency bound [1,2]. The quality of service (QoS) requirements, in terms of desired latency and reliability, varies from application to application. Figure 1.1 shows a typical heterogeneous IoT network where different applications require communication interfaces with diverse QoS requirements. Industrial IoT (IIoT), a subset of IoT, aims to support Industry 4.0 applications [3]. Machine-type communication devices in IIoT networks generate delay-sensitive and delay-tolerant data in periodic and aperiodic manners. Mission-critical IoT (MC-IoT) networks aim to provide ultra-reliable and low latency communications (URLLC) interfaces for transmitting delay-sensitive data and form one of the three primary services in 5G and beyond wireless networks. Public safety, remote sensing, automotive, industrial automation, telesurgery, intelligent transportation, and smart grids are emerging MC-IoT applications. The performance specifications of different mission-critical applications are described in [4].

The design of IoT networks follows a layered approach in which each layer performs a set of specific operations and provides services to the immediate layer. The devices in these networks generate short packets in which the size of control information is

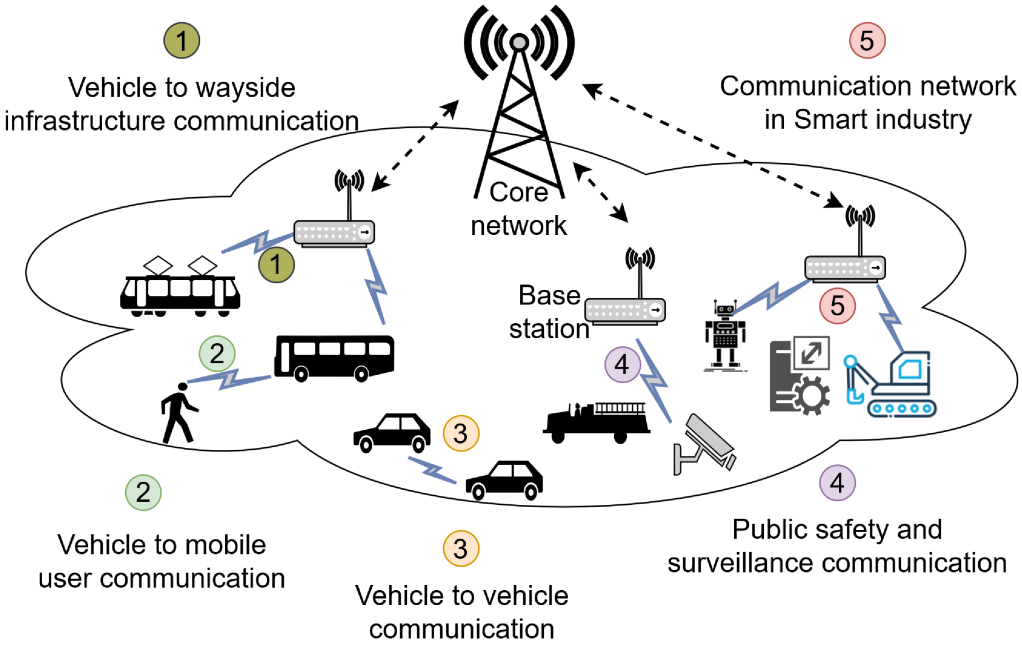

Figure 1.1: Heterogeneous network composed of multiple mission critical IoT groups.

comparable with the size of actual information. Therefore, the overhead caused by the control information becomes significant as it introduces additional latency. Consequently, the classical information theoretic principles for designing the physical (PHY) layer are no longer helpful. This fact motivates the research community to redesign the transmission strategies for MC-IoT networks which can support short packet transmission [5,6]. Simultaneously short packet transmission can cause physical layer security concerns, while the cryptography schemes used at higher layers cause additional latency due to their higher computational complexities. Therefore, instead of using the cryptography schemes, physical layer authentication mechanisms are proposed for MC-IoT [7-9]. MC-IoT applications can encounter situations where the channel changes very frequently. For example, due to mobility, rapid changes in the wireless channel are observed in vehicular networks. On the other hand, smart power grid systems operate under a relatively static environment. Thus, in order to meet the application-specific latency reliability requirements, MC-IoT networks must be capable of adapting to network changes.

The frequency and time resources available in IoT networks for uplink data transmission are small compared to a large number of installed devices. Moreover, the number of active devices at a given time is random. Therefore, fulfilling the QoS requirements becomes challenging when devices communicate over shared radio resources

and network parameters change dynamically. Consequently, efficient network access protocols are crucial in the design of IoT networks supporting mission-critical applications. In this regard, the centralized grant-based network access schemes dedicate resources for data transmission to those devices that remain successful in a random access channel (RACH) phase. Consequently, this approach results in significant latency due to their inherent feedback and control signaling overheads.

On the other hand, the grant-free network access mechanism allows devices to transmit their data over shared radio resources without going through any RACH phase. This approach can avoid excessive control signaling resulting in latency reduction. However, when multiple devices perform transmission over the same channels, the reliability and the system's overall performance are impacted. Thus grant-free access methods with efficient retransmission strategies are required to enhance performance by improving latency and reliability in MC-IoT networks [10-20]. Moreover, grant-free non-orthogonal multiple access methods can further reduce latency and improve system's performance [21]. Furthermore, network slicing, software-defined networks, and network function virtualization [22-31] are promising techniques to prioritize the transmission of mission-critical traffic in the heterogeneous networks.

The 5G and future wireless networks will take advantage of the distributed computing, storage, and control services offered by edge-computing systems in the design of different delay sensitive applications. These features of edge computing can lead to provisioning a platform that is suitable for MC-IoT applications [1]. In this regard, potential enablers for edge computing-based mission-critical applications are discussed in [1]. Due to the distributed nature of edge-computing systems, it becomes possible to process data near the source. Thus edge computing can be used to develop distributed decision-making mechanisms that will enable the end devices and edge nodes to adapt to the network dynamics. Edge-machine learning and federated learning are among the potential enablers for edge computing-based MC-IoT applications over wireless networks. Some recent works have proposed Federated learning-based PHY layer enhancements for MC-IoT networks while focusing on the energy and power optimization [32-36]. Therefore, distributed network access approach and device-level network exploration can play a significant role in designing MC-IoT networks.

1.2 Motivation

Through literature review, it is identified that supporting MC-IoT applications in dynamic heterogeneous networks with a large number of devices is very challenging. It is found that present works are primarily base-station (BS) centered that employ centralized decision-making schemes, which causes additional latency and inefficient use of resources due to periodic transmission of the control signaling. However, minimizing the control signaling overheads is required due to the strict latency and reliability constraints of MC-IoT applications. To this end, device-level learning of network parameters can play a significant role in designing MC-IoT applications by reducing the control signaling and computation burden at the BS. The knowledge available at the end devices can help the BS allocate radio resources for delay-sensitive and delay-tolerant transmissions much more efficiently [37]. However, the on-device limited energy, computation, and storage resources need to be considered while enabling the end devices to explore and adapt to the network dynamics.

Considering the uplink dominant IoT networks, it is identified that efficient adaptive network access mechanisms have to be designed to meet strict QoS requirements when the available time and frequency resources are limited and the number of transmitting devices changes dynamically. Moreover, adaptive network access approaches are required to adapt to the network dynamics when the probability distributions associated with different network parameters are unknown, enabling the end devices to learn these parameters. Motivated by these facts, this research focuses on designing adaptive network access mechanisms to support MC-IoT applications.

1.3 Problem Statement

Mission-critical IoT networks generate delay-sensitive data with diverse latency and reliability requirements which makes meeting QoS requirements over dynamic environments a challenging problem. Moreover, these systems cannot afford the control signaling overheads caused by the existing centralized network access methods. Therefore, we aim to design distributed network access mechanisms enabling end devices to adapt to the network dynamics and meet the application-specific latency-reliability criterion.

1.4 Aims, Objectives and Research Questions

In this thesis, we consider the MAC layer of uplink-dominant communication in IoT networks, where a large number of devices communicate over shared radio resources. Both single and multiple base-station (BS) scenarios are considered, where each BS is equipped with a set of non-overlapping and orthogonal channels. Time is divided into slots, and active devices perform uplink data transmission to the selected BS in a grant-free manner in each slot. We consider PHY-layer abstraction to the MAC layer and focus on the random component of latency caused by the number of retransmissions performed by an intended device for successful transmission. Reliability is defined as the probability that the number of retransmissions does not exceed a given application-specific latency bound.

Under the context mentioned above, this study aims to explore the key enabling mechanisms that can support MC-IoT applications in a dynamic environment. In this regard, this thesis aims to achieve the following objectives:

- To enable IoT devices to explore the network using their transmission history.
- To design device-level learning-based distributed network access mechanisms for MC-IoT networks operating under variable network load.
- To compare the performance of proposed distributed network access strategies and the existing centralized network access mechanisms.

The following are the research questions this thesis addresses to achieve the objectives mentioned earlier:

1. How can end devices predict different network parameters, including the retransmission limit, current network load, probability of successful transmission, and latency offered by the network?

   Considering the multi-channel slotted ALOHA systems, a part of the first research question is addressed in Chapter 3. The proposed mechanism employs a statistical learning approach, enabling the end devices to predict the retransmission limit under a given latency-reliability criterion.

2. How can end devices help the BS in identifying different IoT groups in a

heterogeneous network?

The second research question and the remaining part of the first research question are addressed in Chapter 4, where a statistical learning-based grant-free access scheme is proposed for delay-sensitive IoT applications. The proposed mechanism enables the end devices to predict the current network load, the probability of successful transmission under the proposed scheme, and the average latency offered by the network. Moreover, it is also demonstrated that the BS can identify different groups in the network by allowing the end devices to share their knowledge with the BS.

3. How can end devices utilize the available time and frequency resources for delay-sensitive and delay-tolerant transmissions while avoiding additional control signaling overheads from the BS?

   The third research question is addressed in Chapter 5 while considering the industrial IoT, where devices generate delay-sensitive and delay-tolerant data. In this chapter, a statistical learning-based adaptive network access mechanism is proposed that avoids the excessive control signaling from the BS. It enables the end devices to partition the channels into two disjoint sets so that delay-sensitive and delay-tolerant transmissions are performed on different channels in a dynamic environment.

4. How can end devices improve their BS selection over time to meet the desired latency-reliability criteria in ultra-dense IoT networks where multiple base stations serve a large number of devices?

   The last research question is addressed in Chapter 6 while considering the dense IoT networks where multiple BSs are deployed to serve a large number of devices, generating delay-sensitive and delay-tolerant data. In order to maximize the number of devices meeting the desired latency-reliability criterion, this chapter proposes a multi-agent MAB learning-based grant-free scheme, enabling the end devices to improve their BS selection over time.

1.5 Methodology

We aim to solve the research questions mentioned earlier by using a distributed decision-making approach in which end devices can adapt to the network dynamics and update the transmission strategies accordingly. In this regard, statistical learning and multi-agent multi-armed bandit (MAB) learning are promising tools. Statistical learning is the theoretical foundation of machine learning algorithms. Recently, a statistical learning framework has been proposed in [38] for the physical layer design of URLLC systems. This framework considers the situations when a transmitter has limited knowledge of the channel's distribution, and there can be a mismatch between the model being used by the transmitter and the actual channel model. The proposed statistical learning-based mechanism enables the transmitter to update the transmission rate such that the desired reliability constraint is met probabilistically. This mechanism proposes to use the average reliability (AR) criterion for the URLLC systems where the transmission rate needs to be updated frequently due to the dynamically varying behavior of the channel. At the same time, the probably correct reliability (PCR) criterion is proposed for the URLLC systems operating under relatively static environments. Thus, the device-level knowledge acquired using the proposed statistical learning-based mechanisms enables the end devices to update their transmission rate under different conditions.

On the other hand, MAB learning, a distributed machine learning technique, is considered a promising tool for designing distributed network access and resource scheduling mechanisms for 5G and future wireless networks [39-41]. The MAB learning operates in an online manner and enables end devices to learn different network parameters and update their transmission strategies without requiring additional feedback and control signaling from the BS. These features of MAB learning can potentially address the research problems related to designing adaptive network access mechanisms for MC-IoT networks.

This thesis aims to enable the end devices to explore the network by applying statistical learning techniques to their local observations. The device-level observations can be the outcomes of transmission attempts (success or failure), outage events observed in a given time slot and any other relevant measures. Depending upon the

transmission strategy and nature of the network under consideration. The observations available at the devices can be independent and identically distributed (IID) and non-IID. The end devices predict different time-varying network parameters by applying appropriate statistical learning mechanisms. The number of observations determines the accuracy of the prediction. The end devices are assumed to have reasonable computational resources and the power required to learn the different network parameters. The mean square error (MSE) criterion is used to evaluate the accuracy of the learned parameters. Moreover, a multi-agent MAB learning framework is used to address research question-4 of this thesis, which incorporates the multiple BSs scenario. In this regard, each BS acts as an arm while active devices behave as agents. The devices are enabled to improve their BS selection over time by performing an adaptive exploration and exploitation strategy.

The key aspect of the selected methodology is that the end devices learn different network dynamics based on the locally available data. Since the observation sets at the device level are updated regularly, the network dynamics are captured accordingly. By enabling the end devices to share the learned parameters with the BS, the devices can assist the BS in optimizing the resource allocation strategy to meet the desired latency-reliability criterion. It is worth noting that instead of offloading a large amount of data to the BS, the end devices only share the learned parameters, reducing transmission overheads caused by transmission power consumption and time and frequency resource usage. This methodology can be more useful when the BS cannot retrieve complete information about the network dynamics from the received messages.

1.6 Summary of Contributions

For the selected research direction, a comprehensive literature review is performed. The literature review forms Chapter-2 of the thesis. The literature review helps identify research gaps in the selected topic, formulating different research questions accordingly. The key contributions of this thesis are summarised as follows:

- Firstly, we present a statistical learning-based retransmission mechanism for the multi-channel slotted ALOHA-based systems. The proposed mechanism enables the end devices to use their transmission history to predict the maximum number of retransmissions that can meet the application-specific latency-reliability criterion. This contribution forms Chapter-3 of the thesis and results in publication-2 as mentioned in section 1.7.

- Secondly, we propose a statistical learning-based grant-free network access mechanism for delay-sensitive IoT applications. The proposed mechanism employs a static resource allocation strategy and enables the end devices to predict different network parameters by using their transmission history. Consequently, the BS can identify different IoT groups in the network by using the knowledge shared by end devices. Through simulations, we show that the MSE in predicting different network parameters reduces as the size of the transmission history increases. Therefore, the optimal size of the history window under the given accuracy constraints is also determined. Moreover, it is demonstrated that the proposed device-level network load prediction mechanism is more robust compared to the existing BS-level approach. This contribution forms Chapter-4 of the thesis and results in publication-3 as mentioned in section 1.7.

- Thirdly, we propose a novel statistical learning-based grant-free access scheme for IIoT networks where devices generate delay-sensitive and delay-tolerant data. The proposed mechanism prioritizes the delay-sensitive transmissions and enables the devices to perform delay-sensitive and delay-tolerant transmissions over dynamically partitioned resources. Different parameters of this scheme are predicted through a network exploration phase in which devices transmit delay-sensitive data only using the grant-free access scheme with

static resource allocation. Since the number of active devices varies dynamically, we design an adaptive network access mechanism that enables the devices to choose between grant-free access with static and dynamic resource allocation strategies according to the current network load. This mechanism offers better channel utilization while meeting the application-specific latency bound in IIoT networks operating under a dynamic environment. This contribution forms Chapter-5 of the thesis and results in publication-4 as mentioned in section 1.7.

- Finally, we propose a multi-agent MAB learning-based grant-free access mechanism for dense IoT networks, where multiple base stations serve delay-sensitive and delay-tolerant devices. Delay-sensitive devices are prioritized to choose the base stations with more channels in a probabilistic manner. The proposed mechanism enables the devices to improve their BS selection over time to accommodate the maximum number of devices that can meet a prescribed latency-reliability criterion. Through simulation, we show that the proposed MAB learning-based network access mechanism outperforms the random base station selection strategy in which end devices do not employ any learning scheme to adapt to the network dynamics. This contribution forms Chapter-6 of the thesis and corresponding research paper has been submitted to an IEEE journal as mentioned in section 1.7.

1.7 List of Publications and Thesis Structure

Literature review is presented in Chapter-2. A part of the literature review is published in the following group survey paper (ref. [101]):

1. I. Zhou, I. Makhdoom, N. Shariati, **M. A. Raza**, R. Keshavarz, J. Lipman, M. Abolhasan, and A. Jamalipour, *"Internet of Things 2.0: Concepts, Applications, and Future Directions,"* IEEE Access, vol. 9, pp. 70961-71012, 2021.

Chapter-3 of this thesis is based on the following conference publication (ref. [104]). Improved results are also added in this chapter

2. **M. A. Raza**, M. Abolhasan, J. Lipman, N. Shariati, and W. Ni, *"Statistical Learning-Based Dynamic Retransmission Mechanism for Mission Critical Communication: An Edge-Computing Approach,"* in 2020 IEEE 45th Conference on Local Computer Networks (LCN), 2020, pp. 393-396.

Chapter-4 of this thesis is based on the following journal publication (ref. [111]):

3. **M. A. Raza**, M. Abolhasan, J. Lipman, N. Shariati, W. Ni, and A. Jamalipour, *"Statistical Learning-Based Grant-Free Access for Delay-Sensitive Internet of Things Applications,"* in IEEE Transactions on Vehicular Technology, vol. 71, no. 5, pp. 5492–5506, 2022.

Chapter-5 of this thesis is based on the following journal publication:

4. **M. A. Raza**, M. Abolhasan, J. Lipman, N. Shariati, W. Ni and A. Jamalipour, *"Statistical Learning-based Adaptive Network Access for the Industrial Internet of Things,"* in IEEE Internet of Things Journal, vol. 10, no. 14, pp. 12219-12233, 2023.

Chapter-6 of this thesis is based on the following paper submitted to IEEE Transactions on Cognitive Communications and Networking:

5. **M. A. Raza**, M. Abolhasan, J. Lipman, N. Shariati, W. Ni, and A. Jamalipour, *"Multi-Agent Multi-Armed Bandits Learning-based Grant-Free Access for Ultra-Dense IoT Networks,"* submitted to IEEE Transactions on Cognitive Communications and Networking, 2023.

Section II of publications 2-5 contains the related literature review; therefore, it has been added to Chapter-2 of this thesis. Finally, we conclude this thesis in Chapter-7 while highlighting the significance of this research work and some interesting future research directions.

1.7.1 Thesis by Compilation Declaration

This thesis follows the thesis by compilation format. The required declaration form signed by the graduate student and all co-authors is provided on the following page.

Thesis by Compilation Declaration

Paper Title	List of Authors	Current Status	Student's Contribution	Related Chapter
Statistical Learning-Based Dynamic Retransmission Mechanism for Mission Critical Communication: An Edge-Computing Approach	Muhammad Ahmad Raza Mehran Abolhasan Justin Lipman Negin Shariati Wei Ni	Published in the 45th IEEE Conference on Local Computer Networks, 2020.	Student's contribution is about 90%, comprising analytical work, simulations, and paper drafting. The co-authors provided feedback and comments, which helped improve the paper.	Chapter-3
Statistical Learning-Based Grant-Free Access for Delay-Sensitive Internet of Things Applications	Muhammad Ahmad Raza Mehran Abolhasan Justin Lipman Negin Shariati Wei Ni Abbas Jamalipour	Published in the IEEE Transactions on Vehicular Technology, 2022.	Student's contribution is about 90%, comprising analytical work, simulations, and paper drafting. The co-authors provided feedback and comments, which helped improve the paper.	*Section-II of this paper is added in Chapter-2; rest of the paper is added in Chapter-4
Statistical Learning-based Adaptive Network Access for the Industrial Internet of Things	Muhammad Ahmad Raza Mehran Abolhasan Justin Lipman Negin Shariati Wei Ni Abbas Jamalipour	Published in the IEEE Internet of Things Journal, 2023.	Student's contribution is about 90%, comprising analytical work, simulations, and paper drafting. The co-authors provided feedback and comments, which helped improve the paper.	*Section-II of this paper is added in Chapter-2; rest of the paper is added in Chapter-5
Multi-Agent Multi-Armed Bandit Learning for Grant-Free Access in Ultra-Dense IoT Networks	Muhammad Ahmad Raza Mehran Abolhasan Justin Lipman Negin Shariati Wei Ni Abbas Jamalipour	Submitted to the IEEE Transactions on Cognitive Communications and Networking, 2023.	Student's contribution is about 90%, comprising analytical work, simulations, and paper drafting. The co-authors provided feedback and comments, which helped improve the paper.	*Section-II of this paper is added in Chapter-2; rest of the paper is added in Chapter-6
Internet of Things 2.0: Concepts, Applications, and Future Directions	Ian Zhou Imran Makhdoom Negin Shariati Muhammad Ahmad Raza Rasool Keshavarz Justin Lipman Mehran Abolhasan Abbas Jamalipour	Published in the IEEE Access, 2021.	Student's contribution is about 10%, comprising Section-V of this paper.	Section-V of this paper is added partially in Chapter-2

*Section-II of this paper contains the related literature review.

		Signature	Date
Student	Muhammad Ahmad Raza	Production Note: Signature removed prior to publication.	06-Jun-2023
Co-authors	Mehran Abolhasan	Production Note: Signature removed prior to publication.	06/06/2023
	Justin Lipman	Production Note: Signature removed prior to publication.	06/06/2023
	Negin Shariati	Production Note: Signature removed prior to publication.	06/06/2023
	Wei Ni	Production Note: Signature removed prior to publication.	07.06.2023
	Abbas Jamalipour	Production Note: Signature removed prior to publication.	7/06/2023
	Ian Zhou	Production Note: Signature removed prior to publication.	07/06/2023
	Imran Makhdoom	Production Note: Signature removed prior to publication.	7/6/2023
	Rasool Keshavarz	Production Note: Signature removed prior to publication.	08/06/2023

Chapter 2

Literature Review

Section 2.1 and subsection 2.2.1 of this chapter are published in the following paper: I. Zhou, I. Makhdoom, N. Shariati, **M. A. Raza**, R. Keshavarz, J. Lipman, M. Abolhasan, and A. Jamalipour, *"Internet of Things 2.0: Concepts, Applications, and Future Directions,"* IEEE Access, vol. 9, pp. 70961-71012, 2021.
Moreover, the literature review related to each contribution chapter of this thesis is added under the appropriate sections of this chapter.

2.1 Introduction

Mission-critical communication-based Internet of Things (MC-IoT) networks put stringent requirements on ultra reliable and low latency communication (URLLC) interfaces, and higher system availability [42]. Communication in MC-IoT networks currently takes the form of machine-to-machine (M2M) communication, a.k.a machine-type communication (MTC), where machines need to communicate with each other to perform various delay-sensitive tasks. Remote sensing, automotive, industrial automation, robot control, and telesurgery are among the emerging applications of MC-IoT networks. Moreover, mission-critical communication services are also required in the systems that address situations where human life and any form of infrastructure can be at risk. The M2M communication systems that do not involve the mission-critical element and have massive connectivity are referred to as massive MTC (mMTC) IoT networks [21].

2.1.1 Important Applications of MC-IoT Networks

In order to protect citizens and infrastructure during disasters and emergencies, different public safety organizations are put in place [43, 44]. The emergency first responder is the most crucial entity in all emergency management agencies. Public safety communication (PSC) systems used by these agencies for coordinating teams and providing quick emergency response need to provide ultra-reliable and secure communication links with a minimum latency such that the desired network requirements are met [45]. In this regard, the aerial platforms that provide airborne communication infrastructure are among the potential technologies to design reliable PSC systems [46]. Public warning systems (PWS) also come under the umbrella of PSC systems as they share many of the characteristics of mission-critical communications. A critical use case of PWS is the earthquake and tsunami warning system. The interest in advancing PSC systems has increased significantly in the last few years. Baldini et al. [43], presented a detailed survey on wireless communication technology while covering the different aspects of regulatory, standardization, and research activities in PSC systems. The main focus of this work is on Europe and the USA. In [44], a comparative analysis of legacy and emerging technologies for PSC is presented. Doumi et al. [45], discussed the use of broadband technologies for public safety, considering existing LTE specifications. Gomez et al. [47], proposed a software architecture design and a set of distributed protocols to meet the strict requirements of PSC networks. The use of wireless networks in the mining industry for mobility support, rapid deployment, and scalability within dynamic environments is another use case of the PSC system. Garcia et al. [48] discussed the mission-critical requirements of PSC systems for open-pit mining, and a framework is proposed that integrates mine and radio network planning.

Automated transportation systems are meant to provide mission-critical services to self-driving vehicles, connected cars, road safety, and traffic management systems. These intelligent transportation systems can increase the efficiency of traffic management agencies and provide numerous benefits, including a considerable reduction in the road accident rate. However, to make these systems realizable, the stringent requirements of MC-IoT networks should be fulfilled. Vehicular connectivity, termed V2X, is another use case of MC-IoT networks in which time-critical

data exchange takes place under three different scenarios: vehicle-to-vehicle (V2V), vehicle-to-infrastructure (V2I), and vehicle-to-personal device moving at pedestrian speeds (V2P) [49]. Unmanned aerial vehicles (UAVs), or drones, have potential usages in many MC-IoT networks due to their inherent mobility features, flexibility, and adaptive altitude [50]. Such UAVs-assisted MC-IoT networks can be used to transport essential goods in emergency situations handled by the public safety and rescue systems. UAVs can be part of cellular networks as new type's network end nodes and as flying base stations. UAVs as flying base stations can help increase the coverage, spectral efficiency, and QoS in MC-IoT networks supported by cellular networks. Fotouhi et al. [51], present a comprehensive survey of different types of promising solutions for the smooth integration of UAVs into cellular networks.

Industrial automation involving time-critical processes requires highly reliable data transfer links between sensors, actuators, and controllers and thus is an essential application of MC-IoT networks. Detailed performance requirements of different MC-IoT network applications are listed in [4]. In a typical factory automation scenario, communication is primarily done between the local controller and sensor/actuator, while repeaters can enhance reliability by providing spatial diversity. Remote patient health monitoring systems and the use of remote robots for surgeries are potential applications of MC-IoT networks. Similarly, both augmented reality (AR) and virtual reality (VR) systems require very low end-to-end latency. Another critical use case of MC-IoT networks is found in the smart grid, an advanced form of conventional power grid capable of remote monitoring and power line communication [52].

2.2 Key Enabling Mechanisms for Designing MC-IoT Networks

Several techniques have been proposed to design URLLC-based systems incorporating the physical (PHY), medium access control (MAC), and network layers [1, 2, 53-55]. Short packet transmission, PHY layer authentication, and channel quality-based selection of modulation and coding schemes are prominent strategies addressing the design of URLLC-based systems. On the other hand, grant-free access for uplink-

dominant IoT applications has gained considerable attention as a potential network access mechanism for delay-sensitive IoT applications with a massive number of devices. The resource utilization in the grant-free access approach is further enhanced by using non-orthogonal multiple access (NOMA) methods [21]. Moreover, diversity-based techniques such as automatic repeat request (ARQ) and retransmission schemes enhance reliability in contention-based access methods. In the context of network layer design, network slicing, implemented by software-defined networking (SDN) and network function virtualization (NFV) techniques, is a promising mechanism to address the problem of meeting the diverse QoS requirements in heterogeneous networks. Moreover, using edge and fog computing paradigms provides the benefits of distributed computing, which help reduce overall latency in the computational extensive IoT applications. Distributed computing further leads to the use federated learning paradigm in the design of delay-sensitive IoT applications.

In the following sections, we review recent works proposed for MC-IoT networks, which aim to enhance reliability while following the latency bound. Since this thesis focuses on designing the MAC layer for delay-sensitive IoT networks, the literature review is primarily MAC layer concentrated. We also present a critical analysis of the existing works highlighting different gaps in the literature.

2.2.1 PHY Layer Considerations for MC-IoT Networks

Table 2.1 summarizes works related to PHY layer considerations for mission critical communication networks. For both licensed and unlicensed bands employing URLLC, many promising PHY and MAC layer techniques are discussed in [55]. The following techniques are among the PHY layer mechanisms proposed specifically for MC-IoT networks to meet the associated URLLC requirements.

Short packet transmission

In contrast to conventional wireless communication systems, the traffic in MC-IoT networks generated by different types of devices and sensors contains short packets where the metadata size (control information) is comparable with that of the actual information payload. Thus, new information-theoretic principles are required to design wireless protocols supporting short packets. The authors of [5] reviewed

Table 2.1: Summary of Recent Works Addressing Mission Critical Communication.

Ref.	**Communication Scenario**	**Challenges Addressed**	**Reliability and Latency Improvement Mechanism**
[5]	Point to point, downlink multiuser, and uplink multiuser	Short packet transmission	Trade-off between coding rate and packet length, data concatenation for multiple users, trade-off between the probability of collision and packet error probability
[6]	D2D and cellular modes with single antenna users and multiple antenna base stations	Network availability for short packet transmission	Available range improvement by optimizing transmission duration
[7]	Point to point	Physical layer security	Clustering based upon channel estimates
[8]	Uplink transmission: single antenna users and multiple antennas base stations over a line of sight path	Physical layer security	Feature based physical layer authentication while considering the associated delays
[9]	Downlink transmission: single and multiple antenna base stations, single antenna actuator and multiple antenna eavesdropper	Physical layer security for short packet transmission	Blocklength optimization to maximize the secrecy throughput for different cases
[25]	Vehicle to everything communication	Slicing the RAN and core network for V2X communication	End-to-end network slicing for different scenarios of V2X communication use cases
[26]	Uplink multiuser	RAN resource management for heterogeneous services for 5G	Non-orthogonal slicing of the RAN resources
[28]	Mission critical communication between a server and a mobile user	End-to-end reliability for high data rate	Software-based framework prioritizing mission critical traffic

information-theoretic principles developed for communication systems generating short packets. These principles were applied in different communication scenarios such that the control information is optimized for short packet transmission. Li et al. [56] considered the transmission of short packets in the downlink of multiple-input and single-output (MISO) communication systems where a BS equipped with multiple antennas communicates with single-antenna users. This work addressed the problem of optimal power and symbol period allocation in the targeted communication scenario. Under a given finite block length, the authors presented an approximate closed-form expression that serves as a lower bound on the average data rate.

The probability that a network provides the required level of QoS is called network availability, and in the context of MC-IoT networks, QoS is the set of desired reliability and latency levels [6]. High SNR is required at the receiver to meet the stringent requirements of URLLC in MC-IoT networks, while the SNR of the received signal depends upon the range between the transmitter and the receiver. The authors of [6] proposed a framework to optimize the available range and transmission duration in MC-IoT networks employing short packet transmission. The base station was equipped with multiple antennas to enhance network availability, while the end nodes have only one antenna. This framework can be used in different transmission modes, including device-to-device, amplify and forward, and decode and forward.

Physical layer authentication (PLA)

Although the use of short packets in mission-critical communications systems can lead to the satisfaction of the stringent requirements of URLLC, the impact of finite block-length coding can cause serious physical-layer security issues. The PLA is another promising way of meeting MC-IoT networks' reliability requirements, employing short packet transmission without using cryptographic methods. A common model considered in this regard is composed of three nodes. One node, called Bob, needs to exchange information with the other node, Alice, securely. There is a third node called Eve, physically distanced in the network, which can sniff information being exchanged between Bob and Alice, and thus can send wrong information to the communicating parties. PLA aims to provide information security at the

physical layer such that interference from the undesired nodes can be avoided. A PLA-based mechanism was proposed in [7] as a lightweight authentication in reliable MC-IoT networks. In this work, the receiver employed a Gaussian mixture model (GMM) to make two clusters of the channel estimates, and based on this clustering, it was enabled to predict the actual transmitter. The authors of [8] presented a queuing theory-based detection and delay performance analysis of a PLA protocol for single-input multiple-output (SIMO) MC-IoT networks. This protocol was investigated under different possible attack cases. The authors of [9] analyzed the secrecy throughput of MC-IoT networks while considering single and multiple antenna access points (AP) in the presence of an eavesdropper equipped with multiple antennas and presented the corresponding latency-reliability trade-off analysis. Through simulations, it was demonstrated that as the number of antennas at the AP increased, the secrecy throughput increased accordingly. Along with securing the short packet transmissions, the PLA-based mechanisms, which use radio frequency authentication, have also been proposed for IoT device authentication [57].

The availability of the channel state information at the transmitter and receiver ends plays a crucial role in optimizing the transmission power. Therefore, Li et al. [58] considered the problem of optimizing transmission power for secure downlink transmission of short packets in wireless networks where a single AP communicates with a desired user. The authors proposed a mechanism to optimize AP's transmission power under different CSI settings. Moreover, this work employed an unsupervised deep learning approach to numerically determine the optimal power control policies, which outperformed the existing mechanisms. Along with securing the short packet transmissions (covert communication), the timeliness, characterized by the age of information (AoI), of a data packet needs to be considered in the design of such MC-IoT networks where end devices need to share time-critical information periodically [59]. Therefore, Yang et al. [60] proposed to jointly consider covertness and AoI in the design of secure short packet transmission. In this work, under the additive white Gaussian noise channels, the authors presented a closed-form expression for the average covert age of information (CAoI).

Although MC-IoT applications involve short packet transmission requiring URLLC interfaces, industrial IoT (IIoT) networks generate delay-sensitive and delay-tolerant

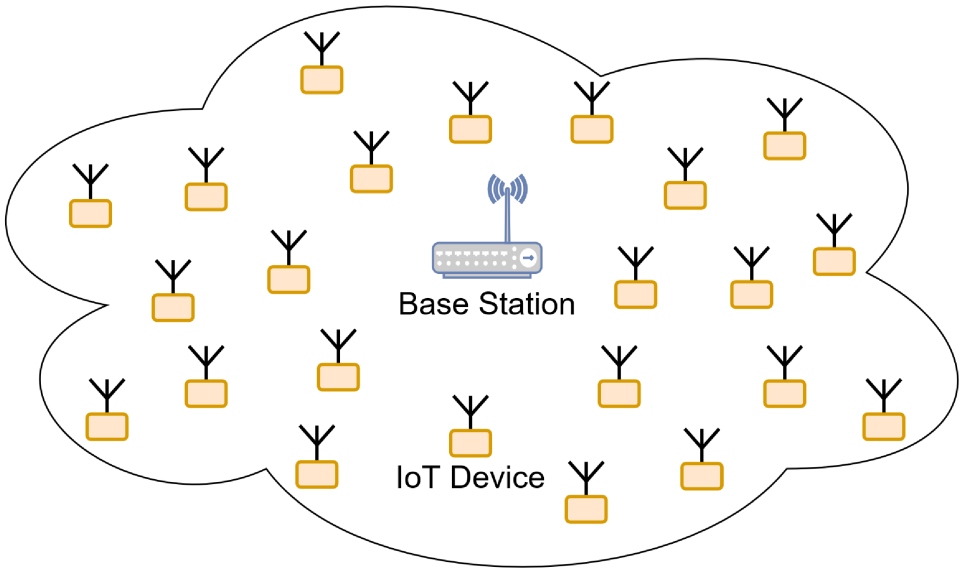

Figure 2.1: A large number of IoT devices performing uplink data transmission over shared radio resources.

data in varying amounts [3]. Moreover, some IIoT applications can require the availability of low-latency communication links for relatively longer time durations, e.g., the use of multimedia applications in IIoT networks. Therefore, the efficient use of available time, frequency and computational resources is essential in IIoT networks [61, 62].

2.3 Centralized Network Access Mechanisms

As shown in Figure 2.1, IoT networks are assumed to be composed of a large number of devices. At a given instant, a random number of devices become active and communicate with one base station (BS). The uplink transmission between the devices and the BS is modeled as a multi-channel slotted ALOHA in which each time slot carries a fixed number of resource blocks (RB), where an RB can be a time, frequency or code-based source. In each slot, an active device selects one RB randomly such that the selection is uniform across all available resources. If two or more devices select the same RB, the transmission fails, and the colliding devices attempt again in the next slot. Throughout this chapter, we use the terms resource blocks and channels interchangeably. The exact value of collision probability in a slot depends upon the number of active devices, available channels/resources, multiple access mechanisms (whether the system employs orthogonal multiple access or

non-orthogonal multiple access), and the type of the receiver being used. Detailed analysis of the collision-probability computation under different system models is presented in [10-12, 63].

The Long Term Evolution (LTE) and LTE-Advanced (LTE-A) technologies provide a four-stage grant-based network access mechanism for communication over limited radio resources [64]. In this approach, the IoT devices first undergo a random access channel (RACH) phase which is implemented by using multi-channel slotted ALOHA strategy [10]. In this phase each device transmits a preamble selected randomly from a pool of available preambles. The successful devices are then granted dedicated resources to transmit their data. While taking into account the case where BS may not be able to distinguish between single transmission and multiple transmissions (collision) over an RB, the corresponding probability mass function is derived in [10]. Due to the inherent signalling overhead, the grant-based access approach is more suitable for delay-tolerant transmission. At the same time, the reservation of available resources in grant-based access methods makes it less efficient for networks with massive IoT devices.

On the other hand, grant-free access avoids the long scheduling delays by allowing transmissions over shared resources without going through a request-grant phase. The grant-free access has gained considerable attention to support IIoT applications in 5G, and future wireless networks [21]. Liu et al. [65] presented a comparative analysis of different types of grant-free access schemes supporting ultra-reliable and low latency communications (URLLC) services. This work considered three types of grant-free access methods named reactive, K-repetition, and proactive grant-free schemes. The reactive grant-free approach allows devices to retransmit their data packets only if they do not receive an acknowledgment. On the other hand, under the K-repetition scheme, the devices transmit K-replicas of a data packet without waiting for an acknowledgment for the first transmission of the same packet. The devices receive feedback from the BS after K-transmissions. Under the proactive scheme, the devices can send maximum K-replicas of their data packet while getting feedback from the BS against each retransmission. The round-trip time is defined as the number of transmission time intervals (TTI) consumed during the transmission of a data packet and getting feedback from the BS. Each grant-free scheme

offers different round-trip times and associated latency in this work. The authors used latent access failure probability to measure the performance of each grant-free scheme. The latent access probability corresponds to the event in which the latency experienced by a device of interest exceeds the application-specific latency bound. This work helps choose a particular grant-free access mechanism depending upon an application-specific latency bound. In this regard, it was shown that the proactive scheme provided better performance for relatively shorter latency bounds, while the K-repetition scheme was more suitable for relatively large values of latency bound.

Choudhury et al. [13], proposed to transmit a fixed number of replicas of a message by using either time diversity or frequency diversity approach. In a frequency diversity method, a user transmits multiple copies of a message over different frequency resources in a frame. While in the time diversity method, the user sends multiple copies of a message over different time slots selected randomly in a slot over the same frequency resource. For frequency diversity, selected channels can be distinct, or some of the replications can be done over the same channel. On the other hand, for the time diversity method, a deterministic number of replicas can be sent in different frames, or after transmitting the first replica, the second replica is transmitted probabilistically. The results showed that deterministic policy was better than the probabilistic one. These diversity schemes provided higher reliability but at the cost of complicated receivers, which can increase latency.

Abreu et al. [14], proposed a scheme in which URLLC users with similar traffic characteristics are grouped by the BS. Users are grouped based upon the block error rate (BLER). Each group uses a pre-scheduled shared-resource for single retransmission if the initial transmission fails. The efficiency of this scheme is heavily dependent upon the right grouping of users at the BS. Abreu et al. [15], proposed a scheme in which active devices performed T attempts such that the first transmission was performed on dedicated channels, while $(T-1)$ retransmissions were performed on shared channels, and the receiver used successive interference cancellation (SIC) for decoding messages over shared resources. In order to assign resources in the initial transmission, the BS should have the knowledge of number of active devices. Otherwise, the system will not be able to use the resources efficiently.

Chiang et al. [16], presented two schemes based on parallel transmission over shared and dedicated resources. Both schemes assumed a SIC based receiver and allowed single retransmission. In one scheme, an active device performed one transmission on a dedicated resource, and sent a replica of the message over one of the shared resources simultaneously. While in the second scheme, first transmission was performed over shared resource. If BS remained unable to decode the message, second transmission was performed over the dedicated resource in designated slot. Significant control signalling is required in these schemes which can cause additional latency.

Galinina et al. [17], presented a scheme in which an active device with a certain transmission probability, sent single or multiple replicas over the shared channels in one slot. In this work, an optimal control algorithm was presented that guaranteed the minimal channel access delay by controlling the probability of transmission and the number of replicas. For both cases of single and multiple transmissions, corresponding practical implementations were also discussed. Probability of transmission and the number of replicas were decided at the BS level.

Boyd et al. [18], proposed two frequency diversity schemes for URLLC networks employing diversity slotted ALOHA. In each slot, diversity was achieved by the K-repetitious of a message over M orthogonal channels. In one scheme, an active device selected K channels randomly to transmit K replicas of its message. While, in the second scheme, an active device performed K repetitions by using a deterministic pattern of the orthogonal channels. In this work, a destructive collision model, and maximum ratio combining based multi-user interference model were used to design the receiver.

Astudillo et al. [19], proposed a standard compatible probabilistic retransmission mechanism for cellular IoT. In this mechanism, the number of active devices was estimated at the device side by counting the number of random access response (RAR) messages and utilizing the access class barring probability, which was periodically broadcasted by the BS. If an MTC device remained unsuccessful in the first transmission, it locally calculated a retransmission probability based upon this estimate. The authors proposed two retransmission schemes. One scheme consid-

ered the detected preambles while the other scheme used the collided preambles in one slot. In both schemes authors used the expected number of collided devices to evaluate the performance.

Gao et al. [66] proposed a distributed coordination-based grant-free access for heterogeneous IIoT networks in which massive IoT devices are deployed in a relatively small geographical area. The QoS requirements for different devices were measured in terms of the maximum affordable latency and packet collision probability. Three different levels were defined for each of the QoS parameters. Based on these levels, the devices were categorized as high, regular, and low priority. This work did not assume any particular packet arrival model and used time-based access of a single channel for uplink data transmission. In order to address the diverse QoS requirements, based on the priority levels, the devices were assigned different mini-slots in a given frame.

Gao et al. [67] developed a centralized scheduling control for the grant-free access proposed in [66]. Due to the large number of installed devices and their diverse QoS requirements, centralized scheduling control becomes complex. Therefore, the proposed algorithm utilized the neural networks approach for low-complexity scheduling. Firstly, while assuming that information regarding the number of devices in each category and protocol parameters was already available, the proposed algorithm assigned time slots to devices according to their categories. Later, a deep neural network-based scheduling scheme was designed to learn different protocol parameters for any given number of devices.

2.3.1 Network Load Aware Medium Access Control

The optimal allocation of available time and frequency resources in a selected network access mechanism is essential to meet the application-specific QoS requirements. The PHY-layer considerations play a significant role in adapting to the network dynamics [68,69]. Along with the physical channel characteristics, the number of active devices at a given time also impacts the resource utilization. While considering PHY-layer abstraction, the optimal number of retransmissions depends upon the number of transmitting devices (network load), available resources, and nature

of the MAC protocol being used. Most of the existing techniques either assume perfect knowledge of the network load or rely on the BS to estimate the number of transmitting devices to update the resource allocation strategy. Since the number of active devices in a network can change over time, the optimal resource allocation strategy being used should be updated dynamically.

Significant research has been done to address the problem of monitoring the network traffic and optimizing the resource allocation strategies accordingly [70-73]. In these works, the access class barring (ACB) probability played a major role in controlling network congestion. However, the network traffic-aware radio resource management in the existing grant-free and grant-based access mechanisms is primarily BS-centered and involves excessive computation overhead. Therefore, new intelligent resource management methods are required for the uplink dominant IIoT networks, which can avoid the computation overheads caused by centralized resource management approaches.

Astudillo et al. [19] proposed a mechanism for Long Term Evaluation (LTE) based cellular IoT networks which enabled the end-devices to estimate the number of active devices in a slot by using the information regarding the number of detected preambles at the BS in that frame. The end-devices can determine the number of detected preambles by counting the number of random access response (RAR) messages sent by the BS. This approach performs well as long as the BS is capable of transmitting the RAR messages against all the detected preambles. In order to perform the estimation under incomplete information at the device-level, which happens when the number of transmitting devices is higher, Astudillo et al. [19] proposed to use the value of Access Class Barring (ACB) probability. The ACB probability is a function of the number of active devices and number of channels, and it is broadcasted by the BS regularly. On the other hand, the computation of ACB-probability at the BS involves estimation of the number of active devices.

Oh et al. [71] proposed a mechanism to estimate the number of active devices at the BS in a given slot by computing the probability that a preamble remained idle in that frame. The proposed mechanism required that the probability of having an idle preamble is non-zero. However, for the higher number of active devices, the number

of idle preambles in a slot can become zero with high probability. Moreover, due to the channel impairments, an RB originally selected by one or more devices can be erroneously detected as an idle one [74]. Thus, the accuracy of this estimation method deteriorates in a dynamic environment.

For the framed-ALOHA networks, Jiang et al. [74], proposed an online supervised learning method that enabled the BS to predict current traffic load. In this work, the BS kept the history of idle, successfully decoded, and collided resource blocks in previous and current frames to predict the current traffic load. This work also incorporated the case where a detection error can occur, and a resource block can be detected as an idle one with a non-zero probability. The proposed mechanism outperformed the existing method of moments (MoM) and maximum likelihood (ML) prediction techniques.

2.3.2 Energy Efficient Grant-Free Network Access

Although device-level learning and grant-free access approaches help reduce the control signaling overheads, the device energy consumption cannot be ignored in the design of IIoT applications. The energy consumption aspect becomes more significant for battery powered IoT devices installed in remote areas where battery replacement is not that straightforward. Li et al. [75] proposed an energy consumption model for MTC devices. The proposed model considered device energy consumption in different phases, including sleep mode, data acquisition and processing, synchronization, and data transmission. This model was then used to derive the network lifetime and analyze network-level efficiency. It was shown that the average transmission rate governed the device's average energy consumption under the fixed power allocation in different phases and data packet size. On the other hand, the average transmission rate depended on available time-frequency resources.

Azari et al. [76] incorporated the device energy consumption along with the latency and reliability in the design of grant-free access for the uplink communication scenario. In this design, transmission power was one of the critical factors controlling the probability of successful transmission. The analysis in [76] assumed fixed transmit power for all transmissions. However, under the identical PHY-layer char-

acteristics, the diverse reliability requirements of traffic generated in IIoT networks can be addressed by assigning different transmit power levels to different types of transmissions. Moreover, under a dynamic environment, the adaptive power allocation approach can potentially enhance the overall energy efficiency of grant-free network access.

Al Homssi et al. [77] considered the uplink dominant IoT networks and used Shannon's channel capacity-based-energy composition model for end devices. Using this model, the authors derived lower bounds on the device's energy consumption under the unrestricted and restricted QoS scenarios. For each scenario, the authors analyzed the end device's energy consumption in different stochastic distributions of the serving BSs.

Optimal power allocation is very crucial in every retransmission scheme so that the desired reliability can be achieved with least amount of power. In type-1 ARQ scheme, an active device can perform a maximum of M attempts to have a successful transmission. If it remains failed in all attempts, the event is declared an outage. Dosti et al. [20], proposed a power allocation scheme for type-1 ARQ protocol employing short packet transmission. This power allocation aimed to minimize the power consumption in multiple transmissions such that it maximizes the throughout in the ultra-reliable region.

Choi et al. [78] proposed two grant-free access schemes named power domain multiple access (PDMA) and a rate domain multiple access (RDMA). Multiple users shared a single channel in these schemes employing a hybrid automatic repeat request with incremental redundancy-based re-transmit diversity. At the same time, a successive interference cancellation (SIC) based receiver is used. The PDMA scheme allowed the end devices to choose a power level from available power levels randomly. Under the RDMA scheme, the devices selected a transmission rate randomly from several possible transmission rates.

Tegos et al. [79] presented two power domain non-orthogonal multiple access (NOMA) schemes for slotted ALOHA systems. In this work, one scheme used a SIC-based receiver while the other scheme performed joint decoding at the receiver. The outage probability was utilized to obtain the average throughput offered by the proposed

schemes over Nakagami-m and Rayleigh fading channels. The proposed schemes provided higher throughput as compared to the slotted ALOHA systems. Moreover, the number of transmitting sources that can meet the desired QoS in the proposed schemes was also higher than supported by the slotted ALOHA systems.

Gharbieh et al. [80] proposed a stochastic geometry and queuing theory-based opportunistic grant-free access mechanism for uplink data transmission. The proposed mechanism enabled the IoT devices to transmit when their channel gains are above a prescribed threshold, and the devices have sufficient energy stored to overcome the path loss. This work assumed that the BSs and devices followed homogeneous Poisson point processes for spatial distribution. The proposed mechanism aims to enhance the utilization of energy harvested by the end devices.

2.3.3 Hybrid Network Access

Since traffic in IIoT networks has both delay-sensitive and delay-tolerant components with varying amounts of data, the coexistence of grant-free and grant-based approaches can potentially address these diverse QoS requirements. Therefore, Choi et al. [81] proposed to enable the end-devices to perform a BS-assisted preamble-based exploration phase prior to the data transmission. The exploration phase was performed over the available channels, and it divides the active devices into two groups of contention-free and collided devices. The available channels were also divided into two subsets accordingly. During the data transmission phase, contention-free devices transmitted data over the channels selected during the exploration phase. However, the devices in contention randomly chose a channel from the remaining channels with an optimal access probability. This mechanism provided significant improvement in the conventional multi-channel ALOHA system. However, in this design, the network access mechanism assumed that the number of active devices followed the Poisson distribution with the arrival rate less than the number of available channels. Consequently, future IIoT applications require more robust network access mechanisms which can be operated under higher network loads.

2.3.4 Critical Analysis

Following are the key critical points and observations found in the literature presented in this section:

- The above mentioned works are BS centred and employ centralized decision-making schemes where a central controller or a BS performs all the network-level decisions, which causes additional latency.

- Due to the centralized decision making, the BS needs to transmit control information periodically, which results in less efficient use of resources. Thus, we need to design such schemes that offer the least amount of control information.

- Moreover, in all these works, the analysis is performed either for single transmission or a fixed number of retransmissions/replications. The limit on the number of retransmissions needs to be adapted dynamically according to the network conditions.

- In the reviewed literature, MTC devices are assumed to be co-located in a common interference region. It is important to investigate the scene where devices belong to different interference regions.

- The techniques presented in these works use iterative solutions that are time-consuming and converge slowly. These iterative algorithms introduce additional latency in the processing of data at the BS. Thus, we need to devise closed-form solutions that can help reduce the latency in MT-MTC networks.

- It becomes very challenging to meet the required latency-reliability criterion when network parameters change dynamically. Distributed or decentralized decision making can help reduce the latency by allowing the devices to adapt to network dynamics. Hence, the network end-nodes must have the capability of learning and adapting the network dynamics.

2.4 Device-Level Learning-based Distributed Network Access

The centralized network schemes rely on the feedback and control information transmitted by the BS, which causes additional latency and under-utilization of available time and frequency resources. Although the grant-free network access approach allows end devices to transmit data over shared channels without going through a resource reservation phase, simultaneous transmissions from multiple devices over the same channel can cause collisions. Consequently, resource utilization is impacted in the systems employing grant-free network access strategies. One possible approach to improve the performance of these systems is enabling the end devices to update their transmission strategies by employing distributed learning algorithms [82]. In this regard, multi-armed bandit (MAB) learning is a promising tool for designing distributed network schemes [39-41]. The key feature of the MAB learning framework is that end devices can explore the network independently and make decisions to update their transmission strategies without requiring additional feedback and control information. Therefore, the resulting distributed network access approach can enhance resource utilization and reduce latency. This section briefly reviews recent works that use the multi-agent MAB learning framework in designing distributed network access mechanisms. We also highlight gaps in the existing works that motivated us to perform the research work presented in chapter-6 of this thesis.

Considering the heterogeneous networks, the design of an appropriate spectrum access mechanism depends on how IoT devices are categorized in the network. Therefore, Bonnefoi et al. [83] analyzed the potential usage of stochastic multi-agent MAB algorithms for IoT networks composed of static and dynamic devices. In this work, the static devices transmitted over fixed channels, while each dynamic device randomly selected a channel, resulting in non-IID rewards. The proposed mechanism improved the probability of successful transmission compared to random policies. However, as the proportion of dynamic devices increases, efficiency of this mechanism decreased. Choi et al. [84] proposed to use the power domain non-orthogonal multiple access (NOMA) for the system model considered in [83] resulting in higher throughput for both dynamic and static devices. Moreover, it was also demonstrated

that allowing the BS to decide the rewards of active dynamic devices makes device-level multi-agent MAB-based learning faster. However, the enhanced performance of the proposed two-sided learning approach suffered from additional computations at the BS and control signaling overheads. Since, the number of active devices can change over time, the static channel allocation can result in lower utilization of the available radio resources.

The QoS experienced by an intended device is significantly impacted by the number of active devices and their locations in the network. Therefore, Avner et al. [85] proposed a coordinated multi-agent MAB learning-based network access mechanism for users experiencing different reward distributions. This work considered that due to the different location profiles of each user, the same channel may behave differently for different users. The proposed mechanism assumed that the number of active users did not exceed the number of available channels. Additionally, the coordination among users required feedback information, resulting in communication overheads.

Gafni et al. [86, 87] proposed a distributed learning-based spectrum access strategy for wireless networks in which the available transmission rate over a given channel can vary for each user. In this mechanism, all users needed to estimate each channel's expected transmission rate through an exploration phase. Magesh et al. [88] proposed an multi-agent MAB learning-based uncoordinated spectrum access mechanism for heterogeneous networks where users can experience a different mean reward for a given channel. Simultaneously, Youssef et al. [82] proposed multi-agent MAB-learning-based uncoordinated spectrum access for networks with heterogeneous reward distributions while allowing users to choose more than one channel for the uplink data transmission. In these works, when two or more users accessed the same channel, the corresponding users receive zero rewards.

MAB learning has recently been used to design uncoordinated spectrum access mechanisms for networks where users accessing the same channel receive non-zero rewards. Shi et al. [89] proposed a multi-agent MAB learning-based information-theoretic channel model incorporating collision-dependent rewards. This work assumed that the number of channels is known to the users; however, the number of

active users is less than or equal to the number of channels. Moreover, the number of active users was estimated by using a sequential hopping protocol. On the other hand, Bande et al. [90] proposed a stochastic multi-agent MAB-based spectrum access mechanism that can generate a non-zero reward for the users occupying the same channel. However, the mean reward became zero when the number of users sharing the same channel was higher than a prescribed threshold. Moreover, the reward distribution was considered to be homogeneous across all users. This work can accommodate users higher than the number of channels. However, information regarding the number of active users is broadcasted during each exploration phase, which adds to the control signaling overhead. On the other hand, Magesh et al. [91] proposed a stochastic multi-agent MAB-based decentralized spectrum access mechanism that supported both the heterogeneous reward distributions and non-zeros rewards for the colliding users.

The multi-agent MAB learning-based uncoordinated spectrum access mechanism supporting non-zero rewards for colliding users can be applied in uplink NOMA systems. Therefore, Youssef et al. [92] considered the self-organizing networks where multiple access points are deployed. This work addressed the problems of designing multi-agent MAB learning-based uncoordinated spectrum access and distributed power allocation in the targeted networks. In order to support the non-zero reward for devices experiencing collisions, this work proposed using a power domain NOMA-based uplink transmission approach. The exploration phase in [90-92] relied on a users-grouping-based method to estimate the number of users sharing each channel, which introduced an additional computation burden at the user level.

2.4.1 Critical Analysis

The above discussion highlights that device-level knowledge regarding the number of active devices is crucial for designing the MAB-DMAC mechanism strategies. However, existing works employ a dedicated stage to estimate the number of active users causing additional computation burden at end devices. Although some of these works classify devices as static and dynamic, the time-varying nature of the number of active devices needs to be accommodated for efficient use of the shared resources. Moreover, some of these works incorporate heterogeneous reward distributions for

different users, which can address variations in the channel's behavior for different users. However, along with the channel's physical characteristics, the diversity in the latency and reliability requirements of different devices needs to be addressed while using multi-agent MAB learning in IoT networks.

2.5 Distributed Computing Services for MC-IoT Networks

It becomes very challenging to meet the required latency-reliability criterion when network parameters change dynamically. The above-mentioned works are BS centered and employ centralized decision-making schemes where a central controller or a BS performs all the network-level decisions, which causes additional latency. Distributed decision making can help reduce the latency by allowing the devices to adopt the network changes. Hence, the end-nodes must have the capability of learning and adopting the network dynamics.

2.5.1 Edge and Fog Computing

Edge computing is an integral part of future wireless networks that enables distributed computing, storage, and control services at the network edge-nodes. These features of edge computing can lead to provide a platform that is suitable for mission-critical applications. In this regard, high-capacity mmWave links, proximity-based computing, edge machine learning, proactive computing, and parallel coded computing are the key enablers to achieve low latency, while multi-connectivity, task replication, edge machine learning and federated machine learning (a form of distributed learning) can provide high reliability in edge computing based MC-IoT networks [1]. In this study, we focus on edge machine learning and distributed learning based systems.

Fog-computing is a distributed computing paradigm that aims to address the bandwidth, latency, and reliability-constrained applications in heterogeneous networks by providing cloud-like functionalities near the data source [93-95]. Mukherjee et at. [93] presented a comprehensive survey highlighting recent works which use fog

computing to design systems supporting MC-IoT applications. In this regard, fog computing was proposed to minimize latency in healthcare systems, to design industrial wireless sensor networks supporting real-time applications, and to address the problem of real-time vehicle tracking in smart cities [93]. Furthermore, considering vehicular networks, the growing number of vehicles equipped with intelligent IoT devices makes it necessary to design vehicular networks where they can learn and adapt to the network dynamics without depending upon additional infrastructures. Therefore, Hou et al. [96] proposed a vehicular fog computing (VFC) design paradigm that used moving and parked vehicles as infrastructures for computation and communication in vehicular networks, which can result in better utilization of the available resources, enhance the overall system performance, and support the latency-sensitive applications in vehicular networks.

Any device which has the required communication, storage, and computational resources can become a fog node (FN). Fog-computing-based radio access networks (F-RANs) proposed for 5G wireless communication systems enable collaboration radio signal processing (CRSP) at the fog and terminal layers [97]. The F-RANs are composed of the terminal, logical fog, and cloud layers. The terminal layer includes IoT devices, also called terminal nodes. The entities of the logical fog computing layer come from the network access layer in the form of fog access points (F-AP) to communicate with the terminal layer; and routers, switches, and gateways to transfer data to the cloud layer, which is responsible for large data storage and complex processing. Although F-RANs help reduce the latency, the communication link between the terminal and fog layers (so called fog-things interface) becomes the bottleneck while achieving the required levels of reliability in the fog-computing-based critical IoT applications.

The growing number of vehicles equipped with intelligent IoT devices makes it necessary to design such vehicular networks in which these vehicles can learn and adapt to the network dynamics by themselves without depending upon the additional infrastructure. Hou et al. [96] proposed a vehicular fog computing (VFC) design paradigm that used moving and parked vehicles as infrastructure for computation and communication in vehicular networks. The VFC paradigm can better utilize the available resources, enhance the overall system performance, and support the

latency-sensitive applications in vehicular networks. In this regard, statistical learning is a promising tool to learn different dynamic network parameters in wireless networks when complete information of the probability distributions associated with the dynamic network parameters is not available [38].

2.5.2 Federated learning

Federated learning (FL) introduced in [98] is a distributed learning approach. In this framework end nodes of a network learn statistical models by applying a particular machine-learning method. These end-nodes share their knowledge of locally learned models with the BS for aggregation, which generates a network-wide accepted model. The whole process repeats regularly. In FL, learning is performed over decentralized data, and instead of sharing the data-sets in FL, the end nodes share the updates of learned parameters of a statistical model. The FL paradigm is more suitable when training data is non-I.I.D, unbalanced, devices are massively distributed, and the number of active devices at a given instant of time is small as compared to total devices in the network. Due to the distributed learning nature of this framework, one of the main advantage is the privacy. In FL the primary goal at BS is to minimize an objective function generated by using the local objective functions [99].

Choi et al. [32], proposed to use multi-channel ALOHA (framed-ALOHA) in the FL systems. In this scheme, during each iteration or update round, the BS allowed M mobile devices to send their local updates to the BS using multi-channel ALOHA. Each device, with its access probability, selected one of the M channels randomly following the uniform distribution and transmits the local update. This work showed that if access probability was less than e^{-1}, the multi-channel ALOHA based FL systems performed better than the polling method in which BS sequentially polled M devices to get their updates. Since the performance of the proposed system depended on the access probability, it was also demonstrated that the access probability can be optimized based upon the availability of local updates, which can improve the overall performance of a multi-channel ALOHA based FL systems.

Yang et al. [33], proposed an energy efficient transmission mechanism for FL-based wireless networks. They presented an iterative algorithm to jointly optimize the

energy and computation resources utilization in an FL system. Yang et al. [34], presented an analytical model for wireless networks employing FL in different scheduling policies. These scheduling policies included random scheduling, round-robin, and proportional fair. This work investigated the performance of FL assisted scheduling policies under different regions of the signal to interference plus noise ratio (SINR) and other channel conditions in-terms of the convergence rate. Chen et al. [35], proposed an FL based framework for wireless networks to jointly optimize the resource allocation at the BS and transmit power allocation at the device level such that the packet error rate was decreased. This FL-based framework aimed to decrease the packet error rate by the joint learning and communication approach. Samarakoon et al. [36], proposed an extreme value theory based FL framework for ultra-reliable low latency vehicular communication. This work jointly optimized the resource allocation and transmit power such that the network-wide power consumption was minimized.

2.5.3 Critical Analysis

The above-mentioned recent studies on FL-based wireless networks primarily focus on the resource and energy/power optimization aspects at the BS and device levels, respectively. Devices sharing parameters of learned models with the BS over shared media may undergo additional latency caused by retransmissions. However, these works do not cover the overheads caused by particular medium access methods being used in these systems.

Moreover, implementation of FL-based solutions in wireless networks faces four main challenges [100]: Firstly, while applying the FL model in networks with a massive number of devices, communication can be costly due to the large number of updates being sent to a central BS for the training purpose. Secondly, due to the heterogeneity of the devices and their applications, the hardware resources may vary from device to device. Thirdly, the variability in applications being used on these devices results in non-I.I.D data. Finally, information privacy is also among the core challenges due to the fact that instead of sharing the raw data, the devices learn and share the parameters of a model with the BS. Thus, the FL-based solutions being implemented in MT-MTC networks should be capable of handling these aspects.

2.6 Conclusion

The literature review presented in this chapter highlights different approaches proposed to design MC-IoT networks. Moreover, critical analysis of this literature helps us identify the gaps in the existing research works. In this thesis, we focus on designing network access mechanisms that can meet the desired latency-reliability criterion in the MC-IoT networks operating under dynamic network load. In this context, it is identified that existing works that employ centralized network access control strategies involve excessive control signaling and feedback information overheads. However, the MC-IoT applications cannot afford these overheads due to their strict latency requirements. Moreover, it is also identified that, in contrast to the grant-based network access mechanism, the grant-free network access approach avoids the resource reservation stage. However, simultaneous transmissions over the same channel can result in collisions that impact the system's performance when the network load changes dynamically. Therefore, to adapt to the network dynamics, end devices need to be capable of exploring the network without requiring additional feedback information from the BS.

Motivated by the identified research challenges in designing MC-IoT networks, we aim to design grant-free network access mechanisms where end devices can learn different network parameters independently and adapt to the network dynamics without relying much on the BS. To this end, statistical and MAB learning are promising tools for designing distributed network access mechanisms. Statistical learning can enable end devices to predict different networks by using their transmission history in a probabilistic manner. On the other hand, when multiple BSs serve a dense IoT network, the MAB learning paradigm can enable the end devices to improve their BS selection over time while avoiding excessive feedback information and control signaling overheads. In the following chapters, we present grant-free network access mechanisms for MC-IoT networks that enable the end devices to adapt to the network dynamics by exploring the network in a distributed manner while avoiding additional control signaling from the BS. Chapters 3-5 consider uplink data transmission over a single BS, while chapter-6 focuses on the uplink data transmission in a dense IoT network where multiple BSs serve a large number of devices.

Chapter 3

Statistical Learning-Based Dynamic Retransmission Mechanism for Mission Critical Communication: An Edge-Computing Approach

This chapter is based on the following conference publication. Improved results are also added in this chapter:

M. A. Raza, M. Abolhasan, J. Lipman, N. Shariati, and W. Ni, *"Statistical Learning-Based Dynamic Retransmission Mechanism for Mission Critical Communication: An Edge-Computing Approach,"* in 2020 IEEE 45th Conference on Local Computer Networks (LCN), 2020, pp. 393-396.

3.1 Introduction

Mission-critical machine type communication (MC-MTC) systems require stringent requirements of ultra-reliable and low-latency communications (URLLC). Remote sensing, autonomous transport, Industry 4.0, robot control, and telesurgery are among the emerging applications of MC-MTC networks. In such systems, messages

from MTC devices need to be delivered successfully at the base station (BS) within a prescribed end-to-end latency of L (ms). From the physical (PHY) layer perspective, the concept of reliability is related to the packet-error rate (PER). However, reliability can also be defined as the probability of satisfying a latency bound L (ms) [1], and this notion of reliability is more useful while addressing URLLC requirements at the medium access control (MAC) layer and the other higher layers. If L_D is the latency experienced by a packet from an MTC device, and ϵ_r is the reliability constraint, the MC-MTC system is required to exhibit $\Pr(L_D \leq L) \geq 1 - \epsilon_r$, where $\Pr(.)$ denotes the probability measure. Future MC-MTC networks aim to achieve $\epsilon_r \leq 10^{-5}$ and $L \leq 1$ (ms) [2].

Several PHY and MAC layer techniques have been proposed to design URLLC based systems [2, 54, 55]. Short packet transmission and grant-free non-orthogonal multiple access methods can reduce latency considerably [21], while the diversity-based and retransmission schemes enhance the reliability [14-18]. It is identified that present approaches are primarily BS centered and employ centralized decision-making schemes where a central controller or a BS performs all the network-level decisions, which causes additional latency. It becomes very challenging to meet the required latency-reliability criterion when network parameters change dynamically. Hence, the network edge-nodes and edge-devices must have the capability of learning and adapting to the network dynamics. Moreover, current literature focuses on the schemes which involve either a single transmission or a fixed number of retransmissions and replications. However, in MC-MTC networks, the retransmissions limit needs to be adapted dynamically according to the network conditions, which is the main focus of this chapter.

Edge computing is an integral part of future wireless networks that enable distributed computing, storage, and control services at the network edge-nodes. These features of edge computing can lead to provisioning a platform that is suitable for mission-critical applications. In this regard, potential enablers for edge computing-based mission-critical applications are discussed in [1]. This chapter considers MC-MTC networks employing framed-ALOHA and uses an edge computing approach to demonstrate how edge-devices can help the edge-node/BS determine the retransmissions limit. The following are the key contributions of this chapter:

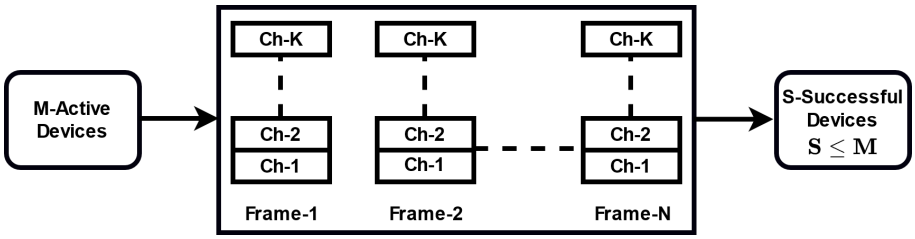

Figure 3.1: Framed-ALOHA based transmission over one MCR composed of N frames.

- For MC-MTC networks employing framed-ALOHA, we present an edge computing based statistical learning mechanism to predict the retransmissions limit N_r, which can meet the desired latency-reliability criterion. A sequence of $(N_r + 1)$ frames is termed as a mission-critical round (MCR), and each device uses its history of previous J MCRs to estimate the collision probability in one frame. This estimate is used to formulate a value at risk (VaR) problem to predict the retransmissions limit under a given latency-reliability constraint. Finally, each device shares the prediction of N_r with the BS.

- Through simulations, we present the performance analysis of a restricted MCR-based framed-ALOHA system in which after the first successful transmission, the device stops transmitting in the current MCR and attempts in the next MCR if it has another packet to transmit. In this regard, we compare the performance of a restricted MCR based framed-ALOHA system with the diversity transmission-based framed-ALOHA (DTFA).

3.2 Retransmissions Limit Prediction

We consider a homogeneous MC-MTC network composed of W MTC-devices in which, at a given instant, $M \leq W$ active devices attempt to communicate with one BS. The uplink transmission between the MTC-devices and the BS is modeled as multi-channel slotted ALOHA or framed-ALOHA, which is also used by Long-Term Evaluation (LTE) during the contention phase [10]. As shown in Fig. 3.1, each frame is composed of K channels or resource blocks, and a sequence of $N = N_r + 1$ frames is called a mission-critical round (MCR). All active devices begin to transmit at the start of an MCR. It is assumed that an active device will always have a packet

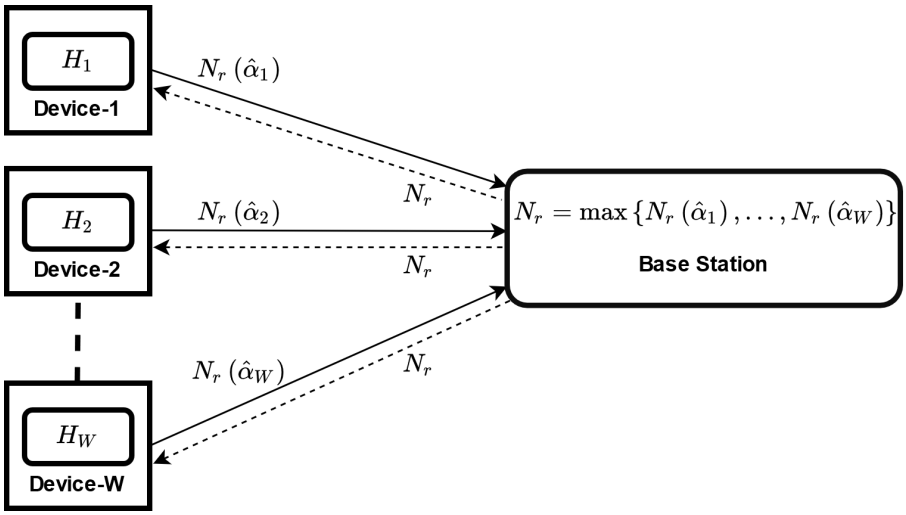

Figure 3.2: MTC devices sharing locally predicted retransmissions limit with the BS.

to transmit throughout the MCR. In each frame, every active device selects one of the K available channels randomly following a uniform distribution independently from other devices. We perform the MAC layer analysis only while considering PHY layer abstraction in which transmission fails if two or more devices select the same channel, and the failed devices attempt again in the next frame. Upon successful transmission, the device receives an acknowledgment from the BS and continues to transmit in subsequent frames. The parameter N_r is the maximum affordable retransmissions, and the value of N_r is determined at the edge dynamically.

An observation interval of $N_h = JN$ slots spanned over J MCRs is considered. The number of active devices in a given observation interval is assumed to remain fixed. However, M can change randomly from one observation interval to another. The end devices and the BS do not know the value of M and the associated probability distribution. If processing and propagation delays are assumed constant, latency (L_D) is primarily a function of N_r. We aim to enable the active devices to estimate the collision probability in one frame and then determine the optimal number of retransmissions at the edge that can meet the desired latency-reliability criterion.

The number of transmission attempts an MTC device performs for a successful transmission depends upon the collision probability in one frame. Given that M devices are active, the probability that an MTC device of interest will collide with

at least one of the $(M-1)$ devices in one frame is given as [11]:

$$\alpha := 1 - \left(1 - \frac{1}{K}\right)^{M-1}. \tag{3.1}$$

Since the devices do not know the exact value of M, they cannot use (3.1) to determine the value of α. Therefore, the devices are enabled to estimate the value of α by using the history of their previous transmissions. For that purpose, each device keeps the record of its last N_h transmissions attempts in a vector $H_m = \left[A_m^{(1)}, A_m^{(2)}, ..., A_m^{(N_h)}\right]$, where each element of H_m is an independent Bernoulli random variable defined as:

$$\left\{A_m^{(n)}\right\}_{\substack{m=1,2,..,W \\ n=1,2,..,N_h}} = \begin{cases} 1, & \text{collision with other device/s;} \\ 0, & \text{successful transmission.} \end{cases} \tag{3.2}$$

The estimate of collision probability at the m^{th} device denoted by $\hat{\alpha}_m$ is computed as

$$\hat{\alpha}_m = \frac{1}{N_h} \sum_{n=1}^{N_h} A_m^{(n)}. \tag{3.3}$$

Risk sensitive learning and control is a promising tool to address URLLC related problems [2]. We use the collision probability estimate $(\hat{\alpha}_m)$ to formulate a value at risk (VaR) problem to predict the number of retransmissions the MTC device is allowed under a given latency-reliability constraint. Let the random variable X_m show the number of collisions faced by m^{th} device before a successful transmission. The random variable X_m follows the geometric distribution, and the probability that a device undergoes up to N_c collisions before having a successful transmission is given as

$$\Pr\left(X_m \leq N_c \mid \hat{\alpha}_m\right) = 1 - \left(\hat{\alpha}_m\right)^{N_c+1}. \tag{3.4}$$

Each retransmission adds to the latency experienced by a data packet in a given MCR, and there exists a maximum value of retransmissions under the given latency-reliability constraint, after which it will be too late to receive that data packet at the BS. Thus, the retransmissions limit N_r can be found by computing the VaR of

X_m as follows:

$$N_r\left(\hat{\alpha}_m\right) = \inf_{N_c}\left\{N_c \geq 0 : \Pr\left(X_m \leq N_c \mid \hat{\alpha}_m\right) \geq 1 - \epsilon_r\right\}. \tag{3.5}$$

An optimal value of N_r that can meet the stringent requirements of the URLLC will require that the collision probability is kept very small. Each device predicts the retransmissions limit $N_r\left(\hat{\alpha}_m\right)$, and shares with the BS as a part of its data packet. As shown in Fig. 3.2, the BS keeps a record of the last update sent by each device in a vector $R = \{N_r\left(\hat{\alpha}_1\right), N_r\left(\hat{\alpha}_2\right), ..., N_r\left(\hat{\alpha}_W\right)\}$. After every F number of MCRs, the BS broadcasts its updated retransmissions limit $N_r = \max\{N_r\left(\hat{\alpha}_1\right), N_r\left(\hat{\alpha}_2\right), ..., N_r\left(\hat{\alpha}_W\right)\}$ to be used by all the devices for determining the size of the MCR, and the outage event, which is part of our future research work. A device is said to be successful in one MCR if it has at least one successful transmission in that MCR, and the probability of this event is given as

$$p_{suc}^{(N)} = 1 - \left(\alpha\right)^N. \tag{3.6}$$

Figure 3.3 provides an insight into the number of retransmissions a system should allow for different values of reliability constraint ϵ_r against the collision probability α. It is interesting to note that a specific value of N_r can be valid for a range of α. Moreover, due to the discrete nature of N_c, Equation (3.5) can yield same value of N_r for two different values of $(1 - \epsilon_r)$ valid over a range of collision probability. In such cases N_r corresponds to retransmissions limit for higher value of $(1 - \epsilon_r)$. Since each active device updates its history vector after each attempt, the BS captures the increasing traffic load and updates value of N_r after every F number of MCRs. Thus, the network adapts to the dynamic changes by learning the network statistics, i.e., the collision probability.

3.3 Simulation Results and Discussion

Extensive simulations are performed in MATLAB to evaluate performance of the proposed system. In Fig. 3.4, for $\epsilon_r = 10^{-5}$ and $N_r = 3$, the normalized mean squared error (NMSE) of $N_r\left(\hat{\alpha}_m\right)$ is plotted against length of the history vector H_m

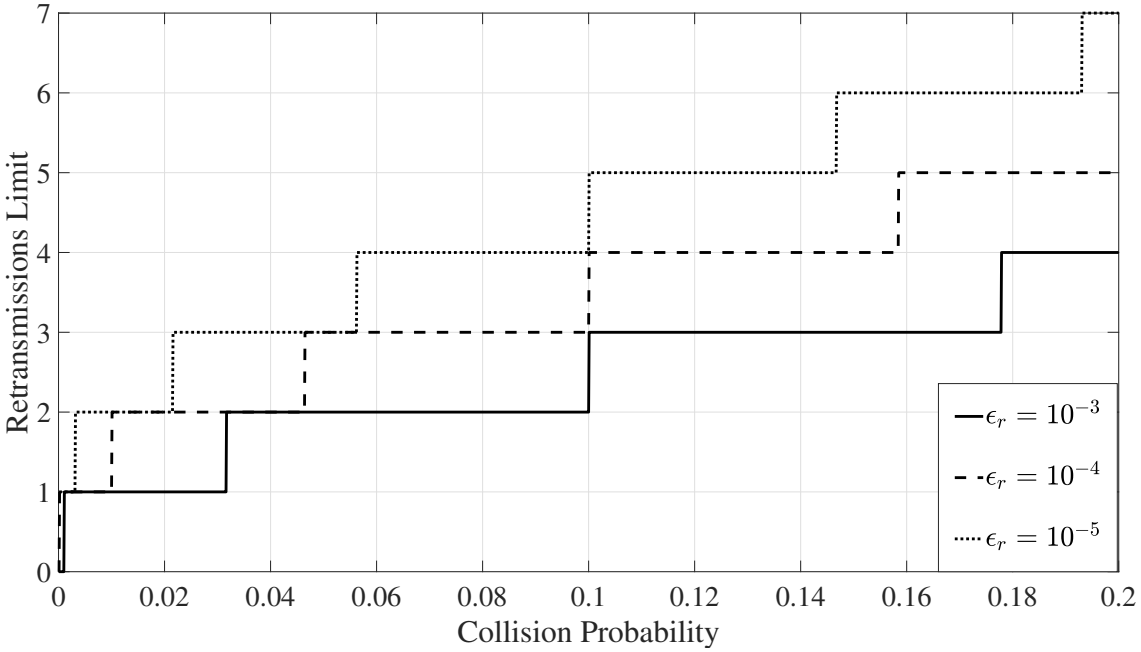

Figure 3.3: Retransmissions limit against the collision probability for different values of reliability constraint ϵ_r.

used to predict the retransmission threshold. The NMSE is defined as: NMSE = $\frac{\text{MSE}}{[N_r(\alpha)]^2}$, and the mean squared error (MSE) is computed as

$$\text{MSE} = \frac{1}{N_s} \sum_{n=1}^{N_s} \left[N_r(\alpha) - N_r^{(n)}(\hat{\alpha}_m) \right]^2, \tag{3.7}$$

where $N_s = 10000$ is the number of iterations performed to compute MSE against one value of N_h, and $N_r^{(n)}(\hat{\alpha}_m)$ is the retransmission limit prediction in n^{th} iteration. As shown in Fig. 3.3, there exists a unique value of $N_r(\alpha)$ for a specific interval of α. We pick three different values of α such that each corresponds to a different value of $N_r(\alpha)$. For each value of α, the NMSE of retransmission threshold prediction is plotted against N_h. It is shown that the NMSE of retransmission threshold prediction decreases randomly when the value of N_h is increased and becomes stable asymptotically when N_h is large.

3.3.1 Restricted-MCR

In restricted-MCR, all the active devices begin to transmit at the start of an MCR. However, after the first successful transmission, the device stops transmitting in the current MCR and attempts in the next MCR if it has another packet to transmit.

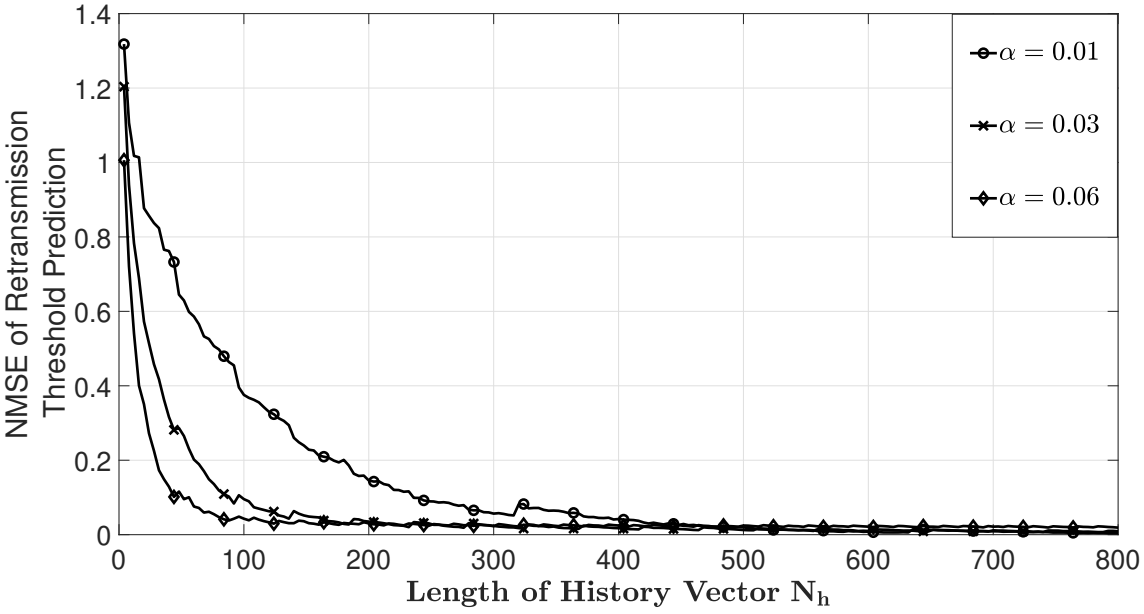

Figure 3.4: NMSE of locally predicted retransmission limit $N_r\,(\hat{\alpha}_m)$ against length of history vector for different values of collision probability.

The restricted transmission strategy helps reduce the collision probability in successive frames of an MCR, which results in latency reduction. On the other hand, in the diversity transmission-based framed-ALOHA (DTFA) method, each active device sends one replica of its message in N frames of an MCR, such that in each frame, it selects one of the K channels randomly. Devices may collide in some frames, but they can also be successful in some other frames. This helps increase the number of successful devices by reducing the overall collision probability. The analytical expression for overall collision probability of the DTFA scheme is provided in [12].

We compare the performance of the restricted-MCR-based framed-ALOHA with the DTFA scheme. The performance is compared in terms of the average successful devices per round and the average retransmission for successful transmission against a range of active devices. For the DTFA strategy, we consider the case where a device is successful if at least one transmission remains successful in one MCR. As shown in Figure 3.5, for the relatively smaller number of active devices, both schemes depict similar behavior with respect to the average successful devices per round. However, the restricted transmission policy outperforms the DTFA scheme under moderate network load. When the network load becomes too large, the average number of successful devices in both schemes approaches zero. Moreover, as illustrated in Figure 3.6, the average number of transmission attempts performed by a successful device

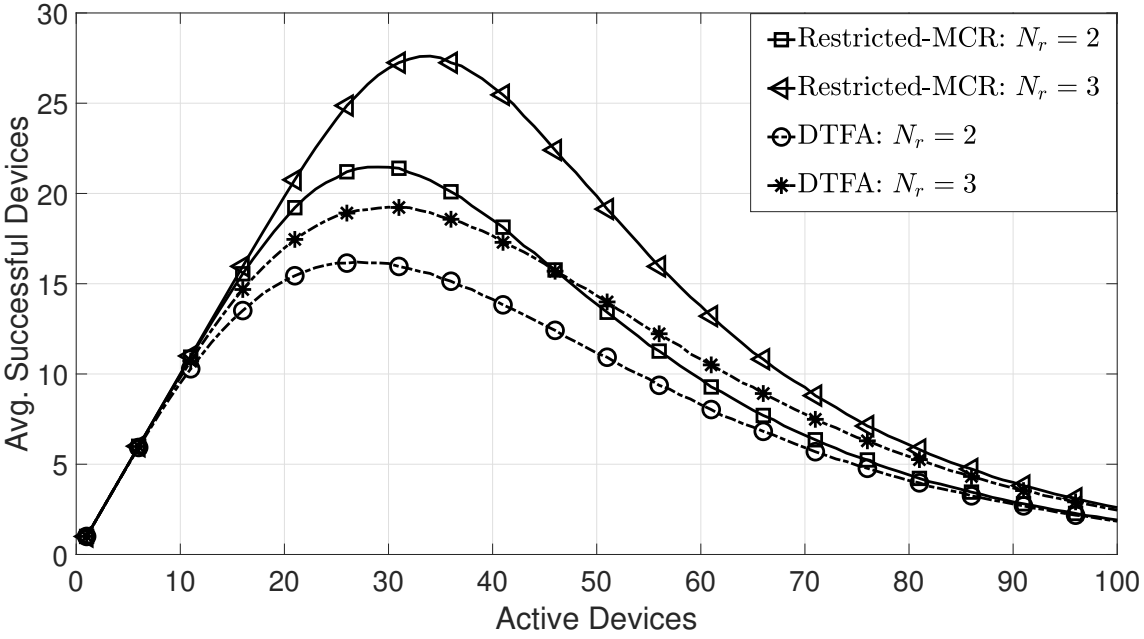

Figure 3.5: Performance comparison of restricted-MCR based framed-ALOHA and DTFA in terms of average successful devices with $K = 20$.

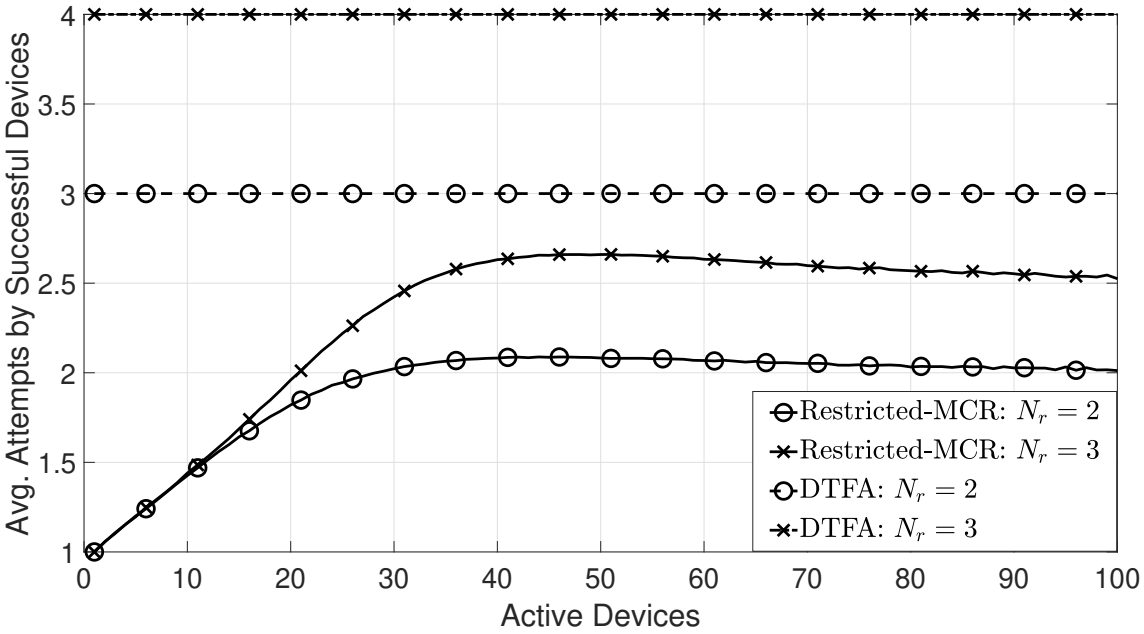

Figure 3.6: Performance comparison of restricted-MCR based framed-ALOHA and DTFA in terms of average attempts by a successful device with $K = 20$.

in the restricted-MCR is less than that of the DTFA method. Thus, the overall average latency can be reduced by using the restricted-MCR based retransmission scheme. (Please note that Figure 3.5 and Figure 3.6 are the improved versions of the respective figures in the corresponding conference paper, obtained after fixing a minor bug in the MATLAB code.)

3.4 Conclusion

By using an edge computing approach, we present a statistical learning-based dynamic retransmission mechanism for MC-MTC networks employing framed-ALOHA. Each MTC device in the network uses its history of the previous transmissions to learn statistically the number of retransmissions it can afford such that the desired latency-reliability criterion is met. In order to have a network-wide uniform value, each device shares its knowledge of retransmissions with the base station (BS). Simulations are performed in MATLAB to evaluate the performance of MC-MTC networks employing a framed-ALOHA system for the case where each active device can have only one successful transmission in one MCR, called a restricted-MCR. For the same average successful devices in one MCR, the restricted-MCR based framed-ALOHA system requires fewer attempts as compared to the DTFA scheme. As future work, we aim to perform the analytical modeling of restricted-MCR-based framed-ALOHA for MC-MTC networks.

Chapter 4

Statistical Learning-Based Grant-Free Access for Delay-Sensitive Internet of Things Applications

This chapter is based on the following journal publication:

M. A. Raza, M. Abolhasan, J. Lipman, N. Shariati, W. Ni, and A. Jamalipour, *"Statistical Learning-Based Grant-Free Access for Delay-Sensitive Internet of Things Applications,"* IEEE Transactions on Vehicular Technology, vol. 71, no. 5, pp. 5492–5506, 2022.

4.1 Introduction

Mission critical Internet-of-Things (IoT) applications require ultra-reliable and low latency communication (URLLC) interfaces to transmit delay-sensitive data. These applications form an essential dimension of IoT 2.0 systems, which includes intelligent transportation systems, unmanned aerial vehicles (UAVs), public safety communication networks, telesurgery, smart grids, and Industry 4.0, covering smart factories [101]. Different mission-critical applications can have different latency and reliability specifications; some of those are highlighted [4]. From the vehicular com-

munication perspective, different vehicle-to-everything (V2X) communication use-cases in which a vehicle communicates with other vehicles (V2V), with wayside infrastructure (V2I) and with mobile users (V2P), can involve delay-sensitive data transmission, which requires ultra-reliability [49], e.g., self-driving vehicles. Similarly, intelligent transportation systems aided by the vehicular ad-hoc networks (VANETs) aim to exchange safety-critical messages under strict latency and reliability requirements. It becomes very challenging to fulfill the desired latency-reliability requirements for the V2X based systems in heterogeneous networks.

Latency experienced by data packets in a wireless communication system is composed of deterministic and random components. The information processing delays at the transmitter and receiver determine the deterministic component, while the delays involved in retransmissions and back-off phases define the random part of the latency [2]. The reliability of a communication system can be affected by many factors, including the time-varying nature of the wireless channel, different sources of interference causing random changes in the signal to noise ratio (SNR) at the receiver, type of a particular constellation being used, error detection and correction codes, and nature of the medium access control (MAC) mechanism [2]. In the context of mission-critical IoT applications, reliability is interpreted as the probability of meeting the prescribed latency bound [1]. The real-time processing of a massive amount of data generated by a large number of sensors in these networks requires that the data be transferred from the source to the data centers within the application-specific latency while ensuring desired levels of reliability. It becomes challenging to meet these requirements in heterogeneous networks where different groups of IoT devices can have different latency-reliability criteria and network parameters change dynamically.

For the optimal utilization of the available radio resources in heterogeneous networks to meet the application-specific latency-reliability criterion, it is essential to know the number of active devices and their latency-reliability requirements. The conventional centralized decision-making approaches in which these tasks are performed at the base station (BS) suffer from heavy computation overheads, which result in higher latency. Therefore, the use of distributed computing and device-level learning of network parameters can play a significant role in designing mission-critical IoT

applications by reducing the computation burden at the BS. Fog computing is a distributed computing paradigm that aims to address the bandwidth, latency, and reliability constrained applications in heterogeneous networks by providing cloud-like functionalities near the data source [93-95]. The growing number of vehicles equipped with intelligent IoT devices makes it necessary to design such vehicular networks in which these vehicles can learn and adapt to the network dynamics by themselves without depending upon the additional infrastructure. Hou et al. [96] proposed a vehicular fog computing (VFC) design paradigm that uses moving and parked vehicles as infrastructure for computation and communication in vehicular networks. The VFC paradigm can better utilize the available resources, enhance the overall system performance, and support the latency-sensitive applications in vehicular networks.

The choice of a particular network access mechanism plays a major role in meeting the application specific QoS requirements. The grant-based MAC protocol in Long Term Evolution (LTE) allows the IoT devices to transmit their data over dedicated resources if they are successful in a contention-based random access channel (RACH) phase. The RACH phase introduces additional signaling overheads, and the grant-based protocols are suitable for a smaller number of IoT devices. In comparison, the data transmission in grant-free network access mechanisms is performed over shared radio resources in a random-access manner without requesting a resource grant. The grant-free network access approach has many benefits over the grant-based strategies to support the uplink connectivity for massive IoT, generating sporadic traffic [21, 102]. However, while achieving the massive connectivity target, the latency and reliability can be compromised in the grant-free MAC protocols. Several retransmission schemes have been proposed to enhance the reliability in mission-critical IoT applications [15-18]. Another important constraint is the energy consumption in critical-IoT applications. Since the IoT devices can have limited power storage capacity, the design of energy-efficient grant-free MAC protocols is indispensable [76].

While communicating over shared radio resources, the availability of knowledge regarding the number of active devices plays a crucial role in optimizing radio resource allocation and to control the congestion efficiently [71, 72]. However, in the absence

of any feedback, the BS lacks the knowledge of the exact cardinality of collisions, i.e., the number of users colliding per channel. In multichannel slotted ALOHA (framed-ALOHA) based systems, the BS can estimate the number of active devices in a frame by using the number of idle channels [71, 103]. However, for heterogeneous networks with dynamically varying parameters, tracking the number of active devices at the BS gets complicated and less accurate under a higher network load.

On the other hand, in order to address the stringent requirements of URLLC for mission-critical IoT applications in heterogeneous networks where network parameters change dynamically, acquiring knowledge of probability distributions associated with these parameters is equally essential [38]. In this regard, statistical learning is a promising tool to learn the network parameters probabilistically in a dynamic environment. Therefore, a statistical learning framework has been proposed in [38] for the physical layer design of URLLC systems. In this framework, the authors considered the limited channel knowledge and model mismatch to design a transmitter that can statistically learn and adapt the transmission rate, such that the desired reliability constraint is met probabilistically. This framework uses two necessary statistical measures for URLLC systems named the average reliability (AR) and the probably correct reliability (PCR). The AR criterion is helpful in a dynamic environment, while the PCR approach is more appropriate for relatively static environments.

The above discussion highlights the fact that supporting mission-critical applications in dynamic heterogeneous networks with a large number of IoT devices is very challenging. This fact motivates us to use the statistical learning paradigm to design such mechanisms where IoT devices can assist the BS in predicting different network parameters and the associated probability distributions.

This chapter considers the MAC layer of the uplink communication interface in heterogeneous networks. A large number of IoT devices communicate with one BS over shared radio resources in a grant-free manner. This uplink communication follows a framed-ALOHA-based restricted transmission strategy. Following are the key contributions and novelty of this chapter:

1. We propose a statistical learning-based device-level network exploration mech-

anism at the MAC layer for delay-sensitive IoT applications. The end-devices are enabled to learn network parameters under a dynamic environment.

2. The proposed mechanism uses the information available at the devices in the history of their previous transmissions and enables the devices to predict different network parameters. Consequently, the end-devices can predict the number of active devices, the probability of collision in each frame, the average number of successful devices per round, and the average behavior of random latency.

3. For the optimal radio resource allocation, the statistical knowledge of dynamic network parameters learned by the end-devices is shared with the BS to identify different IoT groups present in the network. Consequently, the computation burden at the BS is reduced, which can reduce the overall latency offered by the network.

4. Using the mean square error (MSE) criterion, the optimal size of the transmission history window is determined under the given accuracy constraints in predicting different network parameters.

5. The probability of exception is used to measure the robustness of the proposed statistical learning-based device-level network load prediction mechanism. Results show that the proposed mechanism is more robust than the BS-centered approach of [71] under the higher network load.

4.2 System Model

We consider a heterogeneous network composed of $\mathcal{J}$ IoT devices virtually partitioned into $\mathcal{G}$ groups such that each group in the network contains IoT devices with identical latency-reliability requirements. Each group of IoT devices can be part of a particular mission-critical application generating short data packets. The parameter $\mathcal{J}$ is expressed as $\mathcal{J} = \sum_{i=1}^{\mathcal{G}} \jmath^{(i)}$ where $\jmath^{(i)}$ is the number of IoT devices in the i^{th}-group, $\forall i = 1, 2, ..., \mathcal{G}$. The total number of active devices in the network is $M = \sum_{i=1}^{\mathcal{G}} M^{(i)}$, where $M^{(i)} \leq \jmath^{(i)}$ is the number of active devices in the i^{th}-group, $\forall i$. As shown in Figure 4.1, the active devices from different groups communicate

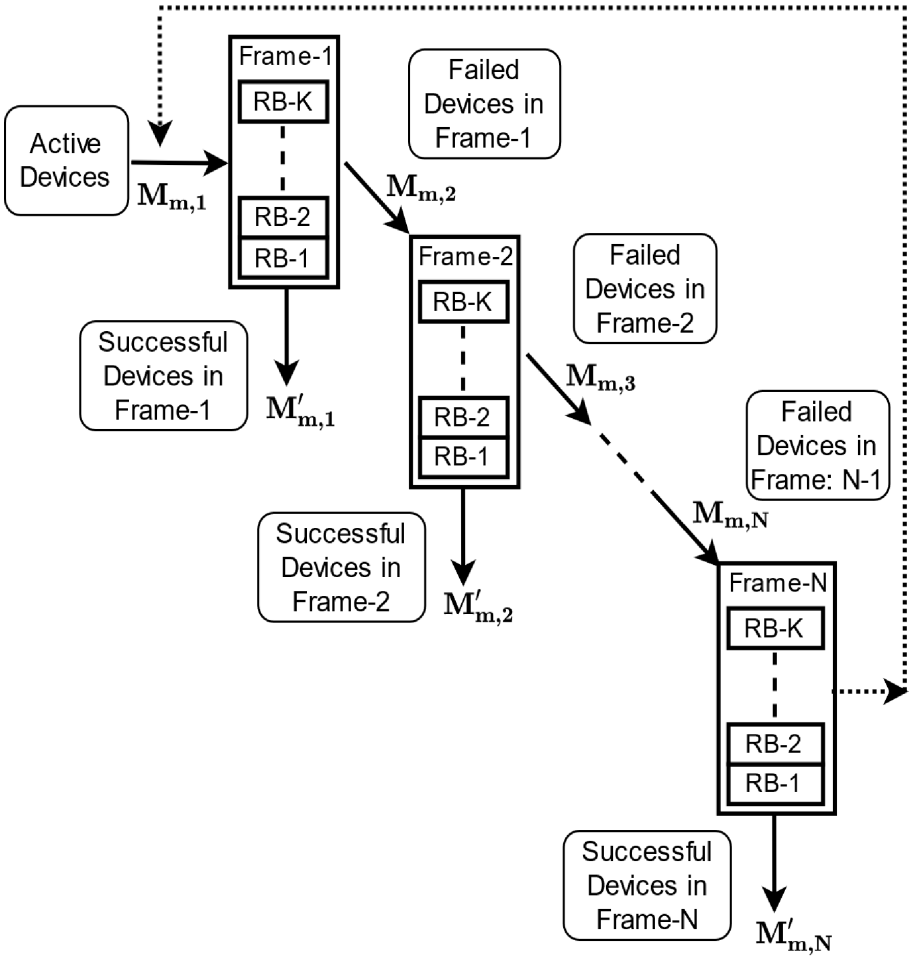

Figure 4.1: Framed-ALOHA-based restricted transmission strategy over N frames in the m^{th} round of an observation interval of R rounds.

over K orthogonal shared resource blocks (RBs) for the transmission of their messages to a single BS in a grant-free manner by employing a framed-ALOHA based restricted transmission policy. In this protocol, each time slot is composed of multiple resource blocks (RB), called a frame, and an RB can be a time, frequency, or code-based resource. In each frame, an active device selects one of the RBs randomly such that the selection is uniform across all the RBs and independent from other active devices. If two or more IoT devices select the same RB, the transmission fails, and the colliding devices attempt again in the next frame. We consider physical layer abstraction to the MAC layer in which transmission fails only because of the collisions. We use the terms RB and channel interchangeably.

All active devices begin to transmit at the start of a round only, which is composed of N-frames, and an observation interval of R independent rounds is considered. Upon successful transmission, the devices receive an acknowledgment from the BS, and

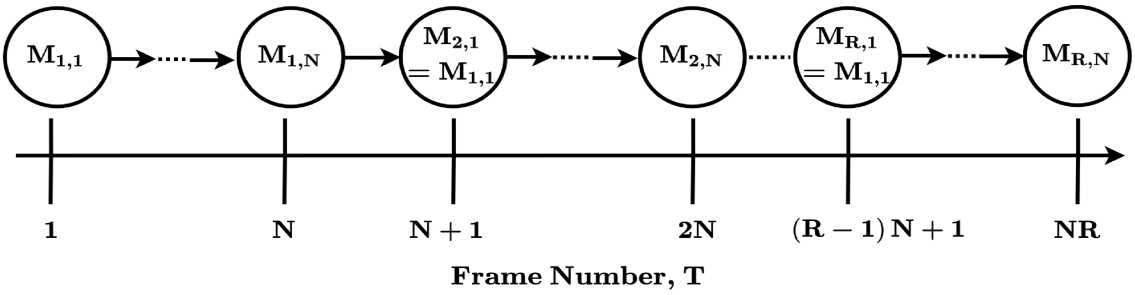

Figure 4.2: Network state: number of active devices in each frame of R rounds.

they stop transmitting in the current round. The restricted transmission strategy helps improve the latency-reliability performance by reducing the collision probability in successive frames of any round. It is assumed that the size of the data packet is the same across all the groups and can be completely transmitted within one frame duration.

The value of parameter M can change from one observation interval to another. The end-devices do not need to know the probability distribution associated with M. The IoT devices capture the status of parameter M regularly in each observation interval and share it with the BS, as explained in the next section. As shown in Figure 4.2, the time index T representing the frame number can be expressed as a function of the round number (m), and the frame number (n) as: $T = (m-1)\,N + n$, where $m = 1, 2, ..., R$ and $n = 1, 2, ..., N$. Figure 4.2 shows the network state in terms of the number of transmitting devices in each frame of the history window. While, the number of transmitting devices in each frame of the m^{th} round is defined as

$$M_{m,n} = \begin{cases} M, & n = 1; \\ M - \sum_{j=1}^{n-1} M'_{m,j}, & n = 2, 3, ..., N. \end{cases} \tag{4.1}$$

where $M'_{m,n}$ denotes the number of successful devices in the n^{th} frame of the m^{th} round. Due to the restricted transmission strategy in each round, we have $M_{m,1} \geq M_{m,2} \geq, ..., \geq M_{m,N} \geq 0,\ \forall m$, and $M_{m,1} = M,\ \forall m$. The number of transmitting devices in a frame depends upon the number of transmitting and successful devices in the previous frame. Thus, two situations can arise: for the first case in which $M_{m,n-1} > K$, we have $(M_{m,n-1} - K) < M_{m,n} \leq M_{m,n-1}$, and in the second case when $M_{m,n-1} \leq K$, we get $0 \leq M_{m,n} \leq M_{m,n-1}$.

The latency-reliability requirements of the V2I communication interface can be different from other IoT devices present in the network. The number of active devices also changes when vehicular IoT entities leave or exit the coverage area of a serving BS. Therefore, the proposed framed-ALOHA-based grant-free network access is suitable for the V2I communication scenario in which vehicular IoT entities communicate with a common BS over shared radio resources under a dynamic network load. Moreover, the proposed grant-free access with a restricted transmission strategy helps end-devices reduce their energy consumption. This is because after having a successful transmission, the corresponding devices stop transmitting in the current round.

Due to the time-varying nature of the number of transmitting devices, it becomes challenging to assess the feasibility of running a particular mission-critical application in heterogeneous networks, and acquiring the statistical knowledge of the network dynamics becomes essential. The following section demonstrates how the end-devices can explore the network to learn different network parameters at the MAC layer.

4.3 Device-Level Network Exploration

In this section, we present a statistical learning-based procedure to explore the network at the device-level. The number of successful devices in each round $S_m = \sum_{n=1}^{N} M'_{m,n}$, is a random quantity, as a statistical measure, we are interested in getting the knowledge of average successful devices per round at the device-level which is defined as

$$S_{av} := \frac{1}{R} \sum_{m=1}^{R} \sum_{n=1}^{N} M'_{m,n}. \tag{4.2}$$

A related parameter is the probability of success per round (P_{s_m}) derived in the Subsection 4.3.1, and it depends on the number of transmitting devices in each frame of the given round. There can be possibly different patterns of the number of active devices in each round; the quantity P_{s_m} can vary from round to round. Thus, acquiring the average behaviour of P_{s_m} denoted by P_s is essential for network

Algorithm 1 Device-Level Network Exploration

Require: K, N and R
Ensure: $\widehat{\mathbf{\Theta}}$, $\widehat{P}_s$, $\widehat{S}_{av}$, $\widehat{\mu}_L$ and $R^{(i)}$

for $m = 1$ to R **do**
  for $n = 1$ to N **do**
    Select a channel randomly
    Transmit data
    if (success) **then**
      $A_{m,n} := 0$
      Stop transmitting in current round
      $h_{m,j} := -1;\ \forall j = n+1, n+2, ..., N$
    else
      $A_{m,n} := 1$
    end if
  end for
end for
Predict $\widehat{\mathbf{\Theta}} = \left[\widehat{M_1}, \widehat{M_2}, ..., \widehat{M_N}\right]$ from (4.16)
Predict $\widehat{S}_{av}$ from (4.20)
Predict $\widehat{P}_s$ from (4.23)
Predict $R^{(i)}$ from (4.24)
Predict $\widehat{\mu}_L$ from (4.30)
Share learned parameters $\widehat{\mathbf{\Theta}}$ and $R^{(i)}$ with the BS
Get the optimal $\widehat{R}$ from the BS
Update number of rounds $R := \widehat{R}$

exploration.

The third important parameter is the latency offered by the network. In this chapter, we focus on the random component of the latency (L) experienced by a data packet due to the retransmissions and its average behavior denoted by μ_L. For mission-critical-IoT applications, a statistical reliability constraint can be defined as: $\Pr\left(L \leq L_{max}^{(i)}\right) \geq 1 - \epsilon_r^{(i)}$, where $\epsilon_r^{(i)}$ and $L_{max}^{(i)}$ are the group-specific reliability criterion and maximum affordable latency, respectively. Under the given values of K and N, each group requires a minimum number of rounds $R^{(i)}, \forall i$ within which it can meet the desired reliability constraint probabilistically. This fourth parameter $R^{(i)}, \forall i$ is also learned dynamically at the device-level and, the end-devices share their knowledge with the BS, which can identify the number of groups present in the network. In summary, we aim to enable the end-devices to predict four important network parameters $\left(S_{av}, P_s, \mu_L, R^{(i)}\right)$ so that the BS can utilize their knowledge for the better utilization of the available resources.

4.3.1 Device-level prediction of P_s and S_{av}

The only information provided to the IoT devices is the number of channels (K) in each frame and the size (N) of a round. The number of transmitting devices ($M_{m,n}$) in each frame of a round is not known by the BS and the IoT devices a-prior. In order to explore the network, each device keeps the record of transmission outcomes from last R rounds. When a device of interest performs a transmission in the n^{th} frame of the m^{th} round, a Bernoulli random variable $A_{m,n}$ is used to show outcome of the transmission as follows:

$$A_{m,n} = \begin{cases} 1, & \text{Collision with other device/s;} \\ 0, & \text{Successful transmission.} \end{cases} \tag{4.3}$$

The probability that a device of interest will have a collision with at least one of the other transmitting devices in the n^{th} frame of the m^{th} round, is computed as

$$\begin{aligned} \alpha_{m,n} &:= \Pr\left(A_{m,n} = 1\right), \\ &= 1 - \left(1 - \frac{1}{K}\right)^{M_{m,n}-1}. \end{aligned} \tag{4.4}$$

The probability of a successful transmission is computed as

$$\Pr\left(A_{m,n} = 0\right) := 1 - \alpha_{m,n}. \tag{4.5}$$

After having a successful transmission, the corresponding devices wait until the next round. The successful devices can use any arbitrary value other than 0 and 1 to keep the history of the frames in which these devices do not perform any transmission. In this work, devices use -1 in case of no transmission. Thus, each element $h_{m,n}$ in the history matrix $\mathbf{H}$ is defined as follows:

$$h_{m,n} = \begin{cases} A_{m,n}, & \text{Grant-free transmission;} \\ -1, & \text{No transmission.} \end{cases} \tag{4.6}$$

Once a device has built its history of R rounds, it can predict different network parameters as explained below.

As shown in Figure 4.1, all the active devices start transmitting at the beginning

of a round, and each device can have only one successful transmission in a round. So, the probability that a device of interest remains successful in the m^{th} round is computed as

$$\begin{aligned} P_{s_m} &:= \sum_{n=1}^{N} (1-\alpha_{m,n}) \prod_{\substack{j=1 \\ n>1}}^{n-1} \alpha_{m,j} \ , \\ &= (1-\alpha_{m,1}) + (1-\alpha_{m,2})\,\alpha_{m,1} + ... + (1-\alpha_{m,N})\,\alpha_{m,1}\alpha_{m,2}...\alpha_{m,N-1} \ , \\ &= 1 - \alpha_{m,1} + \alpha_{m,1} - \alpha_{m,1}\alpha_{m,2} + \alpha_{m,1}\alpha_{m,2} + ... - \alpha_{m,1}\alpha_{m,2}...\alpha_{m,N-1}\alpha_{m,N}. \end{aligned} \tag{4.7}$$

All the terms except first and last terms of (4.7), are cancelled out and (4.7) is reduced to

$$P_{s_m} = 1 - \prod_{n=1}^{N} \alpha_{m,n}. \tag{4.8}$$

Thus P_{s_m} can be computed by applying (4.4) in (4.8) and it gets the following form:

$$P_{s_m} = 1 - \prod_{n=1}^{N} \left\{ 1 - \left(1 - \frac{1}{K} \right)^{M_{m,n}-1} \right\}. \tag{4.9}$$

As indicated in (4.9), for the given values of K and N, the computation of P_{s_m} at device-level requires knowledge of the number of transmitting devices ($M_{m,n}$) in each frame of a round, and this information is not available at the end-devices directly. Although, the number of active devices ($M_{1,m}$) at the start of a round is assumed to remain constant for a given observation interval, but the number of transmitting devices in the successive frames decreases randomly, and the collision probability varies accordingly. Thus, we have: $0 \leq \alpha_{m,N} \leq \alpha_{m,N-1} \leq, ..., \leq \alpha_{m,1} < 1, \ \forall m$. Consequently, the probability of a successful transmission P_{s_m}, can vary in different rounds. So, as a statistical measure of P_{s_m}, we aim to predict the average probability of success P_s in the given observation interval defined as

$$P_s := \frac{1}{R} \sum_{m=1}^{R} P_{s_m}. \tag{4.10}$$

By using (4.9) in (4.10), P_s gets the following form:

$$P_s = \frac{1}{R}\sum_{m=1}^{R}\left[1 - \prod_{n=1}^{N}\left\{1 - \left(1 - \frac{1}{K}\right)^{M_{m,n}-1}\right\}\right]. \tag{4.11}$$

The IoT devices can predict the quantities S_{av} and P_s by first predicting the number of transmitting devices in each frame. For that purpose, we define a parameter vector $\widehat{\mathbf{\Theta}} = \left[\widehat{M}_1, \widehat{M}_2, ..., \widehat{M}_N\right]$, where $\widehat{M}_n$ is the prediction of $M_{m,n}, \forall m$, and accordingly $\widehat{\alpha}_n$ is the prediction of $\alpha_{m,n}, \forall m$. We consider the case where the number of transmitting devices in a given frame of all rounds represents a wide-sense stationary process, and the number of transmitting devices in the n^{th} frame can be predicted as $\mathrm{E}[M_{m,n}]$, and the corresponding collision probability is predicted as $\mathrm{E}[\alpha_{m,n}]$. However, due to the random nature of the number of failures in each frame, the system can have huge number of states, and the computation of $\mathrm{E}[M_{m,n}]$ and $\mathrm{E}[\alpha_{m,n}]$ becomes cumbersome for $n > 1$.

In this chapter, we enable the end-devices to predict the desired quantities S_{av} and P_s statistically from the transmissions history matrix $\mathbf{H}$ which involves the prediction of the number of transmitting devices and the associated collision probability in each frame. The proposed prediction method uses the fact that all elements in the first column of $\mathbf{H}$ are independent and identically distributed (IID) random variables, and the maximum likelihood (ML) estimator of $\alpha_{1,m}, \forall m$ is given as [104]:

$$\widehat{\alpha}_1 = \frac{1}{R}\sum_{m=1}^{R} A_{m,1}. \tag{4.12}$$

Moreover, we can readily show that $\widehat{\alpha}_1$ is an unbiased estimator of $\alpha_{m,1},\ \forall m$, i.e., $\mathrm{E}[\widehat{\alpha}_1] = \alpha_{m,1},\ \forall m$. We can determine $\widehat{M}_1$ by applying $\widehat{\alpha}_1$ in (4.4) and it comes out to be

$$\begin{aligned}\widehat{M}_1 &= 1 + \frac{\ln(1-\widehat{\alpha}_1)}{\ln\left(\frac{K-1}{K}\right)}, \\ &= 1 + \frac{\ln\left(1 - \frac{1}{R}\sum_{m=1}^{R} A_{m,1}\right)}{\ln\left(\frac{K-1}{K}\right)}.\end{aligned} \tag{4.13}$$

When R is large, $\widehat{\alpha}_1$ approaches to $\alpha_{m,1},\ \forall m$, and as a result $\widehat{M}_1$ approaches

$M_{m,1},\ \forall m$. Thus, for the given round size, accuracy in the prediction of $M_{m,1}$ can be enhanced by using an appropriate value of R. Since the failed devices from the current frame transmit in the next frame of a given round, we use the average number of failures from the current frame as a prediction of the number of transmitting devices in the next frame:

$$\begin{aligned}\widehat{M}_n &= \widehat{M}_{n-1}\widehat{\alpha}_{n-1}, \quad n = 2, 3, ..., N \\ &= \widehat{M}_1 \prod_{j=1}^{n-1} \widehat{\alpha}_j. \end{aligned} \tag{4.14}$$

The corresponding average collision probability in each frame for $n > 1$ is predicted as

$$\widehat{\alpha}_n = 1 - \left(1 - \frac{1}{K}\right)^{\widehat{M}_n - 1};\ n = 2, 3, ..., N. \tag{4.15}$$

Thus, the overall process to predict $\widehat{\mathbf{\Theta}}$ at the device-level is described as follows:

$$\widehat{M}_n = \begin{cases} 1 + \frac{\ln\left(1 - \frac{1}{R}\sum_{m=1}^{R} A_{m,1}\right)}{\ln\left(\frac{K-1}{K}\right)}, & n = 1; \\ \\ \left[1 + \frac{\ln\left(1 - \frac{1}{R}\sum_{m=1}^{R} A_{m,1}\right)}{\ln\left(\frac{K-1}{K}\right)}\right] \prod_{j=1}^{n-1} \widehat{\alpha}_j, & \\ \qquad\qquad\qquad\qquad n = 2, 3, ..., N. \end{cases} \tag{4.16}$$

where

$$\widehat{\alpha}_n = \begin{cases} \frac{1}{R}\sum_{m=1}^{R} A_{m,1}, & n = 1; \\ \\ 1 - \left(1 - \frac{1}{K}\right)^{\widehat{M}_n - 1}, & n = 2, 3, ..., N. \end{cases} \tag{4.17}$$

The average number of successful devices in the n^{th}-frame can be predicted as

$\widehat{M}_n\,(1-\widehat{\alpha}_n)$, thus S_{av} is predicted as

$$\begin{aligned}
\widehat{S}_{av} &:= \sum_{n=1}^{N} \widehat{M}_n\,(1-\widehat{\alpha}_n)\,, \\
&= \widehat{M}_1\,(1-\widehat{\alpha}_1) + \widehat{M}_1\widehat{\alpha}_1\,(1-\widehat{\alpha}_2) + \widehat{M}_1\widehat{\alpha}_1\widehat{\alpha}_2\,(1-\widehat{\alpha}_3) + ... + \widehat{M}_1\widehat{\alpha}_1\widehat{\alpha}_2...\widehat{\alpha}_{N-1}\,(1-\widehat{\alpha}_N)\,, \\
&= \widehat{M}_1\,(1-\widehat{\alpha}_1+\widehat{\alpha}_1-\widehat{\alpha}_1\widehat{\alpha}_2+\widehat{\alpha}_1\widehat{\alpha}_2-\widehat{\alpha}_1\widehat{\alpha}_2\widehat{\alpha}_3+...+\widehat{\alpha}_1\widehat{\alpha}_2...\widehat{\alpha}_{N-1}-\widehat{\alpha}_1\widehat{\alpha}_2...\widehat{\alpha}_{N-1}\widehat{\alpha}_N)\,.
\end{aligned} \tag{4.18}$$

All the terms except first and last terms inside the parenthesis are cancelled out, and (4.18) is reduced to

$$\widehat{S}_{av} = \widehat{M}_1\left(1-\prod_{n=1}^{N}\widehat{\alpha}_n\right). \tag{4.19}$$

By using (4.17) in (4.19), $\widehat{S}_{av}$ can be computed as

$$\widehat{S}_{av} = \widehat{M}_1\left[1-\prod_{n=1}^{N}\left\{1-\left(1-\frac{1}{K}\right)^{\widehat{M}_n-1}\right\}\right]. \tag{4.20}$$

We can compute $\widehat{P}_s$ as the prediction of P_s as follows:

$$\begin{aligned}
\widehat{P}_s &:= \sum_{n=1}^{N}(1-\widehat{\alpha}_n)\prod_{\substack{j=1\\ n>1}}^{n-1}\widehat{\alpha}_j, \\
&= (1-\widehat{\alpha}_1) + (1-\widehat{\alpha}_2)\,\widehat{\alpha}_1 + ... + (1-\widehat{\alpha}_N)\,\widehat{\alpha}_1\widehat{\alpha}_2...\widehat{\alpha}_{N-1}, \\
&= 1-\widehat{\alpha}_1+\widehat{\alpha}_1-\widehat{\alpha}_2\widehat{\alpha}_2+\widehat{\alpha}_1\widehat{\alpha}_2+...-\widehat{\alpha}_1\widehat{\alpha}_2...\widehat{\alpha}_{N-1}\widehat{\alpha}_N.
\end{aligned} \tag{4.21}$$

All the terms except first and last terms of (4.21) are cancelled out, and (4.21) is reduced to

$$\widehat{P}_s = 1-\prod_{n=1}^{N}\widehat{\alpha}_n. \tag{4.22}$$

Thus $\widehat{P}_s$ can be computed by applying (4.4) in (4.22) and it gets the following form:

$$\widehat{P}_s = 1-\prod_{n=1}^{N}\left\{1-\left(1-\frac{1}{K}\right)^{\widehat{M}_n-1}\right\}. \tag{4.23}$$

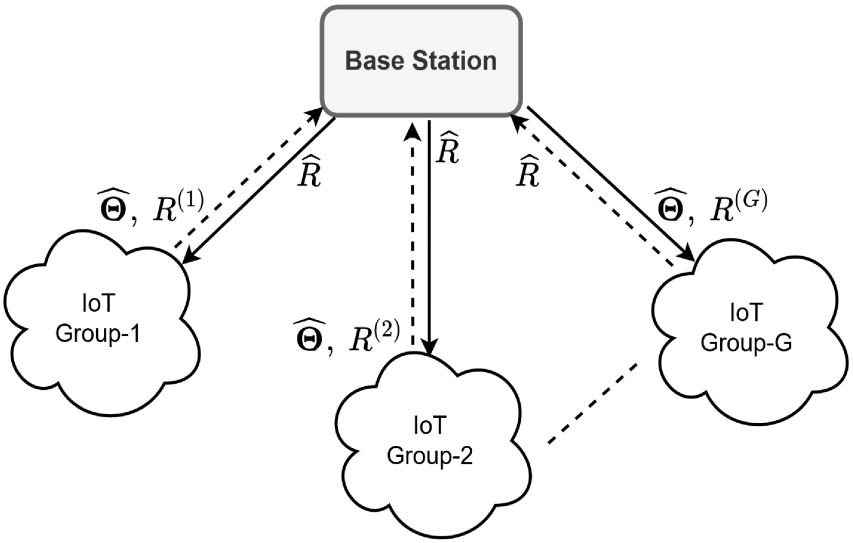

Figure 4.3: Identification of different IoT groups at the BS.

We can see through (4.20) and (4.23) that both parameters $\widehat{S}_{av}$ and $\widehat{P}_s$ are functions of the predicted number of transmitting devices in each frame i.e., the vector $\widehat{\mathbf{\Theta}}$. It is worth noting that the end-devices can predict $\widehat{\mathbf{\Theta}}$, $\widehat{P}_s$ and $\widehat{S}_{av}$ by employing a statistical learning approach that uses the outcomes of their previous transmissions. The end-devices share the predicted network load with the BS as shown in Figure 4.3, which can utilize this knowledge to optimize the radio resource allocation. Moreover, the computation burden at the BS is reduced by allowing the end-devices to predict the network load, which can result in overall latency reduction. This device-level network exploration strategy does not require any additional assistance from the BS except the values of N and K. Thus, we can use these features to design self-configuring networks where network parameters change dynamically.

4.3.2 IoT-groups identification

For URLLC based systems, the reliability is defined as the probability of satisfying a latency bound in a given network [1]. The heterogeneous IoT devices present in a network can be grouped virtually based upon their application specific statistical reliability constraints. This grouping of IoT devices can assist the BS to optimize the radio resource allocation in conditions where network parameters change dynamically. The mobile vehicular IoT entities belong to the same group as long as their latency-reliability requirements do not change and remain in the serving BS's coverage area. However, if they leave the coverage area, the total number of active

devices changes, leading to changes in the resources required by different groups to meet their application-specific QoS requirements.

For the system model under consideration, we develop a statistical learning based strategy to identify different groups at the BS. This scheme involves the device level prediction of the number of rounds required to have a successful transmission such that desired statistical reliability constraint is satisfied. Each device shares this statistical knowledge with the BS which can identify the number groups and their latency-reliability constraints.

Our problem of identifying different groups at the BS reduces to predict the vector parameter $\widehat{\mathbf{\Theta}}$ and $\widehat{P}_s$ at device-level. After predicting $\widehat{\mathbf{\Theta}}$ and $\widehat{P}_s$ the end-devices can compute the optimal number of rounds needed for a successful transmission against their group-specific reliability criterion $\epsilon_r^{(i)}, \forall i = 1, 2, ..., \mathcal{G}$. In order to do that, we let the random variable X indicate the number of rounds that a device from group-i executes to get its first successful transmission, i.e., the device remains unsuccessful in $X-1$ consecutive rounds before getting a successful transmission in the round number X. The random variable X follows the geometric distribution. Under the group-specific reliability constrain $\epsilon_r^{(i)}$, the optimal value of X can be predicted as follows:

$$R^{(i)} = \inf_{X} \left\{ 1 \leq X \leq R_{max}^{(i)} : \widehat{P}_s \sum_{x=1}^{X} \left(1 - \widehat{P}_s\right)^{x-1} \geq 1 - \epsilon_r^{(i)} \right\}. \tag{4.24}$$

where $R_{max}^{(i)}$ is related to the group specific maximum affordable latency. The value of $R_{max}^{(i)}$ depends upon the nature of the environment in which communication is being carried out. If a device could not find an appropriate value of $R^{(i)}$ from (4.24), this indicates that the current environment cannot support the particular mission-critical communication application and the event is termed as an outage. Since the IoT devices can predict the outage event; therefore we can design an intelligent back-off mechanism which is part of our future research work.

As shown in Figure 4.3, each device shares the locally learned value of $R^{(i)}$ with the BS, which uses this information to identify different groups present in the network and also their latency-reliability requirements. In addition to that, the BS can

determine the number of successful devices from each group. The BS can utilize the information shared by the IoT devices to optimize the radio resource allocation based upon the latency-reliability criteria of different groups in the network. Moreover, as explained in Subsection 4.4.2, the BS uses the information of the number of active devices to determine the optimal value of R such that the end-devices can predict different network parameters under desired prediction accuracy constraints.

4.3.3 Device-Level prediction of average latency

When the number of active devices vary dynamically, the random component of latency causes significant variations in the overall latency offered by the network. For example, in V2X communication scenarios, the mobile vehicles can cause random variations in the network latency. So, it becomes very essential for the heterogeneous devices to evaluate the feasibility of executing a particular mission-critical application in a dynamic environment. Acquiring the statistical knowledge of the random latency can be very useful in this regard. The average number of retransmissions performed by a device for a successful transmission is a measure of the average latency (μ_L), and we devise a statistical learning method to acquire knowledge of μ_L at the end-devices.

In order to have an analytical model for the prediction of average latency, which can be used at the device-level, let the random variable Y show the number of rounds a device remained failed before a successful transmission. Since we assume that the number of active devices at the start of each round remains fixed for the given observation interval, this makes all rounds independent of each other with a constant average probability of success per round predicted as $\widehat{P}_s$. Thus, the random variable Y follows the geometric distribution, and the expected value of Y is computed as: $\mathrm{E}[Y] = \frac{1-\widehat{P}_s}{\widehat{P}_s}$. By applying (4.23), the $\mathrm{E}[Y]$ comes out to be

$$\mathrm{E}[Y] = \frac{\prod_{n=1}^{N} \widehat{\alpha}_n}{1 - \prod_{n=1}^{N} \widehat{\alpha}_n}. \tag{4.25}$$

Now given that a device of interest remains successful in the round followed by the Y failed rounds, let the random variable Z denote the number of retransmissions

performed for the successful transmission in that round. Since the probability of collision varies in each frame of a round, the random variable Z follows a truncated geometric distribution with a variable probability of success in each frame. The probability mass function (PMF) of the random variable Z is defined as

$$\Pr(Z=z) = \begin{cases} \dfrac{1}{1-\prod_{n=1}^{N}\widehat{\alpha}_n}\,(1-\widehat{\alpha}_z)\prod\limits_{\substack{j=1\\ z>1}}^{z-1}\widehat{\alpha}_j, & z=1,2,...,N; \\ 0, & \text{Otherwise.} \end{cases} \tag{4.26}$$

We can readily show that $\sum_{z=1}^{N}\Pr(Z=z)=1$. While $\mathrm{E}[Z]$ is computed as

$$\begin{aligned} \mathrm{E}[Z] &:= \sum_{z=1}^{N} z\Pr(Z=z), \\ &= \frac{1}{1-\prod_{n=1}^{N}\widehat{\alpha}_n}\sum_{z=1}^{N} z\,(1-\widehat{\alpha}_z)\prod_{\substack{j=1\\ z>1}}^{z-1}\widehat{\alpha}_z\ , \\ &= \frac{1}{1-\prod_{n=1}^{N}\widehat{\alpha}_n}\left[1-\widehat{\alpha}_1+...+N\,(1-\widehat{\alpha}_N)\prod_{j=1}^{N-1}\widehat{\alpha}_j\right]. \end{aligned} \tag{4.27}$$

(4.27) is reduced to

$$\mathrm{E}[Z] = \frac{1}{1-\prod_{n=1}^{N}\widehat{\alpha}_n}\left(1+\sum_{\substack{z=1\\ N>1}}^{N-1}\prod_{j=1}^{z}\widehat{\alpha}_j - N\prod_{j=1}^{N}\widehat{\alpha}_j\right). \tag{4.28}$$

Thus, the average latency in terms of the number of retransmissions per successful transmission can be predicted as follows:

$$\widehat{\mu}_L := N\,\mathrm{E}[Y] + \mathrm{E}[Z]. \tag{4.29}$$

By using (4.25) and (4.28) in (4.29), we get following expression of $\widehat{\mu}_L$:

$$\widehat{\mu}_L = \frac{1}{1-\prod_{n=1}^{N}\widehat{\alpha}_n}\left(1+\sum_{\substack{z=1\\ N>1}}^{N-1}\prod_{j=1}^{z}\widehat{\alpha}_j\right). \tag{4.30}$$

We can see through (4.30) that the end-devices are enabled to predict average la-

tency present in the network by using the prediction of collision probability in each frame of a round. On the other hand, as shown in (4.17), the computation of collision probability in each frame requires the availability of knowledge regarding the number of transmitting devices which is computed through (4.16). For the system model under consideration, the average latency per successful transmission is upper bounded by $\frac{N}{\widehat{P}_s}$, i.e., $\widehat{\mu}_L \leq \frac{N}{\widehat{P}_s}$.

Remarks: An interesting insight of the PMF given in (4.26) is that the truncated geometric distribution presented in [105] can be obtained directly from (4.26) as a special case when collision probability remains constant in each frame. It is also worth noting that when $N = 1$, (4.30) provides the expectation of a geometric random variable that shows the expected number of retransmissions performed for a successful transmission under constant collision probability, and the optimal number of retransmissions under the given latency-reliability constraint is presented in [104]. Thus, the PMF in (4.26) can be useful in analyzing networks in which the probability of collision varies as a result of the variable number of transmitting devices.

Algorithm 1 describes the steps of the proposed device-level network exploration mechanism, and each active device runs the algorithm every R rounds. The BS periodically broadcasts the values of K, N, and R to be used by the end-devices as the inputs for Algorithm 1. Initially, the BS broadcasts an initial value of R to explore the network. As explained in Subsection 4.4.3, the initial value of R is selected such that the probability of exception in the network load prediction remains negligibly small for relatively low to high network load. After executing R rounds of the restricted grant free transmissions as shown in Figure 4.1, the active devices predict $\widehat{\mathbf{\Theta}}$, S_{av}, P_s, $R^{(i)}$ and μ_L. The devices share their knowledge of the current network load with the BS, as shown in Figure 4.3. For a given network load, the BS broadcasts the optimal value of R, which is computed according to the desired prediction accuracy constraints, as explained in Subsection 4.4.2. Thus after every R rounds, the end-devices update their knowledge of network conditions by capturing the current network load, and the status of different QoS metrics.

4.4 Performance Analysis and Comparison

In this section we discuss the performance of the proposed statistical learning-based device-level network exploration mechanism. Since, for the given values of K and N, the only information available at the end-devices is the history of their transmissions, the performance of the proposed prediction mechanisms under the given network load is affected by the size of the history window. The value of R is also related to the amount of time required by the end-devices to learn different network parameters. So, in order to analyze the performance of the device-level network exploration, we evaluate the MSE associated with the prediction of the parameters S_{av}, P_s, and μ_L denoted by MSE_S, MSE_P, and MSE_μ respectively.

The MSE in the prediction of S_{av} is computed as follows:

$$\text{MSE}_S = \text{E}\left[\left\{S_{av} - \widehat{S}_{av}\right\}^2 \mid \mathbf{H}\right]. \tag{4.31}$$

Expectation is taken with respect to S_{av} defined in (4.2). By using (4.2) and (4.20), in (4.31), the MSE_S can be computed as

$$\text{MSE}_S = \text{E}\left[\left\{\frac{1}{R}\sum_{m=1}^{R}\sum_{n=1}^{N} M'_{m,n} - \widehat{M}_1 + \widehat{M}_1 \prod_{n=1}^{N}\left\{1 - \left(1 - \frac{1}{K}\right)^{\widehat{M}_n - 1}\right\}\right\}^2\right]. \tag{4.32}$$

The MSE in the prediction of average probability of success per round is given as

$$\text{MSE}_P = \text{E}\left[\left\{P_s - \widehat{P}_s\right\}^2 \mid \mathbf{H}\right]. \tag{4.33}$$

Expectation is taken with respect to P_s defined in (4.11). By using (4.11) and (4.23) in (4.33), the MSE_P can also be written as

$$\text{MSE}_P = \text{E}\left[\left\{-\frac{1}{R}\sum_{m=1}^{R}\prod_{n=1}^{N}\left\{1 - \left(1 - \frac{1}{K}\right)^{M_{m,n}-1}\right\} + \prod_{n=1}^{N}\left\{1 - \left(1 - \frac{1}{K}\right)^{\widehat{M}_n - 1}\right\}\right\}^2\right]. \tag{4.34}$$

The MSE in the prediction of average latency is given as

$$\mathrm{MSE}_{\mu} = \mathrm{E}\left[\{\mu_L - \widehat{\mu}_L\}^2 \mid \mathbf{H}\right]. \tag{4.35}$$

Expectation is taken with respect to μ_L defined in (4.37). In order to define μ_L, we use the average collision probability in each frame for the given observation interval defined as

$$\alpha_n := \frac{1}{R}\sum_{m=1}^{R}\alpha_{m,n}. \tag{4.36}$$

By using (4.4) in (4.36), and replacing $\widehat{\alpha}_n$ in (4.30) with the resultant expression of α_n, we get the following expression for μ_L:

$$\mu_L := \frac{1 + \sum\limits_{\substack{z=1\\N>1}}^{N-1}\left[\prod\limits_{j=1}^{z}\frac{1}{R}\sum\limits_{m=1}^{R}\left\{1-\left(1-\frac{1}{K}\right)^{M_{m,j}-1}\right\}\right]}{1-\prod\limits_{n=1}^{N}\frac{1}{R}\sum\limits_{m=1}^{R}\left\{1-\left(1-\frac{1}{K}\right)^{M_{m,n}-1}\right\}}. \tag{4.37}$$

By applying (4.37) and (4.30) in (4.35), the MSE_{μ} gets the following form:

$$\mathrm{MSE}_{\mu} = \mathrm{E}\left[\left\{\frac{1 + \sum\limits_{\substack{z=1\\N>1}}^{N-1}\left[\prod\limits_{j=1}^{z}\frac{1}{R}\sum\limits_{m=1}^{R}\left\{1-\left(1-\frac{1}{K}\right)^{M_{m,j}-1}\right\}\right]}{1-\prod\limits_{n=1}^{N}\frac{1}{R}\sum\limits_{m=1}^{R}\left\{1-\left(1-\frac{1}{K}\right)^{M_{m,n}-1}\right\}} - \frac{1 + \sum\limits_{\substack{z=1\\N>1}}^{N-1}\prod\limits_{j=1}^{z}\left\{1-\left(1-\frac{1}{K}\right)^{\widehat{M}_n-1}\right\}}{1-\prod\limits_{n=1}^{N}\left\{1-\left(1-\frac{1}{K}\right)^{\widehat{M}_n-1}\right\}}\right\}^2\right]. \tag{4.38}$$

Due to the random nature of $M_{m,n}$ and $M'_{m,n}$ in each frame of the history window, it gets complicated to obtain the closed-form expressions of MSEs through Eqs. (4.32), (4.34) and (4.38). In this chapter, we compute them numerically by using the Monte Carlo simulation method.

4.4.1 Simulation results

The Monte Carlo simulation method is used to analyze the performance of the proposed mechanisms for device-level network exploration. First, we analyze the behaviour of different network parameters against varying network load. For different values of N and K, we take a range of the number of active devices and use $R = 10,000$ number of independent rounds for the averaging purpose. The average number of successful devices per round defined in (4.2) is plotted in Figure 4.4. The average probability of success per round is computed according to (4.10) and plotted in Figure 4.5. It is observed that for lower values of M, the parameter P_s does not change much, and consequently, S_{av} increases. However, for the higher values of M, the parameter P_s decreases and S_{av} decreases accordingly. The average number of retransmissions for a successful transmission is presented in Figure 4.6, where we can see that the parameter μ_L increases slowly under the smaller values of M, and rapidly under the larger values of M.

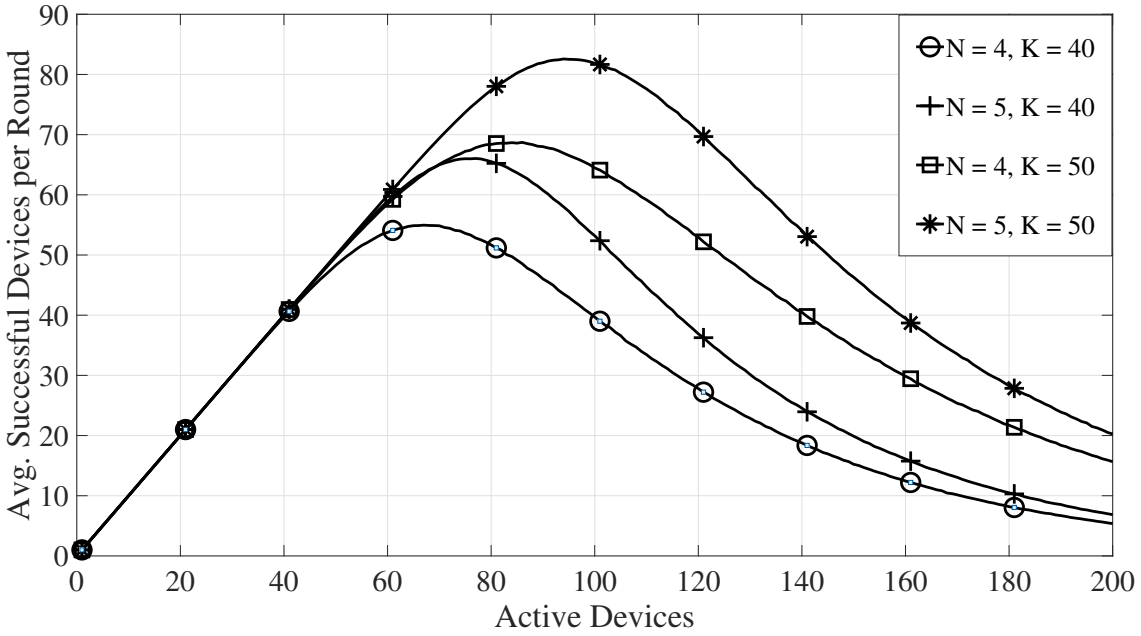

Figure 4.4: Average successful devices per round with different values of K and N against active devices.

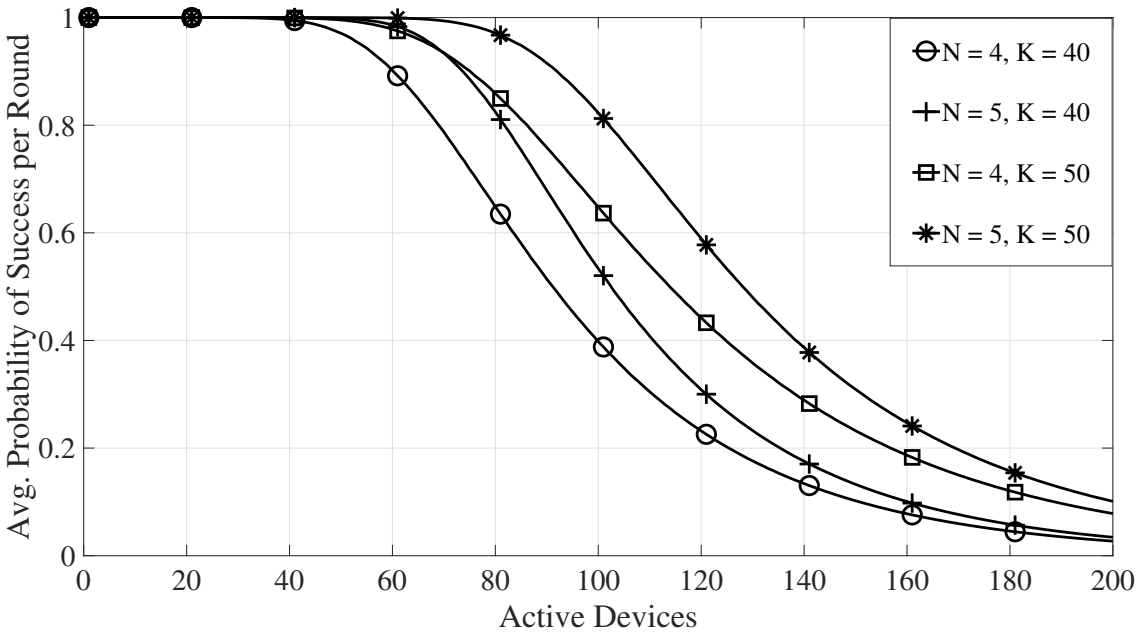

Figure 4.5: Average probability of success per round with different values of K and N against active devices.

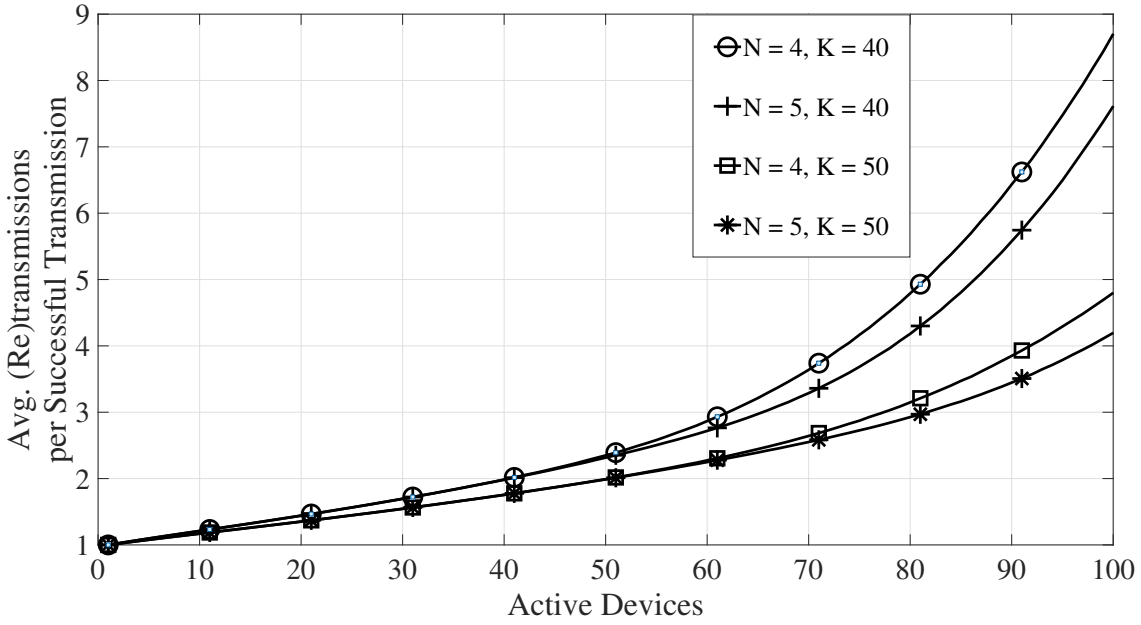

Figure 4.6: Average retransmissions per successful transmission with different values of K and N against active devices.

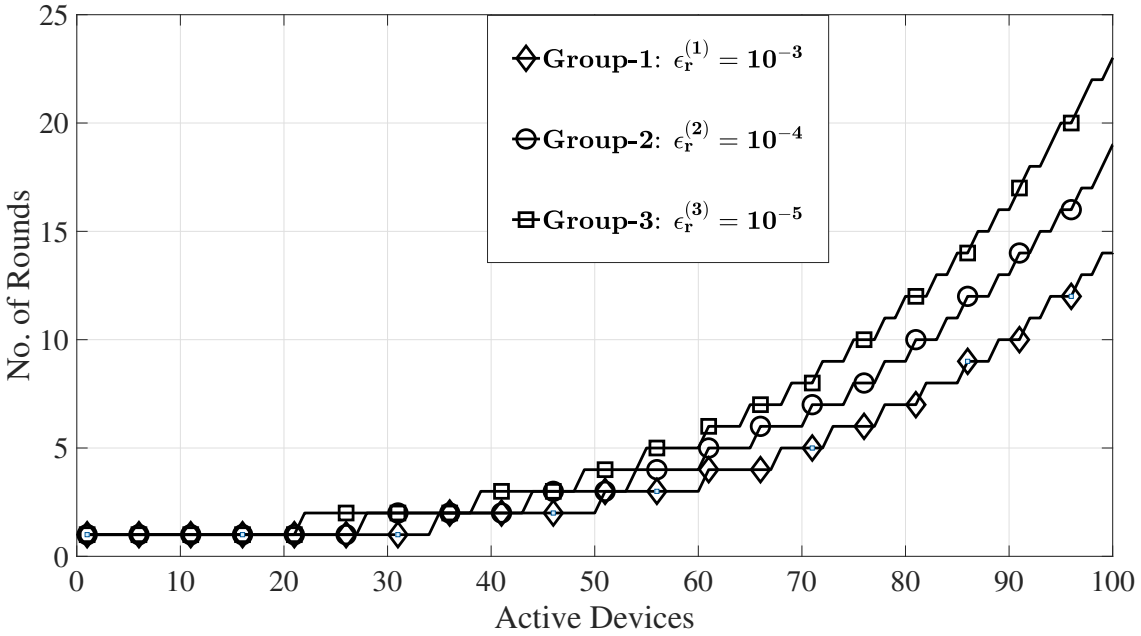

Figure 4.7: No. of rounds required to meet the desired reliability with $K = 40$ and $N = 4$.

For IoT groups identification, three groups are considered with the respective reliability criterion $\epsilon_r^{(1)} = 10^{-3}$, $\epsilon_r^{(2)} = 10^{-4}$, and $\epsilon_r^{(3)} = 10^{-5}$. The optimal number of rounds required by these three different IoT groups to meet the required latency-reliability criteria are plotted in Figure 4.7. It is observed that for the lower number of active devices at the start of each round, due to the discrete nature of the parameter R, different groups can have the same optimal number of rounds against their latency-reliability requirements. However, as the probability of success decreases as a result of an increase in the number of active devices, different groups start attaining distinct values of $R^{(i)}$.

The end-devices are enabled to predict different network parameters as explained in Section 4.3. In order to analyse MSE_S, MSE_P, and MSE_μ, associated with prediction of S_{av}, P_s, and μ_L, respectively, simulations are performed over a range of rounds for different values of M by using $K = 40$ and $N = 4$. While $N_s = 10,000$ iterations are used for each value of R to compute the MSEs numerically. The MSEs of $\widehat{S}_{av}$, $\widehat{P}_s$ and $\widehat{\mu}_L$ are demonstrated in Figure 4.8, Figure 4.9 and Figure 4.10 respectively. It is observed that for a given network load, these MSEs are decreased as the number of rounds is increased. Thus, the desired performance of these prediction methods can be achieved by using an appropriate value of R. In addition to that, as demonstrated

in Figs. 4.8-4.10, when the number of active devices is increased, the IoT devices need to use a higher value of R to maintain the desired MSEs.

Network exploration delay

The time required by IoT devices for network exploration also reflects the performance of the proposed statistical learning-based prediction mechanisms. The end-devices run Algorithm 1 to predict different network parameters after each R number of rounds. Therefore, considering PHY-layer abstraction, the number of rounds executed by the end-devices measures the time required to explore the network. Since each round is composed of N frames, the network exploration delay is NR frames, while the PHY layer defines the frame duration. We can see through Figs. 4.8-4.10, that a higher prediction accuracy requires a larger value of R. In other words, the end-devices would need more time to predict different network parameters if desired accuracy level increases. Moreover, when network load changes, the required number of rounds against the desired prediction accuracy also changes. Therefore, the network exploration delay is variable. In the following subsection, we explain the computation of the optimal value of R under the desired accuracy constraints.

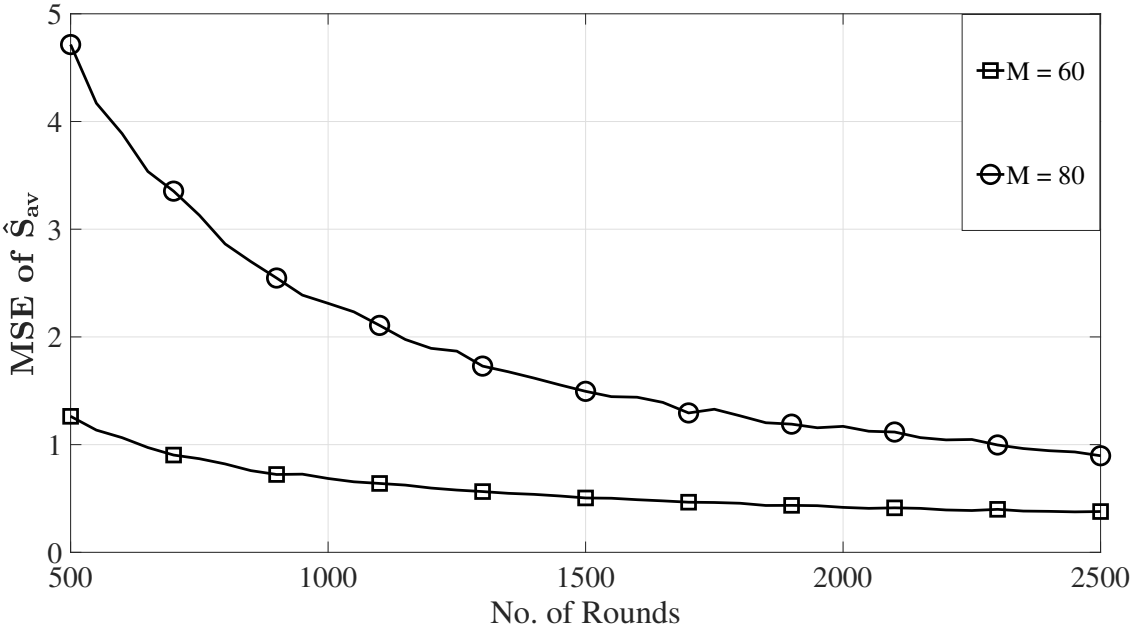

Figure 4.8: MSE in the prediction of average successful devices per round with $K = 40$ and $N = 4$.

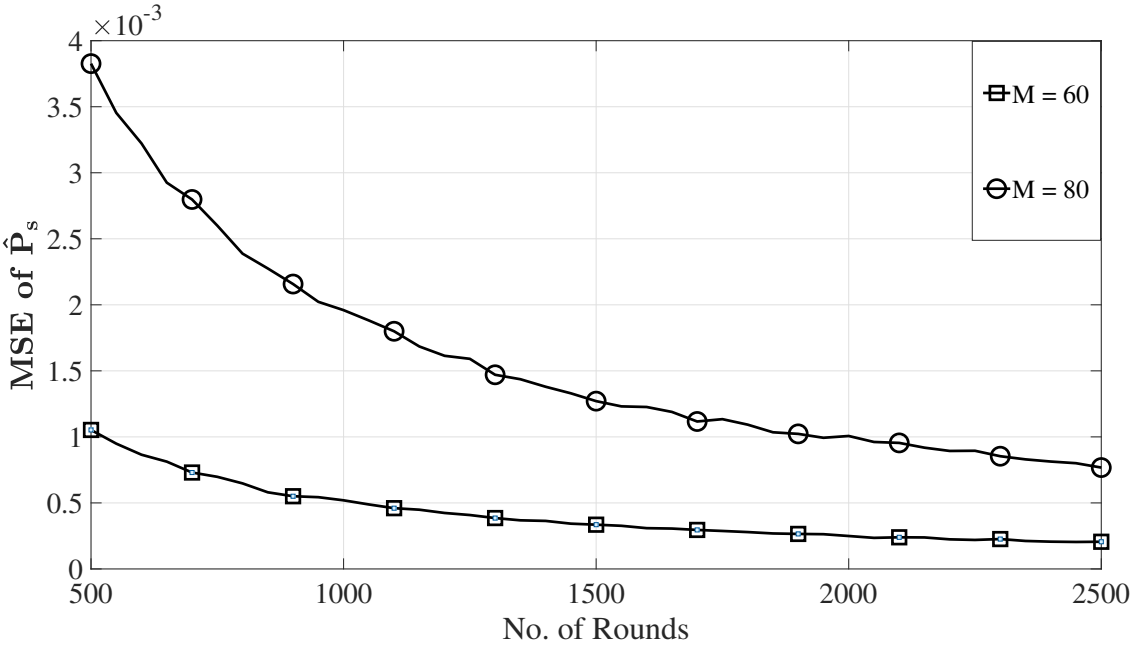

Figure 4.9: MSE in the prediction of average probability of success per round with $K = 40$ and $N = 4$.

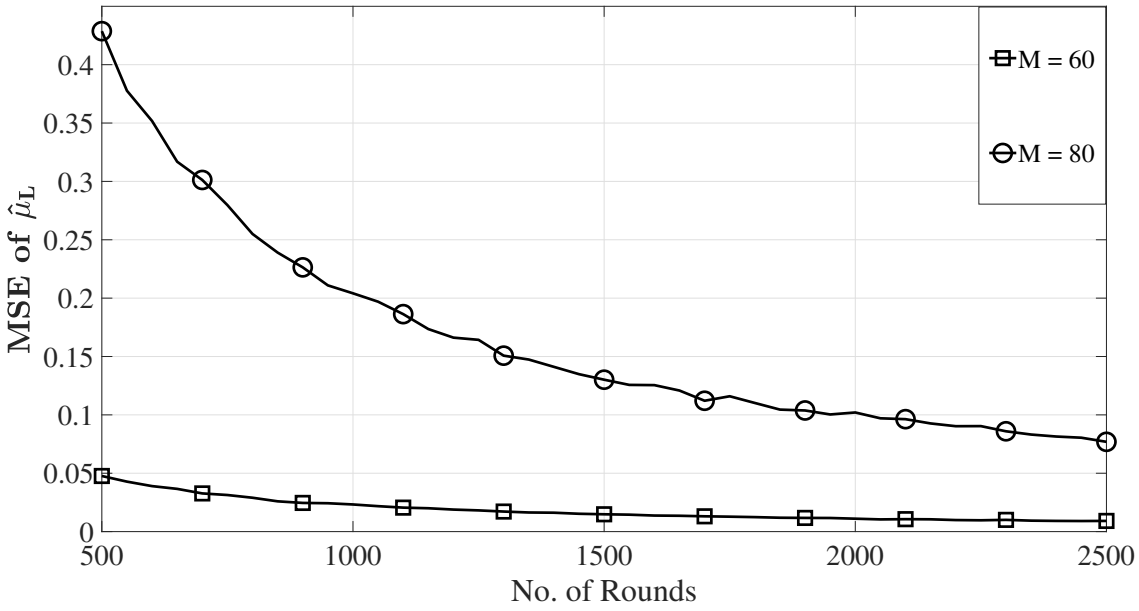

Figure 4.10: MSE in the prediction of average latency with $K = 40$ and $N = 4$.

4.4.2 Optimal size of the history matrix

From the perspective of mission-critical applications, the end-devices need to adapt to the network dynamics in the least possible time. Since the end-devices have limited power, computation, and memory resources, they need the minimum amount of data (transmissions history) to predict different network parameters. On the other hand, the prediction of these parameters should provide reasonable accuracy, which depends on the value of R for the fixed network load. Thus, an optimal value of R is essential to know so that the end-devices can learn different network parameters while meeting the related constraints of time to learn, storage and accuracy. For that purpose, we can use the asymptotic behavior of the above-defined MSEs against R. Let ζ_S, ζ_P and ζ_μ be the acceptable MSE in the prediction of $S_{av}, P_s,$ and μ_L respectively, the optimal number of rounds can be obtained by solving the following:

$$\widehat{R} = \min R \tag{4.39}$$

subject to :

$$R \geq 1,$$
$$\text{MSE}_S \leq \zeta_S,$$
$$\text{MSE}_P \leq \zeta_P,$$
$$\text{MSE}_\mu \leq \zeta_\mu.$$

Since the closed-form expressions of the MSEs related to different parameters are not available, the MSEs are computed numerically for a range of R against different values of the network load. These MSEs decrease monotonically when the value of R is increased, as shown in Figs. 4.8-4.10. Therefore, for each value of M and the given values of K, N, ζ_S, ζ_P, and ζ_L, the BS can have a lookup table to store the corresponding unique value of $\widehat{R}$. Initially, the BS broadcasts an initial value of R such that the end-devices can predict the current network load with a very small probability of exception, as demonstrated in the following Subsection 4.4.3. After receiving the information regarding the current network load from the end-devices, the BS periodically broadcasts the optimal value $\widehat{R}$ according to the desired prediction accuracy constraints and current network load. Thus, the end-devices

can update the size of their history matrix accordingly. We illustrate the impact of M on the computation of $\widehat{R}$ through an example. When $M = 60$, $K = 40$, $N = 4$, $\zeta_S = 1$, $\zeta_P = 0.001$, and $\zeta_\mu = 0.1$, by using the MSEs plotted in Figure 4.8-4.10, we obtain $\widehat{R} \approx 650$. However, for $M = 80$, under the same prediction accuracy constraints, we get $\widehat{R} \approx 2300$.

The significance of the optimal value of R, denoted by $\widehat{R}$, has many folds. The parameter $\widehat{R}$ can be used to determine the devices' storage requirements and the minimum time required to explore and adapt to the network dynamics. In addition, the optimal value of R can be used to determine the energy requirements of the IoT devices for network exploration. In this regard, for the given network load, the transmission energy of $N\widehat{R}$ frames can be used as an upper bound for the energy consumption in device-level network exploration. Since a change in the current network load can impact the value of $\widehat{R}$, the energy consumption during network exploration varies accordingly.

4.4.3 Performance comparison

This Subsection presents a performance comparison regarding the robustness of the proposed statistical learning-based device-level network load prediction and an existing BS-level network load estimation. For the given size of an observation interval R, the performance of the proposed device-level network exploration mechanism is affected by the number of active devices $M_{m,1}$ present in the network. Thus, the accuracy in the prediction of the number of active devices $\widehat{M_1}$ plays a significant role in improving the overall performance of the proposed mechanism. The computation of $\widehat{M_1}$ through (4.13), requires $\widehat{\alpha}_1 < 1$ so that we can have a valid argument for the $\ln(.)$ function. We define exception as an event in which the argument of function $\ln(.)$ becomes zero which corresponds to the case when $\widehat{\alpha}_1 = 1$. The probability of exception η_{M_1} in the computation of $\widehat{M_1}$ is obtained empirically as follows:

$$\eta_{M_1} := \frac{1}{N_s} \sum_{i=1}^{N_s} \mathbf{1}\left(\widehat{\alpha}_1^{(i)} = 1\right). \tag{4.40}$$

where

$$\mathbf{1}\left(\widehat{\alpha}^{(i)}=1\right)=\begin{cases}0 & \text{if} \quad \widehat{\alpha}_1^{(i)}\neq 1;\\ 1 & \text{if} \quad \widehat{\alpha}_1^{(i)}=1.\end{cases} \tag{4.41}$$

For the given value of R, (4.40) provides the relative frequency of the exception occurring in N_s iterations (observation intervals) i.e., the number of times $\widehat{\alpha}_1$ gets value 1 in N_s iterations, while $\widehat{\alpha}_1^{(i)}$ is the prediction of $\alpha_{m,1}$ in the i^{th} iteration, and it is computed through (4.12).

We compare the probability of exception of the proposed device-level method with the one presented in [71, Section IV-C] to estimate the number of active devices at the BS. The estimation method in [71] uses the number of idle preambles in a frame during the contention phase in LTE-A random access procedure. By following the BS centered approach of [71], the number of transmitting devices in each frame can be estimated as follows:

$$\widehat{M}_n^{(BS)}=\frac{1}{R}\sum_{m=1}^{R}\frac{\ln\left(\frac{K_{m,n}}{K}\right)}{\ln\left(\frac{K-1}{K}\right)}. \tag{4.42}$$

where $\widehat{M}_n^{(BS)}$ is an estimate of number of transmitting devices and $K_{m,n}$ is the number of unused channels in the n^{th} frame. This method works well as long as the argument of $\ln(.)$ function is greater than zero i.e., $K_{m,n}>0$. However, when value of $M_{m,n}$ gets larger, the probability of having zero idle channels becomes significantly large. Thus, an exception occurs when $K_{m,n}=0$, and the probability of exception in this case is computed empirically as follows:

$$\eta_{M_n}^{(BS)}:=\frac{1}{N_sR}\sum_{i=1}^{N_s}\sum_{m=1}^{R}\mathbf{1}\left(K_{m,n}^{(i)}=0\right). \tag{4.43}$$

where

$$\mathbf{1}\left(K_{m,n}^{(i)}=0\right)=\begin{cases}0 & \text{if} \quad K_{m,n}^{(i)}\neq 0;\\ 1 & \text{if} \quad K_{m,n}^{(i)}=0.\end{cases} \tag{4.44}$$

where $K_{m,n}^{(i)}$ is the number of idle channels in the n^{th} frame for the i^{th} iteration.

For the given value of R, (4.43) provides the relative frequency of the exception occurring in N_s iterations (observation intervals) i.e., the number of times $K_{m,n}$ gets value 0 in N_s iterations.

In Figure 4.11, we have demonstrated η_{M_1} and $\eta_{M_1}^{(BS)}$ against a range of number of transmitting devices for different values of R with $K = 40$ and $N = 4$. For each value of M, we performed $N_s = 2500$ iterations to compute the probability of exception empirically. It is observed that both η_{M_1} and $\eta_{M_1}^{(BS)}$ are extremely small for a low to moderate network load. However, as the number of active devices is increased further, $\eta_{M_1}^{(BS)}$ becomes significantly large as compared to η_{M_1}. Moreover, for the given network load, η_{M_1} is further reduced by increasing value of R. In contrast to that, the computation of $\widehat{M}_{m,n}^{(BS)}$ only depends upon the number of idle channels in a frame, and increasing value of R does not reduce the probability of exception $\eta_{M_1}^{(BS)}$. Hence, the proposed statistical learning-based device-level network load prediction mechanism is more robust than the BS-centered approach in an environment where a large number of IoT devices communicate with a single BS over limited shared resources.

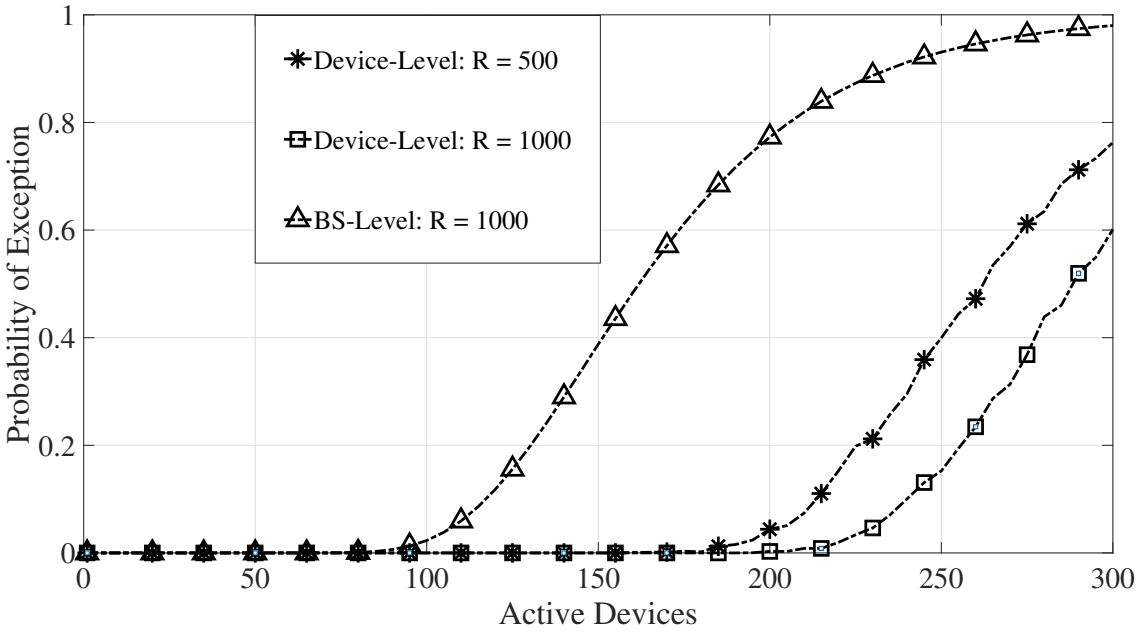

Figure 4.11: Comparison of the probability of exception in the estimation of M

The above discussion highlights that the proposed statistical learning-based network exploration mechanism enables the IoT devices to get an insight of the network condition by predicting S_{av}, P_s, μ_L, and $R^{(i)}$. At the same time, a variation in the number of active devices impacts these network parameters. Therefore, the significance of the knowledge regarding the number of active devices available at the end-devices is further strengthened. It is noteworthy that any change in the number of active devices can be tracked and adapted accordingly by the IoT devices as long as that change remains stable for at least $\widehat{R}$ number of rounds. This feature can be used to design adaptive networks in which end-devices can learn the network dynamics with the least amount of data according to the desired accuracy. Since the BS utilizes information provided by the end-devices, this approach can yield overall latency reduction by reducing the computational overheads at the BS. Therefore, the proposed grant-free access can also improve the energy consumption in the energy-constrained delay-sensitive IoT applications.

4.5 Conclusion

Providing the URLLC interfaces for mission-critical IoT applications in dynamic heterogeneous networks is challenging, and vehicular communication is an important use case of such systems. Statistical learning is a promising tool for predicting dynamically varying parameters and learning associated probability distributions in heterogeneous networks. At the same time, the device-level network exploration can reduce the computation overheads at the BS, which results in overall latency reduction. This chapter presents a statistical learning-based network exploration mechanism for heterogeneous mission-critical-IoT applications employing framed ALOHA-based restricted transmission strategy, enhancing reliability. The proposed grant-free network access mechanism is beneficial for designing heterogeneous networks in which mobile vehicular IoT entities communicate with other IoT devices over shared radio resources. The work presented in this chapter enables the end devices to use their transmission history to predict different dynamic parameters in a probabilistic manner. Through simulations, the performance of the proposed prediction mechanisms is evaluated, and the optimal size of the history matrix is

determined, enabling the end-devices to explore the network under the given accuracy constraints. Compared to the BS-centered approach, the device-level statistical learning-based network load prediction mechanism proposed in this chapter is more robust against heavy network load.

This work can open new research avenues in on-device intelligence for 5G and beyond wireless communication systems. In this regard, as future research work, we aim to extend the current approach for fully decentralized heterogeneous networks while covering device-assisted radio resource management. Moreover, we also aim to design an intelligent back-off algorithm that can be executed by the IoT devices in case of an outage event. Furthermore, the radio channel's condition plays a crucial role in meeting the desired QoS in wireless networks. Therefore, extending the proposed work by considering the channel's behavior can lead to an interesting future research direction.

Chapter 5

Statistical Learning-Based Adaptive Network Access for the Industrial Internet of Things

This chapter is based on the following journal publication:

M. A. Raza, M. Abolhasan, J. Lipman, N. Shariati, W. Ni and A. Jamalipour, *"Statistical Learning-based Adaptive Network Access for the Industrial Internet of Things,"* in IEEE Internet of Things Journal, vol. 10, no. 14, pp. 12219-12233, 2023.

5.1 Introduction

Future wireless networks are envisioned to support Industrial Internet of Things (IIoT) applications that generate network traffic with diverse quality of service (QoS) requirements [3, 61, 101]. Massive machine type communication (MTC) devices deployed in the industrial environment generate delay-sensitive, and delay-tolerant data in cyclic and acyclic manners [3]. Latency requirements for different industrial process automation applications, including safety, control, and monitoring, are described in [106]. Delay-sensitive data needs to be delivered under strict latency and reliability constraints compared to the transmission of delay-tolerant data. Moreover, the amount of data being generated can vary from application to application.

The use of automated guided vehicles and mobile robots has gained considerable attention in industrial operations, including warehouse operations [107]. IIoT networks are used to operate the unmanned vehicles performing time-sensitive (TS) and non-TS tasks in smart warehouses [62]. Furthermore, vehicular IoT entities generate maintenance-critical (delay-sensitive) and maintenance non-critical (delay-tolerant) data of significantly different amounts [108]. The use of multimedia applications in IIoT networks requires the availability of low latency communication links to transmit large amounts of delay-sensitive data. Along with the latency and reliability, the number of successful delay-sensitive transmissions per second and the portions of the bandwidth and computing resources available for delay-tolerant transmission are among the key performance indicators of IIoT networks [61, 62]. Fulfillment of application-specific diverse QoS requirements is challenging when communication is performed over limited radio resources and different network parameters change dynamically [109].

Long Term Evolution (LTE) and LTE-Advanced (LTE-A) technologies provide a four-stage grant-based network access mechanism for communication over limited radio resources [64]. In this approach, the devices first undergo a random access channel (RACH) phase where each device transmits a preamble selected randomly from a pool of available preambles. Collisions happen when multiple devices select the same preamble resulting in RACH failures. The successful devices are granted dedicated resources to transmit their data. Implementing appropriate transmit power control and back-off strategies in successive RACH attempts can improve the probability of success in the RACH phase [110]. However, due to the inherent control signaling overheads, the grant-based network access approach is more suitable for delay-tolerant transmission. Moreover, the reservation of available resources in grant-based access methods makes it less efficient for networks with massive devices. On the other hand, grant-free access avoids long scheduling delays by allowing transmissions over shared resources without going through a request-grant phase. Grant-free access has gained considerable attention to support IIoT applications in 5G and future wireless networks [21]. However, simultaneous transmissions from two or more devices over the same channel can impact the system efficiency and the reliability of delay-sensitive data transmission. Therefore, to evaluate the per-

formance of a particular grant-free access mechanism, both the latency and channel utilization need to be considered.

While communicating over shared radio resources, the number of active devices is one of the critical factors that govern the behavior of the random component of latency experienced by a data packet. Since the number of active devices in IIoT networks can change over time, we can exploit this change to accommodate the transmission of delay-tolerant data resulting in enhanced utilization of the available shared radio resources. Thus when the network load is at a level where transmission of delay-tolerant data does not impact the QoS of delay-sensitive data, the devices can utilize the available resources for the delay-tolerant transmissions. Such an effort would require an adaptive network access mechanism in which end devices can utilize their transmission history to predict the corresponding latency and resource utilization of the network access mechanism under variable network load. Moreover, to avoid the control signaling overheads, end devices need to be able to partition the available resources to accommodate two different types of network traffic without requiring additional feedback information from the BS. The design of such semi-distributed adaptive network access mechanisms involving dynamic resource allocation is challenging under time-varying network conditions. Therefore, distributed computing needs to be explored to address IIoT applications where a large number of devices generate delay-sensitive and delay-tolerant data in a dynamic environment.

The above discussion indicates that the adaptive network access mechanism and device-level learning approach are crucial in designing IIoT networks under limited radio resources and variable network load. The need for adaptive network access approaches is further strengthened when the probability distribution of the time-varying network load is unknown. Moreover, the proportions of the available time, frequency, and energy resources consumed to provide control information to massive end devices become more significant in the BS-centered resource management approaches. On the one hand, existing physical layer enhancements combat the channel's time-varying nature to provide the desired application-specific QoS requirements. On the other hand, statistical learning can be used at the MAC layer to potentially address the problem of adaptive network access to support IoT appli-

cations with diverse latency-reliability constraints [38, 111].

In this chapter, inspired by the need for adaptive network access mechanisms for future IIoT applications, we consider the uplink dominant IIoT networks employing grant-free access. The large number of devices in these networks generate delay-sensitive and delay-tolerant data in random and deterministic manners with varying amounts and diverse QoS requirements. We aim to design a statistical learning-based semi-distributed adaptive network access mechanism that can enable devices to adapt to the network dynamics with limited assistance from the BS. For that purpose, we address the challenge of device-level resource partitioning to accommodate delay-sensitive and delay-tolerant transmissions in IIoT networks. The required parameters related to the device-level resource partitioning are obtained through a statistical learning based-*Network Exploration Phase* designed in Chapter 4, which is based on [111]. The key contributions of this chapter are summarized as follows:

- We propose a statistical learning-based novel grant-free access scheme in which end devices are enabled to dynamically partition the available channels for two different types of transmissions. The proposed scheme prioritizes delay-sensitive transmissions over delay-tolerant transmissions and provides an almost constant collision probability for delay-sensitive transmissions in each slot.

- We design an adaptive network access mechanism that enables end devices to choose between the grant-free access schemes with fixed and dynamic resource allocations under dynamically varying network load. The devices are also enabled to predict outages where current network load is too high to meet desired latency bound for delay-sensitive data, and devices perform a random back-off.

- The proposed adaptive network access operates in a semi-distributed manner and relies on the transmission history of end devices. It avoids additional feedback information from the BS, reducing control signaling overheads while efficiently managing transmission of different types of network traffic in a dynamic environment.

Through simulations, we show that average latency and channel utilization vary in

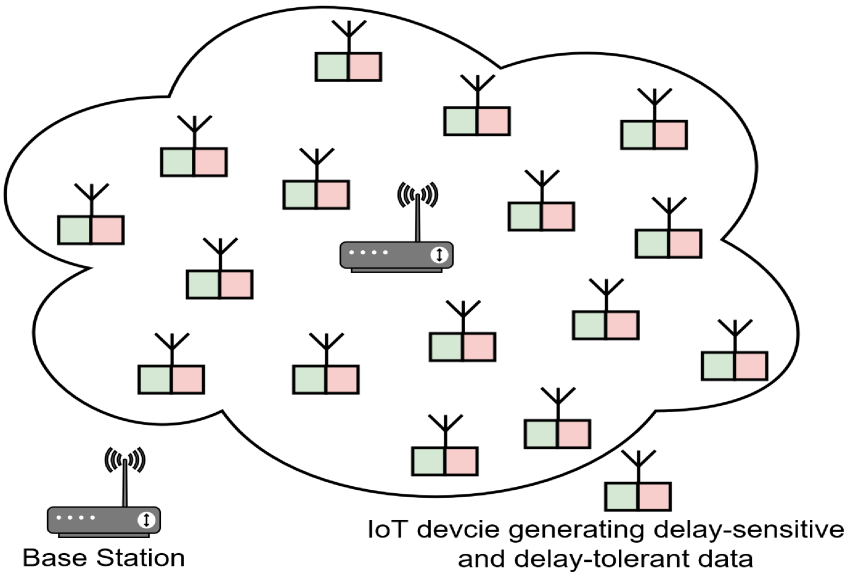

Figure 5.1: IoT devices in an industrial environment generating delay-sensitive and delay-tolerant data and communicating with a single BS over shared radio resources in a grant-free manner.

different access mechanisms under the given network load. Therefore, the device-level decision-making capability enables end devices to adapt to the network dynamics and efficiently utilize available radio resources.

The rest of the chapter is organized as follows: The system model is described in Section 5.2, while Section 5.3 outlines the steps of the proposed adaptive network access mechanism. Section 5.4 presents the design and analysis of the proposed grant-free access with dynamic resource allocation. Device-level prediction of different parameters related to the proposed scheme is discussed in Section 5.5. Simulation results are presented in Section 5.6, and the chapter is concluded in Section 5.7 while highlighting future research directions.

5.2 System Model

As shown in Figure 5.1, we consider uplink communication scenario in IIoT networks composed of massive devices and a single base station (BS). The devices, shown by using two colors in Figure 5.1, generate delay-sensitive and delay-tolerant data. Each device has a scheduler to prioritize the transmission of delay-sensitive data, and all devices perform uplink data transmissions to the BS. Time is divided into slots. A sequence of N consecutive slots makes one round, and a window comprises $2R$

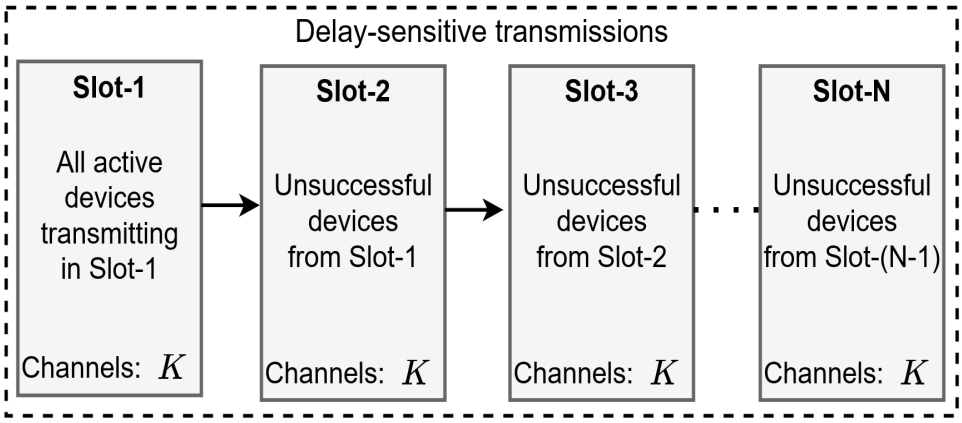

Figure 5.2: The status of different slots in the m^{th} round of *Network Exploration Phase* with $m = 1, 2, ..., R$. In each round devices transmit delay-sensitive by employing the SRA scheme.

rounds.

At the start of each window, M devices become active and communicate with the BS over shared radio resources. The number of active devices remains fixed in a given window; however, the value of M is unknown to the BS. Moreover, M can randomly change from one window to the other while the probability distribution of M is unknown. Active devices use the first half of each window, for rounds $m = 1, 2, ..., R$, to explore the network, including the network load prediction. While the second half of each window, for rounds $m = R + 1, ..., 2R$, is used to adapt to the network dynamics. It is assumed that each device can completely transmit its data packet in one slot.

Each slot is equipped with K orthogonal channels $\mathcal{C} = \{C_1, C_2, ..., C_K\}$, where each channel in $\mathcal{C}$ can be a frequency or code-based resource. The uplink data transmission in each slot follows the grant-free approach where each active device selects a channel randomly and independently from other devices. Moreover, the channel selection is uniform across the available channels. We consider a physical layer abstraction to the MAC layer in which a transmission is unsuccessful if two or more devices select the same channel in a given slot. On the other hand, if a device does not collide with any other devices, the transmission is successful, i.e., the BS can decode the message, and an acknowledgment is sent by the BS. In this chapter, we consider the reactive grant-free approach in which a device retransmits its data packet only if it does not get an acknowledgment from the BS. Throughout this

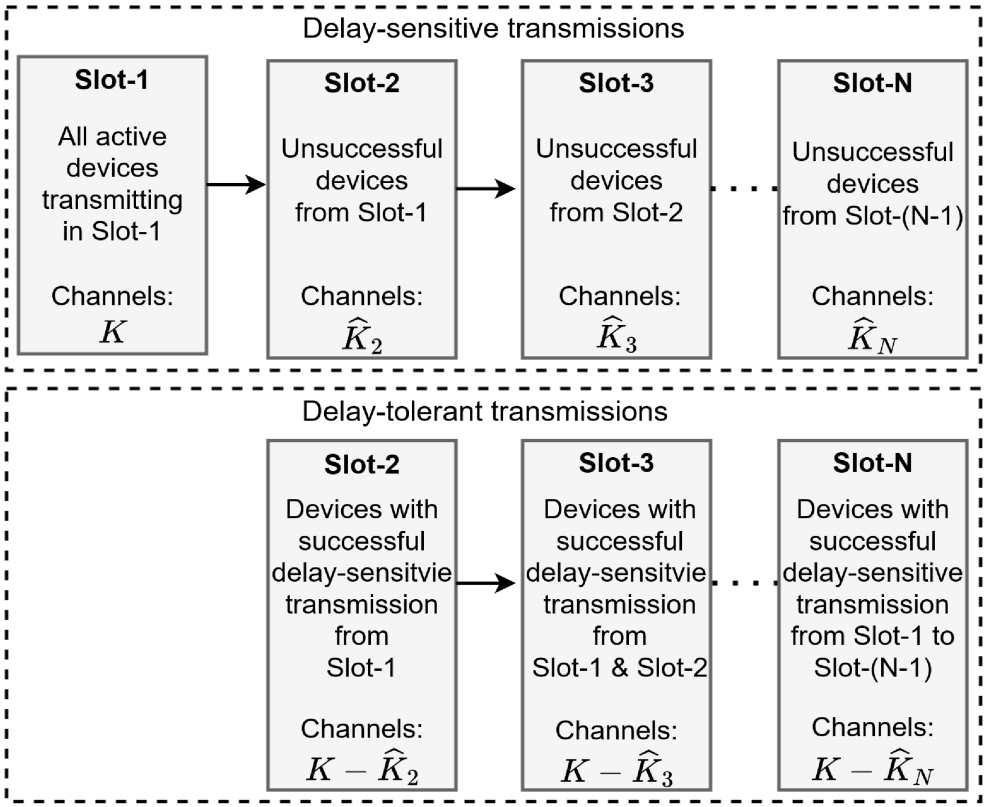

Figure 5.3: Under the condition: $\widehat{\mu}_{\mathrm{ds}}^{(\mathrm{DRA})} \leq \mathcal{L}_{\max}$, status of different slots in each round for $m = R+1, R+2, ..., 2R$ where devices transmit delay-sensitive and delay-tolerant data by employing the DRA scheme.

chapter, we use the terms resource and channel interchangeably.

We consider the random component of latency ($\mathcal{L}$) introduced by the number of (re)transmissions for a successful transmission in the contention-based grant-free access mechanisms. It is assumed that each device can store a newly generated data packet until it is transmitted successfully. Thus, the average latency (μ_L) experienced by a data packet is defined as the average number of (re)transmissions required for successful transmission. In this chapter, we use μ_L to evaluate the possibility of executing a particular IIoT application. Let $\mathcal{L}_{max}$ be the application-specific maximum affordable average latency. The current network conditions are considered feasible for the desired IIoT application as long as $\mu_L \leq \mathcal{L}_{max}$. On the contrary, when $\mu_L > \mathcal{L}_{max}$, we call this event an outage. The channel utilization (η_r) is defined as the average number of successful transmissions per channel per slot, where $0 \leq \eta_r \leq 1$.

Our objective in this chapter is to design a grant-free access mechanism in which

end devices can dynamically partition the resource set $\mathcal{C}$ to accommodate the delay-sensitive and delay-tolerant transmissions under the variable network load. The proposed scheme with dynamic resource allocation is called the DRA scheme. As explained in section 5.5, end devices first undergo a statistical learning-based *Network Exploration Phase*. This phase enables the active devices to predict required parameters by employing a static resource allocation-based grant-free access scheme of [111] called the SRA scheme. The SRA scheme allows each active device one successful delay-sensitive transmission per round.

In contrast to the SRA scheme, as explained in sections 5.4, the DRA scheme proposed in this chapter, enables the end devices to partition the set of available channels in each slot into two disjoint subsets. Consequently, active devices transmit delay-sensitive and delay-tolerant data over dynamically partitioned resources. Since the number of transmitting devices impacts the latency and channel utilization offered by each scheme, we design an adaptive network access mechanism that exploits the change in the current network load and enables the end devices to choose an appropriate grant-free access mechanism under a dynamic environment while avoiding additional feedback information from the BS. The proposed adaptive network access mechanism enhances the channel utilization while meeting the desired latency bound of delay-sensitive data.

In the following section, we provide an overview of the proposed adaptive network access mechanism, followed by the design of grant-free access with dynamic resource allocation.

5.3 Adaptive Network Access

Algorithm-2 explains different steps of the proposed adaptive network access to be executed by each device. As shown in Figure 5.2, using the entire set $\mathcal{C}$, active devices perform delay-sensitive transmissions during the first R rounds of each window, called *Network Exploration Phase*. For this phase, active devices apply the SRA scheme in which every active device can have only one successful delay-sensitive transmission per round. As explained in Section-5.5, the *Network Exploration Phase* enables end devices to predict the current network load ($\widehat{M}$), average latency in the

delay-sensitive transmission $\left(\widehat{\mu}_{\text{ds}}^{(\text{SRA})}\right)$, and channel utilization $(\widehat{\eta}^{(\text{SRA})})$ offered by the SRA scheme.

On the other hand, as shown in Figure 5.3, under the DRA scheme, channels available for delay-sensitive transmissions in the n^{th} slot of a round are given as: $\widehat{\mathcal{C}}_n^{(\text{ds})} = \left\{C_1, C_2, ..., C_{\widehat{K}_n}\right\}$, where $\left|\widehat{\mathcal{C}}_n^{(\text{ds})}\right| = \widehat{K}_n$ and $\widehat{\mathcal{C}}_1^{(\text{ds})} = \mathcal{C}$. While the channels available for delay-tolerant transmissions in the n^{th} slot of a round are given as: $\widehat{\mathcal{C}}_n^{(\text{dt})} = \left\{C_{\widehat{K}_n+1}, C_{\widehat{K}_n+2}, ..., C_K\right\}$, where $\left|\widehat{\mathcal{C}}_n^{(\text{dt})}\right| = K - \widehat{K}_n$ and $\widehat{\mathcal{C}}_1^{(\text{dt})} = \{\emptyset\}$. Thus, in each slot, the available channels are partitioned into two disjoint subsets, i.e., $\mathcal{C} = \widehat{\mathcal{C}}_n^{(\text{ds})} \cup \widehat{\mathcal{C}}_n^{(\text{dt})}$. The resource set $\mathcal{C}$ is partitioned in each slot of a round such that the probability of collision for delay-sensitive transmission remains almost the same as in the first slot. We define a vector parameter $\widehat{\Gamma} := \left[\widehat{K}_1, \widehat{K}_2, ..., \widehat{K}_N\right]$. The *Network Exploration Phase* also enables the active devices to predict $\widehat{\Gamma}$, average latency in the delay-sensitive transmission $(\widehat{\mu}_{\text{ds}}^{(\text{DRA})})$, and the channel utilization $(\widehat{\eta}^{(\text{DRA})})$ offered by the DRA scheme.

After executing the *Network Exploration Phase* if the active devices observe that the current network load is at level where $\widehat{\mu}_{\text{ds}}^{(\text{SRA})} \leq \mathcal{L}_{\max}$, the devices can evaluate the possibility of transmitting delay-tolerant data in the remaining R rounds of the current window by employing the DRA scheme. If the DRA scheme does not cause an outage, active devices transmit delay-sensitive and delay-tolerant data in the next R rounds by employing the DRA scheme. Otherwise, the devices continue to transmit delay-sensitive data in the remaining R rounds of the current window following the SRA scheme.

On the other hand, when current network load is too high to meet the prescribed latency bound for the delay-sensitive data, the *Network Exploration Phase* yields $\widehat{\mu}_{\text{ds}}^{(\text{SRA})} > \mathcal{L}_{\max}$. Therefore, in case of an outage, the devices transmit only delay-tolerant data in each slot of the next R rounds using the multichannel slotted ALOHA (MSA) scheme. Under the MSA approach, in each slot, every active device selects a channel from $\mathcal{C}$ randomly and independently from other devices and (re)transmits the delay-tolerant data. Moreover, the devices perform a random-back-off where each device decides to skip next W_b windows independently from other active devices, where W_b is a random number selected from $\{1, ..., W_{\max}\}$ fol-

lowing uniform distribution. The parameter $W_{\max}$ shows the maximum number of windows a device can skip, and BS periodically broadcasts the parameter $W_{\max}$. The random-back-off strategy provides a fair opportunity for the newly active devices to perform the uplink data transmission.

In summary, the proposed adaptive network access mechanism enables end devices to choose an appropriate grant-free access scheme under a dynamic environment. The only feedback devices need from the BS is the outcome of their transmissions. The end devices use their transmission history to predict different parameters employing the statistical learning approach. Therefore, the proposed adaptive network access mechanism operates in a semi-distributed manner, and avoids excessive control signaling overheads. We first discuss the design of the proposed DRA scheme. Later, we explain the *Network Exploration Phase* to predict the required parameters for the SRA and DRA schemes.

5.4 Grant-Free Access with Dynamic Resource Allocation

The proposed grant-free access scheme with dynamic resource allocation aims to enable end devices to transmit the delay-sensitive and delay-tolerant data over non-overlapping groups of channels. As shown in Figure 5.3, the delay-sensitive transmissions are prioritized over the delay-tolerant transmissions. Under this scheme, the devices after having a successful delay-sensitive transmission in the n^{th} slot perform delay-tolerant transmission in the remaining $N - n$ slots of a given round. Thus, each slot of a round, except Slot-1, can carry the both types of data. Active devices keep the history of their transmission outcomes. Let the random variable $B_{m,n}$ show the outcome of an indented device's transmission in the n^{th} slot of the m^{th} round for $m = R + 1, ..., 2R$ defined as

$$B_{m,n} := \begin{cases} 1, & \text{Successful transmission;} \\ 0, & \text{Collision with other device/s.} \end{cases} \tag{5.1}$$

Algorithm 2 Adaptive Network Access

Require: $\mathcal{C}$, R, N, $\mathcal{L}_{\max}$, $W_{\max}$

Run Algorithm-3 to obtain $\widehat{\mu}_{\text{ds}}^{(\text{SRA})}$, $\widehat{\mu}_{\text{ds}}^{(\text{DRA})}$, $\widehat{\Gamma}$
if $\left(\widehat{\mu}_{\text{ds}}^{(\text{SRA})} \leq \mathcal{L}_{\max}\right)$ **then**
  if $\left(\widehat{\mu}_{\text{ds}}^{(\text{DRA})} \leq \mathcal{L}_{\max}\right)$ **then**
    for $m = R+1$ to $2R$ **do**
      Delay-Tolerant-Flag := 0
      for $n = 1$ to N **do**
        Determine $\widehat{\mathcal{C}}_n^{(\text{ds})}$ and $\widehat{\mathcal{C}}_n^{(\text{dt})}$
        if Delay-Tolerant-Flag == 0 **then**
          Select a channel randomly from $\widehat{\mathcal{C}}_n^{(\text{ds})}$
          Transmit/retransmit delay-sensitive data
          if success **then**
            Delay-Tolerant-Flag := 1
          end if
        else
          Select a channel randomly from $\widehat{\mathcal{C}}_n^{(\text{dt})}$
          Transmit/retransmit delay-tolerant data
        end if
      end for
    end for
  else
    for $m = R+1$ to $2R$ **do**
      for $n = 1$ to N **do**
        Select a channel randomly from $\mathcal{C}$
        Transmit/retransmit delay-sensitive data
        if success **then**
          Stop transmitting in current round: $n := N+1$
        end if
      end for
    end for
  end if
else
  Transmit delay-tolerant data in each slot of the next R rounds using the MSA scheme
  Select W_b from $\{1, ..., W_{\max}\}$ randomly
  Skip next W_b windows
end if

The channels available for delay-sensitive transmissions in the n^{th} slot of the m^{th} round are given as: $\mathcal{C}_{m,n}^{(\text{ds})} = \left\{C_1, C_2, ..., C_{K_{m,n}}\right\}$, where $\left|\mathcal{C}_{m,n}^{(\text{ds})}\right| = K_{m,n}$ and $\mathcal{C}_{m,1}^{(\text{ds})} = \mathcal{C}$. While the channels reserved for delay-tolerant transmissions comes out to be: $\mathcal{C}_{m,n}^{(\text{dt})} = \left\{C_{K_{m,n}+1}, C_{K_{m,n}+2}, ..., C_K\right\}$, where $\left|\mathcal{C}_{m,n}^{(\text{dt})}\right| = K - K_{m,n}$ and $\mathcal{C}_{m,1}^{(\text{dt})} = \{\emptyset\}$. We define a vector parameter $\Gamma_m := [K_{m,1}, K_{m,2}, ..., K_{m,N}]$. Thus, in Slot-2 to Slot-N,

the available channels are partitioned into two disjoint subsets, i.e., $\mathcal{C} = \mathcal{C}_{m,n}^{(ds)} \cup \mathcal{C}_{m,n}^{(\mathrm{dt})}$. As explained below, different elements of Γ_m are determined such that the delay-sensitive transmissions can get the desired QoS in each slot of a round.

5.4.1 Device-Level Resource Partitioning:

In this subsection, we discuss the computation of Γ_m. Under the DRA scheme, the number of devices transmitting delay-sensitive data in the n^{th} slot of the m^{th} round is represented by $V_{m,n}$ and defined as

$$V_{m,n} := \begin{cases} M, & n = 1; \\ M - \sum_{j=1}^{n-1} V'_{m,j} \ , & n = 2, 3, ..., N. \end{cases} \tag{5.2}$$

where $V'_{m,j}$ is the number of devices having successful delay-sensitive transmissions in the j^{th} slot. The probability that delay-sensitive transmission of an intended device faces a collision is given as

$$\begin{aligned} \beta_{m,n} &:= \Pr\left(B_{m,n} = 0 \mid \text{delay-sensitive transmission}\right), \\ &= 1 - \left(1 - \frac{1}{K_{m,n}}\right)^{V_{m,n}-1}, \quad n = 1, 2, ..., N. \end{aligned} \tag{5.3}$$

Active devices begin to transmit delay-tolerant data after successful delay-sensitive transmission. The number of devices transmitting delay-tolerant data in each slot is given as

$$W_{m,n} = \begin{cases} 0, & n = 1; \\ \sum_{j=1}^{n-1} V'_{m,j} \ , & n = 2, 3, ..., N. \end{cases} \tag{5.4}$$

Given that an intended device has a successful delay-sensitive transmission, the probability that its delay-tolerant transmission remains unsuccessful in a given slot is computed as

$$\begin{aligned} \gamma_{m,n} &:= \Pr\left(B_{m,n} = 0 \mid \text{delay-tolerant transmission}\right), \\ &= 1 - \left(1 - \frac{1}{K - K_{m,n}}\right)^{W_{m,n}-1}, \quad n = 2, 3, ..., N. \end{aligned} \tag{5.5}$$

While considering PHY-layer abstraction, different dynamic resource allocation schemes can provide different latency for delay-sensitive and delay-tolerant transmissions under the given set of channels, round size, and the number of active devices. In the proposed DRA scheme, the resource set $\mathcal{C}$ is partitioned in each slot such that all active devices can experience almost the same probability of collision for delay-sensitive transmissions throughout R rounds. We define α_1 as

$$\alpha_1 := 1 - \left(1 - \frac{1}{K}\right)^{M-1}. \tag{5.6}$$

In this chapter, we compute Γ_m by keeping the probability of collision in each slot equal to the probability of collision in the first slot, i.e., $\beta_{m,n} = \alpha_1,\ \forall n = 1, 2, ..., N$. Thus, the number of channels available for the delay-sensitive-data transmission in each slot comes out to be

$$K_{m,n} = \begin{cases} K, & n = 1; \\ \left\lceil \left\{ 1 - \left(1 - \frac{1}{K}\right)^{\frac{M-1}{V_{m,n}-1}} \right\}^{-1} \right\rceil, & n = 2, 3, ..., N. \end{cases} \tag{5.7}$$

where $V_{m,n} > 1\ \forall n = 1, 2, ..., N$, and the ceiling function $\lceil x \rceil$ represents the smallest integer value larger than or equal to x. Due to the discretization in (5.7), we have $\beta_{m,n} \simeq \alpha_1,\ \forall n = 1, 2, ..., N$.

5.4.2 Channel Utilization:

The computation of channel utilization in the DRA scheme requires availability of average number of successful delay-sensitive and delay-tolerant transmissions per round. The average successful delay-sensitive transmissions per round is computed as

$$\mathcal{S}_{\text{ds}}^{(\text{DRA})} := \frac{1}{R} \sum_{m=1}^{R} \sum_{n=1}^{N} V'_{m,n}. \tag{5.8}$$

While, the average successful delay-tolerant transmissions per round is computed as

$$\mathcal{S}_{\text{dt}}^{(\text{DRA})} := \frac{1}{R}\sum_{m=1}^{R}\sum_{n=2}^{N} V''_{m,n}. \tag{5.9}$$

where $V''_{m,n}$ is the number of successful delay-tolerant transmissions in the n^{th} slot of the m^{th} round. Thus, the average number of successful transmissions per round comes out be

$$\begin{aligned}\mathcal{S}^{(\text{DRA})} &:= \mathcal{S}_{\text{ds}}^{(\text{DRA})} + \mathcal{S}_{\text{dt}}^{(\text{DRA})}, \\ &= \frac{1}{R}\sum_{m=1}^{R}\left(\sum_{n=1}^{N} V'_{m,n} + \sum_{n=2}^{N} V''_{m,n}\right).\end{aligned} \tag{5.10}$$

Finally, the channel utilization for the DRA scheme is computed by

$$\eta^{(\text{DRA})} := \frac{\mathcal{S}^{(\text{DRA})}}{KN}. \tag{5.11}$$

By applying (5.10) in (5.11), $\eta^{(\text{DRA})}$ comes out to be

$$\eta^{(\text{DRA})} = \frac{1}{KNR}\sum_{m=1}^{R}\left(\sum_{n=1}^{N} V'_{m,n} + \sum_{n=2}^{N} V''_{m,n}\right). \tag{5.12}$$

In Section 5.5.1, we explain the prediction of channel utilization and average latency offered by the DRA scheme which involves the prediction of Γ_m, $\beta_{m,n}$, and $\gamma_{m,n}$.

5.4.3 Probabilistic Analysis

In this subsection, we perform the probabilistic analysis for the different events related to the DRA scheme. Under this scheme, in each round, a device can undergo one of the three mutually exclusive events: E_1, E_2, and E_3. The event E_1 is defined as the case where a device of interest, after successful delay-sensitive transmission, gets at least one successful delay-tolerant transmission. The probability for the

occurrence of E_1 in the m^{th} round is computed as

$$\mathcal{P}_m(E_1) := \sum_{n=1}^{N-1} \underbrace{(1-\beta_{m,n}) \prod_{\substack{j=1 \\ n>1}}^{n-1} \beta_{m,j}}_{\text{I}} \underbrace{\left(1 - \prod_{\substack{j=n \\ n>1}}^{N} \gamma_{m,j}\right)}_{\text{II}}. \tag{5.13}$$

The expression I in (5.13) is the probability that the intended device gets successful delay-sensitive transmission in the n^{th} slot, while II in (5.13) shows the probability of having at least one successful delay-tolerant transmission in the remaining $N-n$ slots of the m^{th} round.

On the other hand, event E_2 arises when the intended device has one successful delay-sensitive transmission but does not get any successful delay-tolerant transmissions. The probability for the occurrence of E_2 in the m^{th} round is computed as

$$\mathcal{P}_m(E_2) := \sum_{n=1}^{N-1} \underbrace{(1-\beta_{m,n}) \prod_{\substack{j=1 \\ n>1}}^{n-1} \beta_{m,j}}_{\text{I}} \underbrace{\prod_{\substack{j=n \\ n>1}}^{N} \gamma_{m,j}}_{\text{II}} + \underbrace{(1-\beta_{m,N}) \prod_{n=1}^{N-1} \beta_{m,n}}_{\text{III}}. \tag{5.14}$$

The expression I in (5.14) is the same as in (5.13), while II in (5.14) is the probability that after having a successful delay-sensitive transmission, all delay-tolerant transmissions from the intended device are unsuccessful in the remaining slots of that round. The expression III in (5.14) shows the probability of having successful delay-sensitive transmission in the last slot of the m^{th} round. The event E_3 arises when the intended device does not get any successful delay-sensitive transmission and ultimately no successful delay-tolerant transmissions. The probability for the occurrence of E_3 in the m^{th} round is computed as

$$\mathcal{P}_m(E_3) := \prod_{n=1}^{N} \beta_{m,n}. \tag{5.15}$$

The probabilities $\mathcal{P}_m(E_1)$, $\mathcal{P}_m(E_2)$, and $\mathcal{P}_m(E_3)$ satisfy $\mathcal{P}_m(E_1)+\mathcal{P}_m(E_2)+\mathcal{P}_m(E_3) = 1$. By using $\{\beta_{m,n}\}_{n=1}^{N} \simeq \alpha_1,\ \forall m = 1, 2, ..., R$, the probabilities $\mathcal{P}_m(E_1)$, $\mathcal{P}_m(E_2)$,

and $\mathcal{P}_m(E_3)$ are approximated as follows:

$$\mathcal{P}_m(E_1) \simeq \sum_{n=1}^{N-1} (1-\alpha_1)\, \alpha_1^{n-1} \left(1 - \prod_{\substack{j=n \\ n>1}}^{N} \gamma_{m,j} \right). \tag{5.16}$$

$$\mathcal{P}_m(E_2) \simeq \sum_{n=1}^{N-1} (1-\alpha_1)\, \alpha_1^{n-1} \prod_{\substack{j=n \\ n>1}}^{N} \gamma_{m,j} + (1-\alpha_1)\, \alpha_{m,1}^{N-1}. \tag{5.17}$$

$$\mathcal{P}_m(E_3) \simeq \alpha_1^N. \tag{5.18}$$

The average probability that a device of interest has a successful delay-sensitive transmission, whether it gets any delay-tolerant transmissions or not, is given as:

$$\begin{aligned} \mathcal{P}_{\text{ds}}^{(\text{DRA})} &:= \frac{1}{R} \sum_{m=1}^{R} \left(\mathcal{P}_m(E_1) + \mathcal{P}_m(E_2) \right), \\ &= 1 - \frac{1}{R} \sum_{m=1}^{R} \mathcal{P}_m(E_3). \end{aligned} \tag{5.19}$$

By using (5.18) in (5.19), $\mathcal{P}_{\text{ds}}^{(\text{DRA})}$ is computed as

$$\mathcal{P}_{\text{ds}}^{(\text{DRA})} \simeq 1 - \alpha_1^N. \tag{5.20}$$

While the average probability that a device of interest will have at least one delay-tolerant transmission, denoted by $\mathcal{P}_{\text{dt}}^{(\text{DRA})}$, is given by

$$\mathcal{P}_{\text{dt}}^{(\text{DRA})} := \frac{1}{R} \sum_{m=1}^{R} \mathcal{P}_m(E_1). \tag{5.21}$$

By applying (5.16) in (5.21), $\mathcal{P}_{\text{dt}}^{(\text{DRA})}$ is computed as

$$\mathcal{P}_{\text{dt}}^{(\text{DRA})} \simeq \frac{1}{R} \sum_{m=1}^{R} \sum_{n=1}^{N-1} (1-\alpha_1)\, \alpha_1^{n-1} \left(1 - \prod_{\substack{j=n \\ n>1}}^{N} \gamma_{m,j} \right). \tag{5.22}$$

Algorithm 3 Network Exploration Phase for Adaptive Network Access

Require: $\mathcal{C}$, R, N
Ensure: $\widehat{\mu}_{\text{ds}}^{(\text{SRA})}$, $\widehat{\mu}_{\text{ds}}^{(\text{DRA})}$, and $\widehat{\Gamma}$.

```
for m = 1 to R do
    for n = 1 to N do
        Select a channel randomly from C
        Transmit/retransmit delay-sensitive data
        if success then
            if n == 1 then
                A_{m,1} := 0
            end if
            Stop transmitting in current round: n := N + 1
        else
            if n == 1 then
                A_{m,1} := 1
            end if
        end if
    end for
end for
Predict M̂ using (5.24)
Predict μ̂_ds^(SRA) from Eq. (5.26)
Predict Γ̂ using (5.32)
Predict μ̂_ds^(DRA) from Eq. (5.34)
```

In the following section, we discuss the prediction of different parameters related to the SRA and DRA schemes.

5.5 Network Exploration Phase

As shown in Figure 5.2, during *Network Exploration Phase*, all the active devices perform delay-sensitive transmissions following the SRA scheme of [111]. Under this scheme, each active device can have only one successful transmission per round. The probability ($\alpha_{m,n}$) that an intended device's transmission faces a collision with one or more other transmitting devices in the n^{th} slot of the m^{th} round is computed by

$$\alpha_{m,n} = 1 - \left(1 - \frac{1}{K}\right)^{M_{m,n}-1}, \tag{5.23}$$

where $M_{m,n}$ is the number of transmitting devices in the n^{th} slot of the m^{th} round, and we have $M = M_{m,1}$ $\forall m = 1, 2, ..., 2R$. Thus for $n = 1$, (5.6) and (5.23) generate the same expressions.

During the *Network Exploration Phase*, all active devices maintain the history of their transmissions outcomes in a vector: $\mathbf{h} = [A_{1,1}, A_{2,1}, ..., A_{R,1}]$, where each element of $\mathbf{h}$ is a Bernoulli random variable i.e, $A_{m,1} \in \{0, 1\}$, $\forall m = 1, 2, ..., R$. The random variable $A_{m,1} = 1$ if the intended device's transmission faces a collision with one or more other active devices in Slot-1 of the m^{th} round. Finally using the statistical learning approach, end devices are enabled to predict the number of transmitting devices ($\widehat{M}_n$) and the corresponding collision probability ($\widehat{\alpha}_n$) in different slots of each round of the *Network Exploration Phase* as follows [111]:

$$\widehat{M}_n = \begin{cases} 1 + \frac{\ln\left(1-\frac{1}{R}\sum_{m=1}^{R} A_{m,1}\right)}{\ln\left(\frac{K-1}{K}\right)}, & n = 1; \\ \left[1 + \frac{\ln\left(1-\frac{1}{R}\sum_{m=1}^{R} A_{m,1}\right)}{\ln\left(\frac{K-1}{K}\right)}\right] \prod_{j=1}^{n-1} \widehat{\alpha}_j \ , & \\ & n = 2, 3, ..., N. \end{cases} \tag{5.24}$$

$$\widehat{\alpha}_n = \begin{cases} \frac{1}{R}\sum_{m=1}^{R} A_{m,1}, & n = 1; \\ 1 - \left(1 - \frac{1}{K}\right)^{\widehat{M}_n - 1}, & n = 2, 3, ..., N. \end{cases} \tag{5.25}$$

where $\widehat{M}_n$ and $\widehat{\alpha}_n$ are the predictions of $M_{m,n}$ and $\alpha_{m,n}$ $\forall m = 1, 2, ..., R$, respectively, and $\widehat{M} = \widehat{M}_1$.

Consequently, active devices predict the average latency of delay-sensitive transmissions in the SRA scheme using [111, Eq. (30)] as follows:

$$\widehat{\mu}_{\text{ds}}^{(\text{SRA})} := \frac{1}{1 - \prod_{n=1}^{N} \widehat{\alpha}_n} \left(1 + \sum_{\substack{z=1 \\ N>1}}^{N-1} \prod_{j=1}^{z} \widehat{\alpha}_j\right). \tag{5.26}$$

Along with $\widehat{\mu}_{\text{ds}}^{(\text{SRA})}$, end devices predict the channel utilization ($\widehat{\eta}^{(\text{SRA})}$) of the SRA scheme as follows:

$$\widehat{\eta}^{(\text{SRA})} := \frac{\widehat{M}\left(1 - \prod_{n=1}^{N} \widehat{\alpha}_n\right)}{KN}. \tag{5.27}$$

where $\widehat{M}\left(1-\prod_{n=1}^{N}\widehat{\alpha}_n\right)$ is the prediction of average successful devices per round in the SRA scheme.

5.5.1 Prediction of Average Latency in the DRA Scheme

If the current network conditions are such that $\widehat{\mu}_{\text{ds}}^{(\text{SRA})} \leq \mathcal{L}_{max}$, end devices can further explore the possibility of transmitting delay-tolerant data followed by the delay-sensitive transmissions using the DRA scheme. For this purpose, end devices need to predict the vector parameter $\widehat{\Gamma}$ and the average latency ($\widehat{\mu}_{\text{ds}}^{(\text{DRA})}$) offered by the proposed DRA scheme. The end devices apply their knowledge of the current network load prediction, obtained from (5.24), in (5.7) and predict the number of channels reserved for delay-sensitive transmissions in the n^{th} slot of a round as follows:

$$\widehat{K}_n = \begin{cases} K, & n = 1; \\ \left\lceil \left\{ 1 - \left(1 - \frac{1}{K}\right)^{\frac{\widehat{M}-1}{\widehat{V}_n - 1}} \right\}^{-1} \right\rceil, & n = 2, 3, ..., N. \end{cases} \tag{5.28}$$

where $\widehat{V}_n$ is the prediction of $V_{m,n}$ $\forall m = 1, 2, ..., R$ and it is computed by

$$\widehat{V}_n := \widehat{V}_1 \prod_{\substack{j=1 \\ n>1}}^{n-1} \widehat{\beta}_j, \quad n = 1, 2, ..., N. \tag{5.29}$$

where $\widehat{V}_1 = \widehat{M}$ and $\widehat{\beta}_j$ is the prediction of $\beta_{m,j},\ \forall m = 1, 2, ..., R$.

Since the proposed DRA scheme aims to keep the probability of collision for delay-sensitive transmissions almost the same in all slots of a round while accommodating the transmission of delay-tolerant data; by using $\widehat{\beta}_n \simeq \widehat{\alpha}_1,\ \forall n = 1, 2, ..., N$; $\widehat{V}_n$ is approximated as follows:

$$\widehat{V}_n \simeq \widehat{M}\widehat{\alpha}_1^{n-1}. \tag{5.30}$$

By substituting (5.24) and (5.25) in (5.30), $\widehat{V}_n$ is computed as

$$\widehat{V}_n \simeq \left\{1 + \frac{\ln\left(1 - \frac{1}{R}\sum_{m=1}^{R} A_{m,1}\right)}{\ln\left(\frac{K-1}{K}\right)}\right\}\left(\frac{1}{R}\sum_{m=1}^{R} A_{m,1}\right)^{n-1}. \tag{5.31}$$

Finally, by substituting (5.30) in (5.28), different elements in $\widehat{\Gamma}$ are computed by

$$\widehat{K}_n := \begin{cases} K, & n = 1; \\ \left\lceil \left\{1 - \left(1 - \frac{1}{K}\right)^{\frac{\widehat{M}-1}{\widehat{M}\widehat{\alpha}_1^{n-1}-1}}\right\}^{-1} \right\rceil, & \\ & n = 2, 3, ..., N. \end{cases} \tag{5.32}$$

Thus by using (5.31) and (5.32) in (5.3) end devices can compute $\widehat{\beta}_n$ as follows:

$$\widehat{\beta}_n = 1 - \left(1 - \frac{1}{\widehat{K}_n}\right)^{\widehat{V}_n - 1}, \qquad n = 1, 2, ..., N. \tag{5.33}$$

Once end devices have computed $\widehat{\Gamma}$ and $\widehat{\beta}_n$, the average latency in delay-sensitive transmission for the DRA scheme is computed as

$$\widehat{\mu}_{\text{ds}}^{(\text{DRA})} \simeq \frac{R}{R - \sum_{m=1}^{R} A_{m,1}}. \tag{5.34}$$

Derivation of (5.34)

Since each active device can have only one successful delay-sensitive transmission per round in the DRA scheme, the devices can predict the average latency for their delay-sensitive transmissions as follows [111]:

$$\widehat{\mu}_{\text{ds}}^{(\text{DRA})} := \frac{1}{1 - \prod_{n=1}^{N} \widehat{\beta}_n}\left(1 + \sum_{\substack{z=1 \\ N>1}}^{N-1}\prod_{j=1}^{z}\widehat{\beta}_j\right). \tag{5.35}$$

By using $\widehat{\beta}_n \simeq \widehat{\alpha}_1,\ \forall n = 1, 2, ..., N$ in (5.35), the devices can approximate $\widehat{\mu}_{\text{ds}}^{(\text{DRA})}$ as follows:

$$\widehat{\mu}_{\text{ds}}^{(\text{DRA})} \simeq \frac{1 + \sum_{n=1}^{N-1} \widehat{\alpha}_1^n}{1 - \widehat{\alpha}_1^N}. \tag{5.36}$$

The right hand side of (5.36) can be expanded as

$$\begin{aligned} \widehat{\mu}_{\text{ds}}^{(\text{DRA})} &\simeq \frac{1 + \widehat{\alpha}_1^N - \widehat{\alpha}_1^N + (1 - \widehat{\alpha}_1)^{-1} \sum_{n=1}^{N-1} (1 - \widehat{\alpha}_1) \widehat{\alpha}_1^n}{1 - \widehat{\alpha}_1^N}, \\ &= 1 + \frac{\widehat{\alpha}_1 (1 - \widehat{\alpha}_1)^{-1} \sum_{n=1}^{N} (1 - \widehat{\alpha}_1) \widehat{\alpha}_1^{n-1}}{1 - \widehat{\alpha}_1^N}, \end{aligned} \tag{5.37}$$

where

$$\sum_{n=1}^{N} (1 - \widehat{\alpha}_1) \widehat{\alpha}_1^{n-1} = 1 - \widehat{\alpha}_1 + \widehat{\alpha}_1 - \widehat{\alpha}_1^2 + ... + \widehat{\alpha}_1^{N-1} - \widehat{\alpha}_1^N. \tag{5.38}$$

All the terms except the 1st and the last terms at the right hand side of (5.38) are cancelled out and (5.38) is reduced to

$$\sum_{n=1}^{N} (1 - \widehat{\alpha}_1) \widehat{\alpha}_1^{n-1} = 1 - \widehat{\alpha}_1^N. \tag{5.39}$$

By substituting (5.39) in (5.37), we get

$$\widehat{\mu}_{\text{ds}}^{(\text{DRA})} \simeq \frac{1}{1 - \widehat{\alpha}_1}. \tag{5.40}$$

By substituting $\widehat{\alpha}_1$, obtained through (5.25), in (5.40), $\widehat{\mu}_{\text{ds}}^{(\text{DRA})}$ gets the following form:

$$\widehat{\mu}_{\text{ds}}^{(\text{DRA})} \simeq \frac{R}{R - \sum_{m=1}^{R} A_{m,1}}. \tag{5.41}$$

This completes the derivation of (5.34).

After completing the exploration phase, end devices compute, $\widehat{\mu}_{\text{ds}}^{(\text{SRA})}$ and $\widehat{\mu}_{\text{ds}}^{(\text{DRA})}$ through (5.26) and (5.34), respectively. If the average latency in the delay-sensitive transmission offered by the SRA scheme does not exceed the latency bound, i.e., $\widehat{\mu}_{\text{ds}}^{(\text{SRA})} < \mathcal{L}_{max}$, the devices can evaluate the possibility of accommodating the delay-

tolerant transmissions in the next R rounds. Under the given current network load, if the DRA scheme follows the latency bound i.e., $\widehat{\mu}_{\text{ds}}^{(\text{DRA})} < \mathcal{L}_{max}$, the devices select the DRA scheme for the next R rounds. Otherwise, the devices continue using the SRA scheme during the second half of the current window. Thus, the possibility of executing the DRA is determined before executing it with the help of an exploration phase. Moreover, as demonstrated in the following section, allowing the transmission of delay-tolerant data increases channel utilization. The relationship between $\widehat{\mu}_{\text{ds}}^{(\text{SRA})}$ and $\widehat{\mu}_{\text{ds}}^{(\text{DRA})}$ is described in Proposition 1.

Proposition 1 *The average latency of a successful delay-sensitive transmission with static resource allocation under the SRA and with dynamic resource allocation under the DRA are related as*

$$\widehat{\mu}_{ds}^{(SRA)} \leq \widehat{\mu}_{ds}^{(DRA)}. \tag{5.42}$$

Proof of Proposition 1

For the grant-free based restricted transmission strategy of the SRA scheme we have $0 \leq \widehat{\alpha}_1 \leq \widehat{\alpha}_2 \leq ... \leq \widehat{\alpha}_N < 1$, which satisfies the followings:

$$\prod_{i=1}^{n} \widehat{\alpha}_i \leq \widehat{\alpha}_1^n, \ \forall n = 1, 2, ..., N, \tag{5.43}$$

From (5.43) we have

$$1 + \sum_{n=1}^{N-1} \prod_{i=1}^{n} \widehat{\alpha}_i \leq 1 + \sum_{n=1}^{N-1} \widehat{\alpha}_1^n. \tag{5.44}$$

Also from (5.43)

$$\frac{1}{1 - \prod_{i=1}^{N} \widehat{\alpha}_i} \leq \frac{1}{1 - \widehat{\alpha}_1^N}. \tag{5.45}$$

Combining (5.44) and (5.45) yields the following:

$$\frac{1}{1 - \prod_{n=1}^{N} \widehat{\alpha}_n} \left(1 + \sum_{\substack{z=1 \\ N>1}}^{N-1} \prod_{j=1}^{z} \widehat{\alpha}_j \right) \leq \frac{1 + \sum_{j=1}^{N-1} \widehat{\alpha}_1^j}{1 - \widehat{\alpha}_1^N}. \tag{5.46}$$

Comparing the left and right hand sides of (5.46) with (5.26) and (5.36), respectively, we get (5.42).

Latency for delay-tolerant transmissions

Although the proposed adaptive network access mechanism requires end devices to predict the average latency for delay-sensitive transmissions to adapt to the network dynamics, we also analyze the latency experienced by delay-tolerant data. For that purpose, we recall that each active device begins to transmit delay-tolerant data packets after having a successful delay-sensitive transmission. Therefore, the latency experienced by an intended device's first delay-tolerant data packet is composed of the delay introduced by the successful delay-sensitive transmission and the number of (re)transmissions performed to transmit the delay-tolerant packet successfully.

Active devices can use their transmission history from the second half of the current window to predict the average latency for delay-tolerant transmissions. Let t_m denote the slot number in the m^{th} round in which the delay-sensitive packet from the intended is transmitted successfully, where $1 \leq t_m \leq N$. The intended device then performs $N - t_m$ delay-tolerant-transmissions in the m^{th} round. Thus, the average latency for a delay-tolerant transmission can be predicted as follows:

$$\widehat{\mu}_{\mathrm{dt}}^{(\mathrm{DRA})} := \widehat{\mu}_{\mathrm{ds}}^{(\mathrm{DRA})} + \frac{\sum_{m=R+1}^{2R} (N - t_m)}{\sum_{m=R+1}^{2R} \sum_{x=t_m+1}^{N} B_{m,x}}. \tag{5.47}$$

In (5.47), the term $\sum_{m=R+1}^{2R} (N - t_m)$ provides the total number of delay tolerant transmissions performed by the intended device, while the term $\sum_{m=R+1}^{2R} \sum_{x=t_m+1}^{N} B_{m,x}$ provides the number of successful delay-tolerant transmissions obtained by the intended device in R rounds. Thus the term $\frac{\sum_{m=R+1}^{2R}(N-t_m)}{\sum_{m=R+1}^{2R}\sum_{x=t_m+1}^{N} B_{m,x}}$ shows the average number of (re)transmissions per successful delay-tolerant transmission. By substituting (5.34) in (5.47), $\widehat{\mu}_{\mathrm{dt}}^{(\mathrm{DRA})}$ is computed by

$$\widehat{\mu}_{\mathrm{dt}}^{(\mathrm{DRA})} = \frac{R}{R - \sum_{m=1}^{R} A_{m,1}} + \frac{\sum_{m=R+1}^{2R} (N - t_m)}{\sum_{m=R+1}^{2R} \sum_{x=t_m+1}^{N} B_{m,x}}. \tag{5.48}$$

Thus we can see from (5.48) that end devices can use the transmission history of each window to predict the average latency of successful delay-tolerant transmission.

5.5.2 Prediction of Channel Utilization in the DRA Scheme

In order to predict the channel utilization, end devices need to predict the average successful delay-sensitive and delay-tolerant transmissions per round defined in (5.8) and (5.9), respectively. Once end devices have computed $\widehat{\Gamma}$, they can predict the average number of successful delay-sensitive transmissions per round as follows:

$$\widehat{\mathcal{S}}_{\text{ds}}^{(\text{DRA})} := \sum_{n=1}^{N} \widehat{V}_n \left(1 - \widehat{\beta}_n\right). \tag{5.49}$$

On the other hand, the devices can predict the number of delay-tolerant transmissions in each slot as follows:

$$\widehat{W}_n := \sum_{i=1}^{n-1} \widehat{V}_i \left(1 - \widehat{\beta}_i\right), \quad n = 2, 3, ..., N. \tag{5.50}$$

By applying (5.29) in (5.50), $\widehat{W}_n$ is computed as

$$\widehat{W}_n = \widehat{M} \left(1 - \prod_{i=1}^{n-1} \widehat{\beta}_i\right). \tag{5.51}$$

The number of channels reserved for delay-tolerant transmissions in each slot comes out be: $K - \widehat{K}_n,\ \forall n = 2, 3, ..., N$. The probability that the transmission of an intended device collides with at least one of the other devices transmitting their delay-tolerant data in the n^{th} slot, is predicted as

$$\widehat{\gamma}_n = 1 - \left(1 - \frac{1}{K - \widehat{K}_n}\right)^{\widehat{W}_n - 1}, \quad n = 2, 3, ..., N. \tag{5.52}$$

Thus the average number of successful delay-tolerant transmissions per round is predicted as:

$$\widehat{\mathcal{S}}_{\text{dt}}^{(\text{DRA})} := \sum_{n=2}^{N} \widehat{W}_n \left(1 - \widehat{\gamma}_n\right). \tag{5.53}$$

The channel utilization in the DRA is predicted as follows:

$$\begin{aligned}\widehat{\eta}^{(\mathrm{DRA})} &:= \frac{\widehat{\mathcal{S}}_{\mathrm{ds}}^{(\mathrm{DRA})} + \widehat{\mathcal{S}}_{\mathrm{dt}}^{(\mathrm{DRA})}}{KN}, \\ &= \frac{1}{KN}\left\{\sum_{n=1}^{N}\widehat{V}_n\left(1-\widehat{\beta}_n\right) + \sum_{n=2}^{N}\widehat{W}_n\left(1-\widehat{\gamma}_n\right)\right\}, \\ &= \frac{1}{KN}\left\{\sum_{n=1}^{N}\left(\widehat{V}_1\prod_{\substack{j=1\\n>1}}^{n-1}\widehat{\beta}_j\right)\left(1-\widehat{\beta}_n\right) + \sum_{n=2}^{N}\widehat{M}\left(1-\prod_{i=1}^{n-1}\widehat{\beta}_i\right)\left(1-\widehat{\gamma}_n\right)\right\}.\end{aligned} \tag{5.54}$$

Finally, end devices can approximate $\widehat{\eta}^{(\mathrm{DRA})}$ using $\widehat{\beta}_n \simeq \widehat{\alpha}_1,\ \forall n = 1, 2, ..., N$ in (5.54) as follows:

$$\widehat{\eta}^{(\mathrm{DRA})} \simeq \frac{1}{KN}\left\{\widehat{M}\sum_{n=1}^{N}\widehat{\alpha}_1^{n-1}\left(1-\widehat{\alpha}_1\right) + \widehat{M}\sum_{n=2}^{N}\left(1-\widehat{\alpha}_1^{n-1}\right)\left(1-\widehat{\gamma}_n\right)\right\}. \tag{5.55}$$

(5.55) is simplified to

$$\widehat{\eta}^{(\mathrm{DRA})} \simeq \frac{\widehat{M}}{KN}\left[N - \sum_{n=1}^{N}\widehat{\alpha}_1^{n} - \sum_{n=2}^{N}\left(1-\widehat{\alpha}_1^{n-1}\right)\left\{1-\left(1-\frac{1}{K-\widehat{K}_n}\right)^{\widehat{M}\left(1-\widehat{\alpha}_1^{n-1}\right)-1}\right\}\right]. \tag{5.56}$$

Since computation of $\widehat{K}_n$ also depends on $\widehat{M}$ and $\widehat{\alpha}_1$, we can readily show that for the given values of N, K, and R, the channel utilization of the DRA in (5.56) becomes a function of $\widehat{M}$ and $\widehat{\alpha}_1$. While the closed-form expressions of both $\widehat{M}$ and $\widehat{\alpha}_1$ use the on-device transmission history. Therefore, the statistical learning-based network exploration enables end devices to predict each scheme's average latency and channel utilization in closed form.

Accuracy in predicting average latency and channel utilization for the SRA and DRA schemes is evaluated using the mean square error (MSE) criterion. The MSE in the prediction of $\eta^{(\mathrm{DRA})}$ is denoted by $\mathrm{MSE}_{\eta}^{(\mathrm{DRA})}$ and defined as

$$\mathrm{MSE}_{\eta}^{(\mathrm{DRA})} := \mathrm{E}\left[\left(\eta^{(\mathrm{DRA})} - \widehat{\eta}^{(\mathrm{DRA})}\right)^2\right]. \tag{5.57}$$

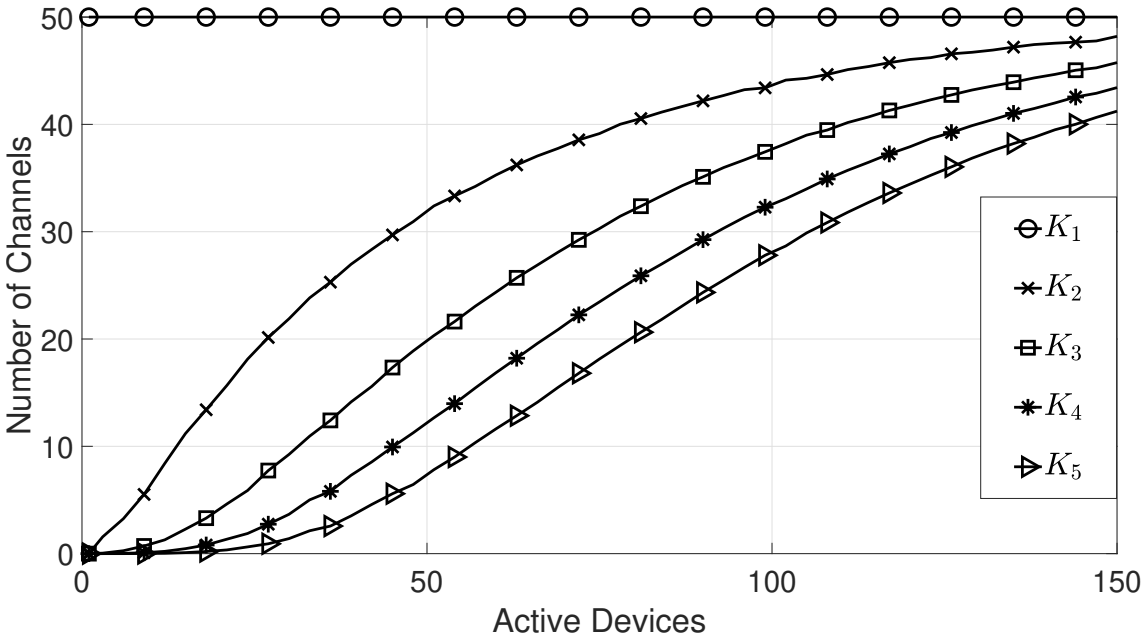

Figure 5.4: Average number of channels available for delay-sensitive transmissions in each slot with $K = 50$ and $N = 5$.

The MSE in the prediction of $\mu_{\text{ds}}^{(\text{DRA})}$ is denoted by $\text{MSE}_{\mu}^{(\text{DRA})}$ and defined as

$$\text{MSE}_{\mu}^{(\text{DRA})} := \text{E}\left[\left(\mu_{\text{ds}}^{(\text{DRA})} - \widehat{\mu}_{\text{ds}}^{(\text{DRA})}\right)^2\right]. \tag{5.58}$$

The MSE in predicting different parameters related to the SRA scheme decreases as the size of transmission history is increased [111]. In the following section we demonstrate that the MSE in the prediction of average latency and channel utilization for the DRA scheme also decreases as the size of transmission history is increased.

The complexity of Algorithm-3 is described in terms of the time required to predict desired parameters. The *Network Exploration Phase* is spanned over R rounds, where each round is composed of N slots. Therefore, for a given maximum acceptable MSE in predicting each parameter, the optimal number of rounds in the *Network Exploration Phase* can be computed by following [111]. Furthermore, Algorithm-2 allows each active device to have one successful delay-sensitive transmission per round in the *Network Exploration Phase*. In addition to that, Algorithm-2 operates in an online manner as devices use their transmission history to predict desired parameters by employing closed-form expressions (26), (28), (34), and (36). On the other hand, if the current network load allows, end devices choose the DRA scheme and perform transmission in each slot of the next R round, as explained in Section-

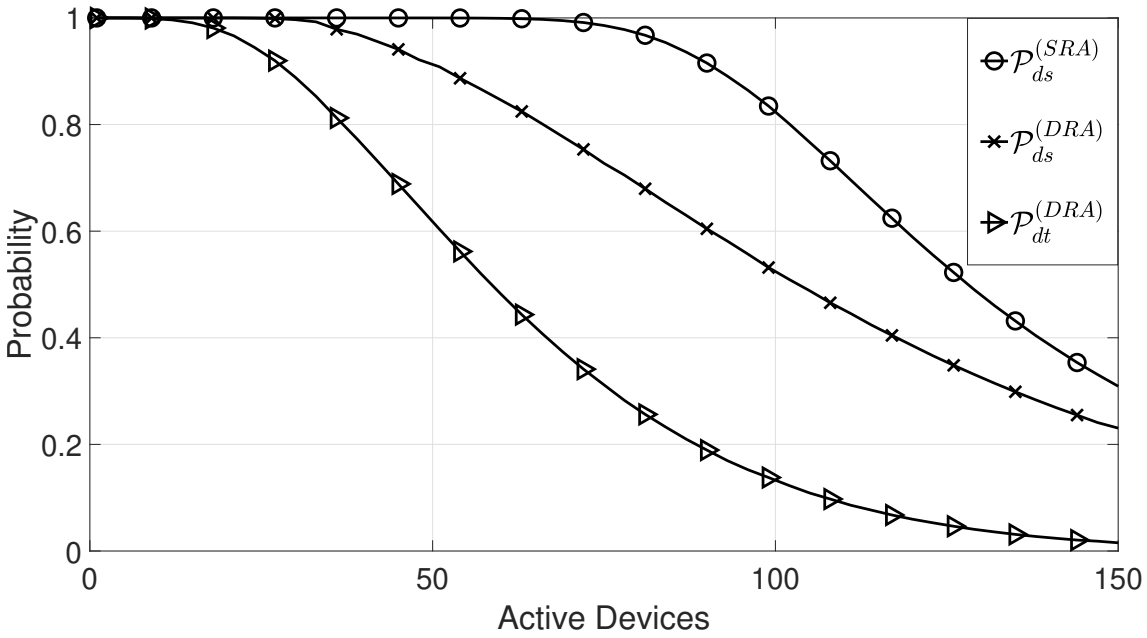

Figure 5.5: Average probabilities of successful delay-sensitive and delay-tolerant transmissions per round with $K = 50$ and $N = 5$.

5.4. These features of the proposed adaptive network access make it suitable for IIoT networks where devices have limited computation power.

Moreover, in this chapter, all active devices undergo network exploration in each window to predict the current network load. However, the frequency of executing the *Network Exploration Phase* depends on how frequently the network load varies. In our future work, we intend to incorporate the nature of network load variation to determine the frequency of executing the *Network Exploration Phase*.

5.6 Simulation Results and Discussion

This section presents simulation results of the proposed adaptive network access mechanism. Along with analyzing different parameters related to the proposed DRA scheme, we also compare average latency and channel utilization of the DRA scheme with the SRA and conventional MSA systems. We apply the Monte Carlo simulation method with $K = 50$ channels and $N = 5$ slots per round for several active devices, while $R = 10,000$ independent rounds are used to analyze the behavior of different parameters against the varying network load. The average number of channels (K_n), computed by $K_n = \frac{1}{R}\sum_{m=1}^{R} K_{m,n}$, reserved for delay-sensitive transmissions in each slot are plotted in Figure 5.4. The average number of channels allocated for delay-

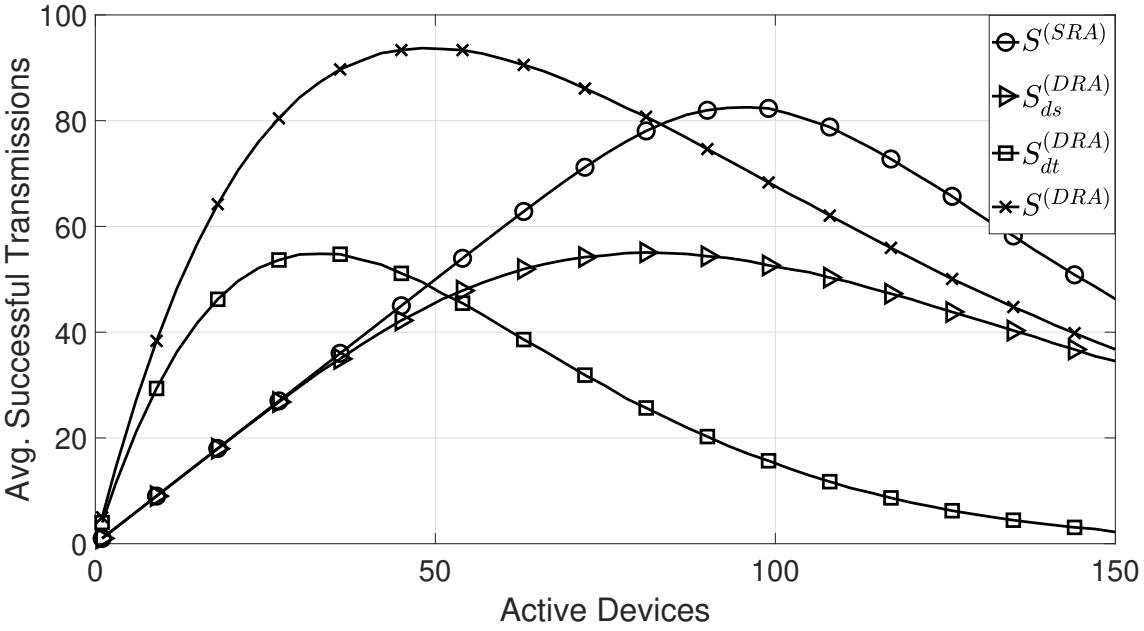

Figure 5.6: Average successful delay-sensitive and delay tolerant transmissions per round with $K = 50$ and $N = 5$.

tolerant transmissions can be computed as: $K - K_n$. It is observed that for the given network load, K_n decreases in each slot; however, it approaches K when the number of active devices increases.

Figure 5.5 plots $\mathcal{P}_{\text{ds}}^{(\text{DRA})}$ and $\mathcal{P}_{\text{dt}}^{(\text{DRA})}$ for the DRA scheme. In Figure 5.5, we have also plotted the average probability of a successful delay-sensitive transmission per round ($\mathcal{P}_{\text{ds}}^{(\text{SRA})}$) in the SRA scheme defined by [111, Eq. (11)]. We can observe that $\mathcal{P}_{\text{ds}}^{(\text{SRA})}$ and $\mathcal{P}_{\text{ds}}^{(\text{DRA})}$ are similar for the lower network load. However, $\mathcal{P}_{\text{ds}}^{(\text{SRA})}$ is higher than $\mathcal{P}_{\text{ds}}^{(\text{DRA})}$ when the number of active devices becomes large. On the other hand, $\mathcal{P}_{\text{dt}}^{(\text{DRA})}$ follows $\mathcal{P}_{\text{ds}}^{(\text{SRA})}$ and $\mathcal{P}_{\text{ds}}^{(\text{DRA})}$ when the number of active devices is very small, and becomes significantly less than $\mathcal{P}_{\text{ds}}^{(\text{SRA})}$ and $\mathcal{P}_{\text{ds}}^{(\text{DRA})}$ when network load increases.

Figure 5.6 plots $\mathcal{S}_{\text{ds}}^{(\text{DRA})}$, $\mathcal{S}_{\text{dt}}^{(\text{DRA})}$, and $\mathcal{S}^{(\text{DRA})}$ defined in (5.8), (5.9), and (5.10), respectively. Moreover, Figure 5.6 also plots the average number of successful delay-sensitive transmissions ($\mathcal{S}^{(\text{SRA})}$) in the SRA scheme computed through [111, Eq. (2)]. It is observed that $\mathcal{S}^{(\text{SRA})}$ is similar to $\mathcal{S}_{\text{ds}}^{(\text{DRA})}$ for low to moderate network load; however, $\mathcal{S}^{(\text{SRA})}$ becomes higher than $\mathcal{S}_{\text{ds}}^{(\text{DRA})}$ when the number of active devices increases. On the other hand, $\mathcal{S}_{\text{dt}}^{(\text{DRA})}$ is higher than both $\mathcal{S}_{\text{ds}}^{(\text{SRA})}$ and $\mathcal{S}_{\text{ds}}^{(\text{DRA})}$ under low to moderate network load. However, $\mathcal{S}_{\text{dt}}^{(\text{DRA})}$ decreases rapidly when the number of active devices gets larger. Furthermore, $\mathcal{S}^{(\text{DRA})}$ is higher than $\mathcal{S}^{(\text{SRA})}$ for relatively

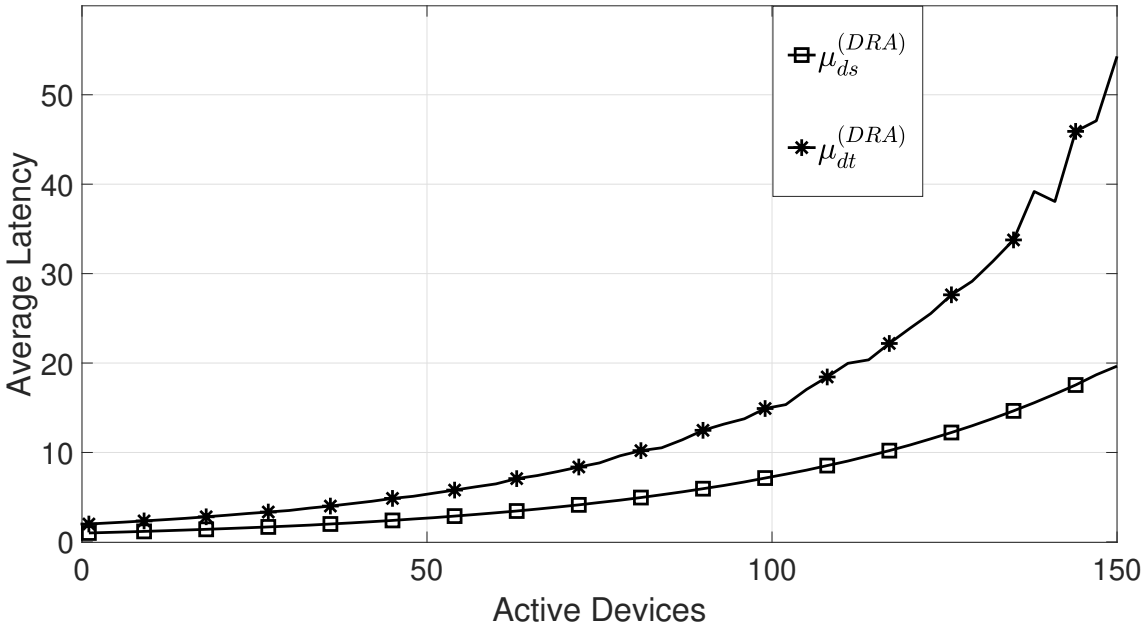

Figure 5.7: Average latency for a successful delay-sensitive and delay-tolerant transmissions with $K = 50$ and $N = 5$.

lower network load; however for moderate to high network load $\mathcal{S}^{(\mathrm{SRA})}$ is greater than $\mathcal{S}^{(\mathrm{DRA})}$. Finally, both $\mathcal{S}_{\mathrm{ds}}^{(\mathrm{SRA})}$ and $\mathcal{S}^{(\mathrm{DRA})}$ approach zero when M becomes too large.

Figure 5.7 plots the average latency for a successful delay-sensitive and delay-tolerant transmissions under the DRA scheme denoted by $\mu_{\mathrm{ds}}^{(\mathrm{DRA})}$, and $\mu_{\mathrm{dt}}^{(\mathrm{DRA})}$ respectively. We compute $\mu_{\mathrm{ds}}^{(\mathrm{DRA})}$ from (5.40) while replacing $\widehat{\beta}_n$ with $\frac{1}{R}\sum_{m=1}^{R}\beta_{m,n}$. On the other hand, we compute $\mu_{\mathrm{dt}}^{(\mathrm{DRA})}$ from (5.47) while replacing $\widehat{\mu}_{\mathrm{ds}}^{(\mathrm{DRA})}$ with $\mu_{\mathrm{ds}}^{(\mathrm{DRA})}$. Since delay-tolerant data is transmitted after successful delay-sensitive transmission, it is observed that $\mu_{\mathrm{dt}}^{(\mathrm{DRA})}$ is significantly higher than $\mu_{\mathrm{ds}}^{(\mathrm{DRA})}$ for the whole range of the number of active devices. Figure 5.8 plots the average latency for a successful delay-sensitive transmission offered by the SRA and DRA schemes. We compute average latency in the SRA scheme, denoted by $\mu_{\mathrm{ds}}^{(\mathrm{SRA})}$, using [111, Eq. (37)]. It is observed that $\mu_{\mathrm{ds}}^{(\mathrm{SRA})}$ and $\mu_{\mathrm{ds}}^{(\mathrm{DRA})}$ show similar behavior for low network load. However, as the number of active devices increases, accommodating delay-tolerant transmissions in the grant-free access with dynamic resource allocation results in higher latency. Therefore, the SRA scheme is more suitable under higher network load for delay-sensitive transmissions.

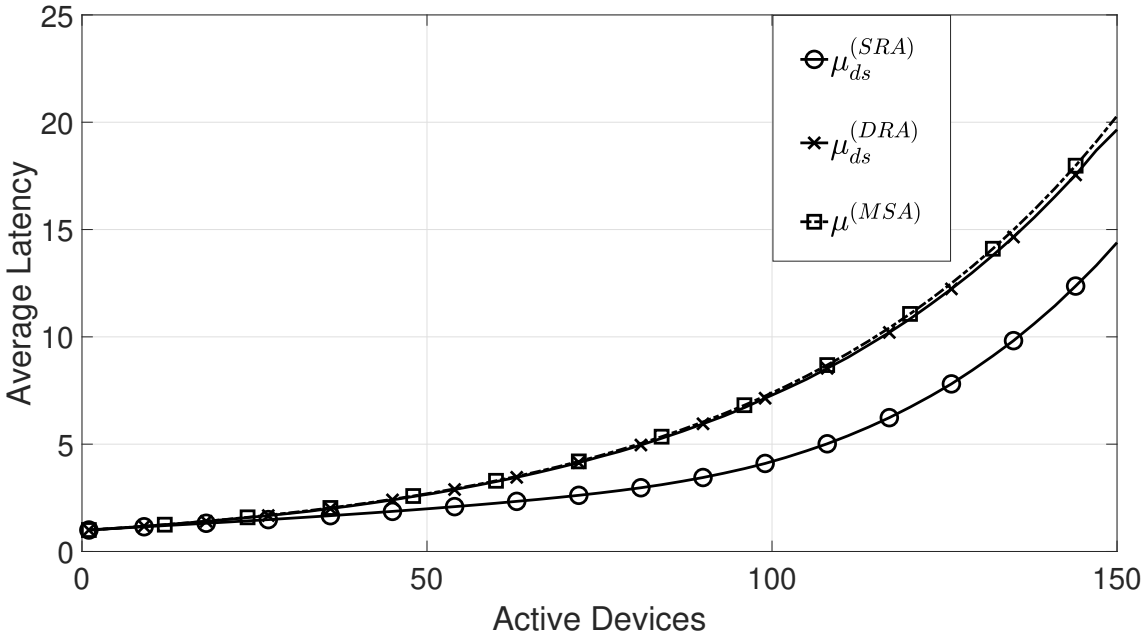

Figure 5.8: Performance comparison in terms of the average latency with $K = 50$ and $N = 5$.

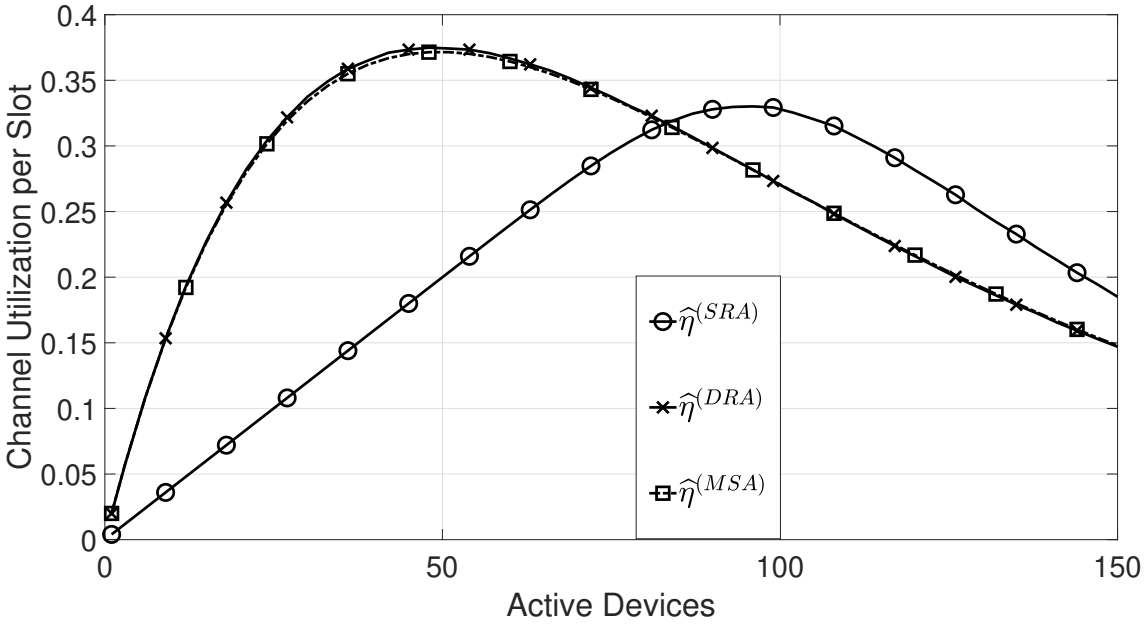

Figure 5.9: Performance comparison in terms of the channel utilization with $K = 50$ and $N = 5$.

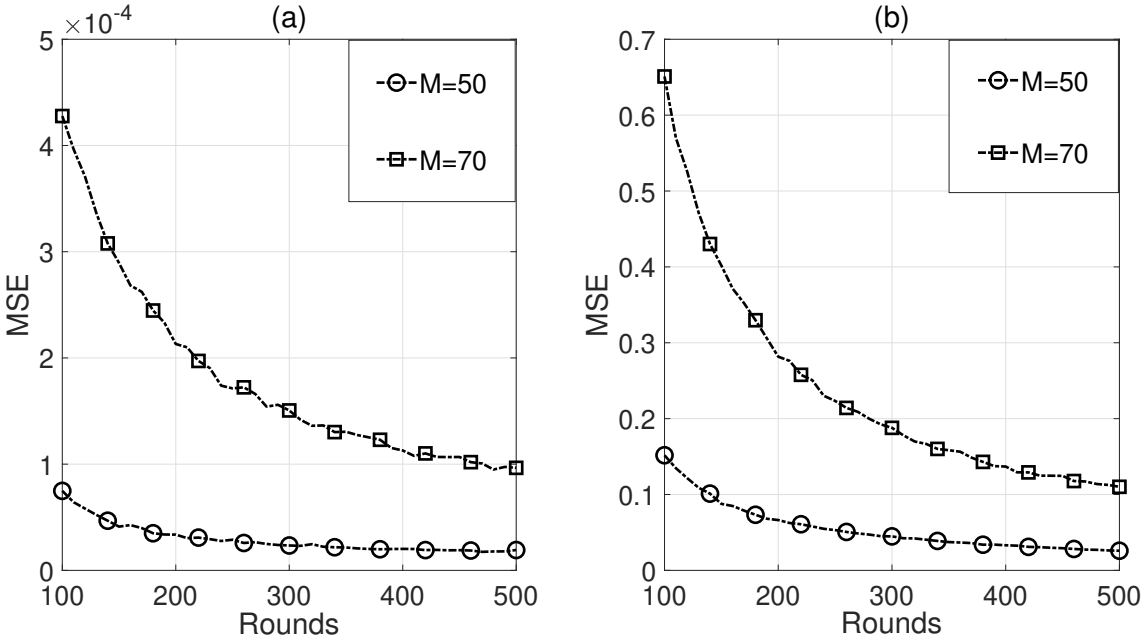

Figure 5.10: Prediction accuracy against number of rounds with $K = 50$ and $N = 5$: (a) MSE in device-level prediction of $\eta^{(\mathrm{DRA})}$. (b) MSE in device-level prediction of $\mu_{\mathrm{ds}}^{(\mathrm{DRA})}$.

Figure 5.9 demonstrates channel utilization in the DRA and SRA schemes denoted by $\eta^{(\mathrm{DRA})}$ and $\eta^{(\mathrm{SRA})}$, respectively. Where $\eta^{(\mathrm{DRA})}$ is defined in (5.12), and $\eta^{(\mathrm{SRA})} := \frac{\mathcal{S}^{(\mathrm{SRA})}}{KN}$. It is observed that $\eta^{(\mathrm{DRA})}$ is higher than $\eta^{(\mathrm{SRA})}$ for a relatively lower network load. While, for moderate to higher network load, $\eta^{(\mathrm{SRA})}$ becomes larger than $\eta^{(\mathrm{DRA})}$. Both $\eta^{(\mathrm{DRA})}$ and $\eta^{(\mathrm{SRA})}$ depict similar asymptotic behaviour against M. Figure 10(a) and Figure 10(b) plot the MSE in device-level prediction of $\eta^{(\mathrm{DRA})}$ and $\mu_{\mathrm{ds}}^{(\mathrm{DRA})}$, respectively, where $10,000$ iterations are performed to compute the MSE for each number of rounds. It is observed that under a given network load, the MSEs in predicting channel utilization and average latency decrease as the number of rounds in the *Network Exploration Phase* increases.

5.6.1 Performance Comparison

We compare the performance of the proposed adaptive network access with the conventional MSA systems. In the MSA systems, every active device selects a channel randomly and independent in each slot without executing any learning strategy. The average latency in the MSA system $\left(\mu^{(\mathrm{MSA})}\right)$ is defined as: $\mu^{(\mathrm{MSA})} := \frac{1}{\left(1-\frac{1}{K}\right)^{M-1}}$. Since the probability of collision in each slot is almost constant under the DRA scheme, Figure 5.8 shows that $\mu_{\mathrm{ds}}^{(\mathrm{DRA})}$ is similar to $\mu^{(\mathrm{MSA})}$. We also plot the channel

utilization of the MSA system defined as $\eta^{(\mathrm{MSA})} := \frac{M}{K}\left(1-\frac{1}{K}\right)^{M-1}$. As demonstrated in Figure 5.9, the channel utilization in the DRA scheme is similar to that of the MSA systems.

It is noteworthy that channel utilization in the DRA scheme is based upon dynamic resource allocation of the available resources in each slot for delay-sensitive and delay-tolerant transmission. On the contrary, channel utilization in the MSA systems does not incorporate dynamic resource allocation. Moreover, the proposed grant-free access scheme separates the devices transmitting delay-sensitive data from those transmitting delay-tolerant data in each slot. This separation is based on the subset of channels used for each transmission type. Therefore, allowing end devices to share $\widehat{\Gamma}$ with the BS, the DRA scheme can enable the BS to distinguish between delay-sensitive and delay-tolerant transmissions. The BS in turn can use this knowledge to optimize the number of channels in $\mathcal{C}$.

Moreover, the above discussion highlights that DRA and SRA schemes have advantages under different network loads. Thus the proposed adaptive network access enables end devices to choose the appropriate scheme for a given network load. Therefore, in contrast to the conventional MSA-based systems where devices do not employ any learning strategy, the proposed adaptive network access enables the end devices to adapt to the network dynamics.

5.7 Conclusion

Uplink-dominant IIoT networks operate under time-varying network load and generate data with diverse QoS requirements. Therefore, adaptive network access mechanisms are essential to utilize available shared radio resources efficiently. This chapter uses a statistical learning approach to enable end devices to perform delay-sensitive and delay-tolerant transmissions over dynamically partitioned resources in a grant-free manner. Consequently, the proposed DRA scheme accommodates delay-tolerant transmissions under favorable network conditions while delay-sensitive transmissions follow the prescribed latency bound. Moreover, devices perform random back-off in case of an outage providing fairness to newly active devices in accessing shared radio resources. The resultant adaptive network access mechanism enables end devices to

choose an appropriate network access strategy under time-varying network load. In contrast to the existing centralized network access methods, the proposed mechanism operates in a semi-distributed manner and avoids excessive feedback overheads while adaptively managing two different types of network traffic.

This chapter classified data generated in IIoT networks into delay-sensitive and delay-tolerant types. Moreover, the proposed adaptive network access considers the same latency bound for all devices in an IIoT network. Our future research aims to design an adaptive network access mechanism suitable for heterogeneous IIoT networks by accommodating multiple latency requirements.

Chapter 6

Multi-Agent Multi-Armed Bandit Learning for Grant-Free Access in Ultra-Dense IoT Networks

This chapter is based on the following research paper submitted to IEEE Transactions on Cognitive Communications and Networking. Additional results are also added in this chapter:

M. A. Raza, M. Abolhasan, J. Lipman, N. Shariati, W. Ni, and A. Jamalipour, *"Multi-Agent Multi-Armed Bandits Learning-based Grant-Free Access for Ultra-Dense IoT Networks,"* submitted to IEEE Transactions on Cognitive Communications and Networking, 2023.

6.1 Introduction

The growing number of devices and the increasing diversity in their quality-of-service (QoS) requirements are among the key characteristics of Internet of Things (IoT) applications envisioned by the fifth generation (5G) and future wireless networks [109]. Ultra-reliable and low latency communication (URLLC)-based industrial IoT networks cannot afford the excessive control signaling overheads offered by centralized coordination [3, 61, 101]. Moreover, diversity in the amounts and patterns of data generated by end devices introduces additional complexity in the network design.

Furthermore, energy consumption in battery-powered IoT devices is another critical design parameter that affects the overall performance of a network [76, 112-114].

The characteristics mentioned earlier of IoT networks make it challenging to use the available shared radio resources efficiently in the dense and uplink communication dominant networks. Grant-free medium access control (MAC) avoids the control signaling overheads inherent in grant-based network access protocols, thus making it suitable for latency-critical IoT applications. However, as the number of transmitting devices increases, the efficiency of contention-based network access mechanisms deteriorates due to collisions. The spectral efficiency of grant-free access mechanisms can be improved using power-domain non-orthogonal multiple access (NOMA)-based data transmission [115]. Regarding the design of the PHY layer in IoT networks, under the incomplete knowledge of a channel's probability distribution function (PDF), the URLLC transmitter can use statistical learning methods to estimate the corresponding PDF. As a result of this statistical learning step, the transmitter can choose the maximum transmission rate under any given reliability constraint [38, 116].

Distributed network access can potentially avoid excessive control signalling overheads caused by centralized systems. Therefore, the use of distributed machine learning techniques has gained considerable attention in designing wireless networks supporting dense and heterogeneous IoT networks [109, 117]. Multi-armed bandits (MAB) learning paradigm has emerged as a promising tool to enhance the performance of distributed network access, and resource scheduling for 5G and future wireless networks [39-41]. In existing multi-agent MAB learning-based spectrum access methods, channels are treated as arms and users behave as agents. Active users choose an arm to perform the uplink data transmission in each time slot. As a result of these actions, each user obtains a reward following a reward distribution unknown to the users. Thus by exploring different channels, the users improve their knowledge of network conditions over time. The expected difference between the observed and optimal rewards is called regret, which is a key performance indicator. The multi-agent MAB learning-based network access mechanisms aim to achieve a sub-linear cumulative regret, as time increases.

The multi-agent MAB learning is used to address different aspects of IoT networks. This learning framework enables end devices to efficiently use shared radio resources in heterogeneous IoT networks where a group of devices transmits over fixed channels while other devices randomly select a channel for uplink data transmission [83, 84]. Since a channel can behave differently for different users depending on their locations in the network, designing an appropriate distributed network access mechanism becomes even more challenging. Multi-agent MAB learning employing heterogeneous reward distributions can potentially address the problem of distributed network access in a dynamic environment [82, 85-88]. Although many existing works assume that the users accessing the same channel get zero rewards due to collision, multi-agent MAB learning has also been used to address network access problems, where reward distribution for colliding users is non-zero [89-92]. Moreover, by installing multiple BSs in dense IoT networks, distributed network access can potentially meet the diverse latency requirements.

The existing works employing multi-agent MAB learning for distributed spectrum access primarily focus on the physical characteristics of shared radio resources by incorporating appropriate channel models. However, considering physical layer abstraction, for the given number of channels and a transmission scheme, the number of active devices becomes a key parameter impacting the reward observed by each user. Since the number of active devices is random, devices can update their exploration strategy accordingly by predicting the current network load. A related parameter is the maximum number of active devices supported by a particular network access mechanism under a given latency-reliability criterion. Thus the number of devices performing uplink data transmissions over shared channels needs to be controlled accordingly. Therefore, device-level network exploration is essential to enable end devices to adapt to the network dynamics [117]. To this end, active devices can use their transmission history to predict different network parameters, including current network load and average latency by employing statistical learning approach [104, 111].

In this chapter, we consider dense IoT networks having multiple BSs and a large number of devices. The devices are classified as delay-sensitive and delay-tolerant devices. Active devices communicate with a selected BS using the grant-free ac-

cess proposed in [111]. Firstly, under the given number of channels and a latency-reliability criterion, we compute the maximum number of active devices supported by the grant-free access scheme of [111]. Later, we propose a two-stage distributed network access control using multi-agent MAB learning. The proposed mechanism limits the number of active devices, according to the maximum network load support. Moreover, it enables the end devices to choose a BS that can meet the desired latency-reliability criterion in a dynamic environment. A key feature of this mechanism is that, instead of using dedicated training data, it relies on the devices' transmission history to predict different network parameters. The key contributions of this chapter are summarized as follows:

- We propose a multi-agent MAB learning-based grant-free access (MAB-GFA) mechanism in which devices are enabled to perform a Bernoulli bandit learning-based adaptive BS selection strategy. Consequently, the end devices improve their BS selection choice over the time, maximizing the number of devices meeting a given latency-reliability criterion.

- To analyze the convergence of the proposed MAB-GF mechanism, we compute the expected time to reach the stable state when the number of devices performing exploration becomes zero. Moreover, simulation results show that the proposed mechanism achieves a sub-linear regret against time.

- We design a distributed device elimination (DDE) mechanism that enables the end devices to predict excessive network load as a difference between the active devices and maximum network load support. Consequently, the DDE phase probabilistically limits the number of devices performing MAB-GF-based uplink data transmission.

Simulations are performed to compare the performance of the proposed mechanism with the random BS selection (RBSS) strategy in which devices do not employ any learning scheme. Results show that the proposed MAB-GFA mechanism outperforms the RBSS approach regarding the average number of devices meeting the desired latency-reliability criterion as time increases. Moreover, we present a centralized medium access control (CMAC) as an alternative to the proposed distributed network access mechanism. Under the CMAC approach, each BS controls the num-

ber of devices performing uplink transmission over that BS. Simulation results show that the performance of the proposed MAB-GFA mechanism increasingly approaches that of the CMAC method as time elapses.

The rest of this chapter is organized as follows: Section-6.2 describes the system and transmission models used in this chapter. Section-6.3 discusses the initialization phase of the proposed method. The multi-agent MAB learning-based data transmission phase is presented in Section-6.4. Simulation results are discussed in Section-6.5. Finally, the chapter is concluded in Section-6.7.

6.2 System Model

As shown in Figure 6.1, we consider the uplink communication scenario in a massive IoT network composed of B BSs, M_{ds} delay-sensitive devices, and M_{dt} delay-tolerant devices deployed in a relatively small geographical area. We have $M_{\text{o}} = M_{\text{ds}} + M_{\text{dt}}$, and devices are labelled uniquely from the set $\mathcal{M} = \{1, ..., M_{\text{o}}\}$. The devices in the delay-sensitive class generate data that exhibit strict latency requirements, compared to the latency requirements of devices in the delay-tolerant class. The BSs are indexed uniquely from a set $\mathcal{B} = \{1, 2, ...B\}$. Each BS is equipped with K_i non-overlapping and orthogonal channels to be used by the end devices for uplink data transmission. The set $\omega_i = \left\{C_i^{(1)}, C_i^{(2)}, ..., C_i^{(K_i)}\right\}$ contains the channels allocated to BS-i. An initialization phase composed of B number of slots is used to broadcast the resource information of each BS. Each BS uses a shared channel to broadcast its resource information in a dedicated time slot from this phase. The index of a BS also represents the sequence number of a control slot assigned to that BS. Thus the network utilizes $\sum_{i=1}^{B} K_i$ uplink data channels and one downlink control channel.

An epoch is defined as a sequence of R rounds, where each round is composed of N slots. The time duration of each slot, measured in milliseconds, is denoted by T_s. Figure 6.2 shows the structure of a window composed of an initialization phase comprising B time slots, a DDE phase (epoch-0), and a multi-agent MAB learning-based data transmission phase spanned over $T_{\max}$-epochs. At the start of each window, M devices are activated, where M is random and $M \leq M_{\text{o}}$. The numbers of active delay-sensitive and delay-tolerant devices are denoted by X_{ds} and

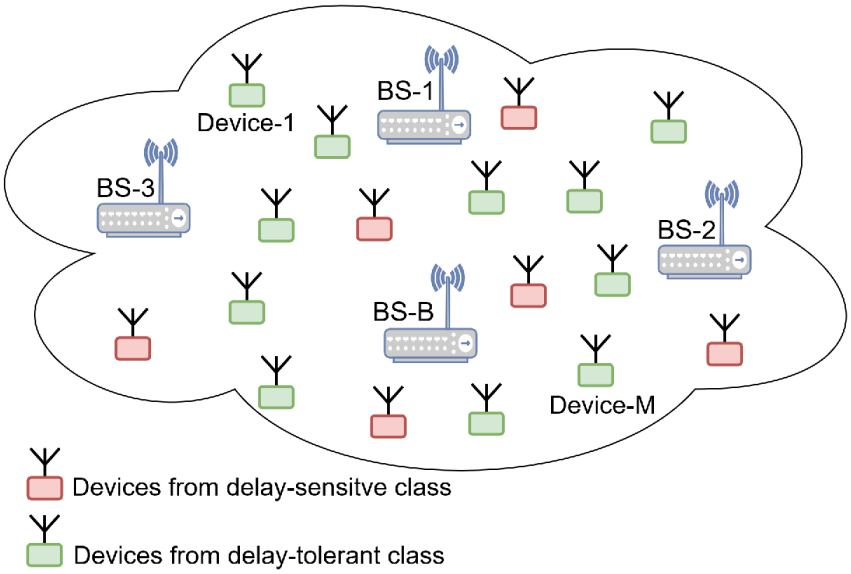

Figure 6.1: Active IoT devices from delay-sensitive and delay-tolerant classes are performing uplink data transmission employing the proposed the MAB-GFA mechanism in a dynamic environment.

Y_{dt}, respectively, where $M = X_{\text{ds}} + Y_{\text{dt}}$. It is assumed that M, X_{ds} and Y_{dt} do not change in a given window. However, the analysis presented in this chapter does not assume any specific probability distributions associated with the random variables M, X_{ds} and Y_{dt}.

6.2.1 Transmission Model

In the proposed multi-agent MAB learning paradigm, each BS is an arm while each active device acts as an agent. In each epoch, the active devices select a BS according to the proposed adaptive BS selection mechanism and perform uplink data transmission employing grant-free access. An intended device executes the exploration step in an epoch if it performs the BS selection step. On the other hand, an exploitation action is a case when the intended device keeps the same BS in the current epoch as selected in the last epoch. An intended device's state in epoch-t represents the BS selected by that device due to the exploration or exploitation activities.

The MAB-GFA mechanism proposed in this chapter is generic and can be adapted for any grant-free transmission scheme. We use the grant-free access scheme proposed in Chapter 4, which is based on [111], to support delay-sensitive transmissions.

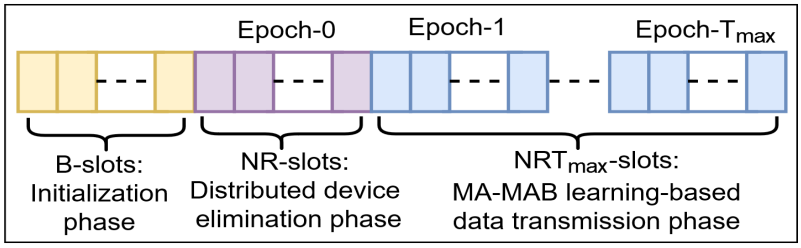

Figure 6.2: Structure of a window in the proposed MAB-GFA mechanism.

Under this scheme, all active devices start transmitting at the start of a round and can have only one successful transmission per round. Considering PHY-layer abstraction, an uplink data transmission with BS-i remains unsuccessful if two or more devices select the same channel and this event is called collision. Moreover, due to the high density of installed devices, each BS is assumed to be accessible to all devices. However, under the given PHY-layer design parameters, the minimum transmission power for uplink data transmission depends on the distance between a BS and the transmitting device. In this chapter, we assume that each device knows the transmit power threshold of each BS.

6.2.2 Latency and Reliability Model

The application-specific latency bound ($\mathcal{L}_{\max}$) represents the maximum number of (re)transmissions allowed to get a successful transmission. Outage is defined as an event when the number of (re)transmissions increases $\mathcal{L}_{\max}$. Let the random variable L denote the number (re)transmissions performed by an active device to have successful transmission. Under given M and K_i, the probability of outage is computed by

$$\mathcal{P}_{\text{out}}\left(M, K_i\right) = 1 - \sum_{t=1}^{\mathcal{L}_{\max}} \Pr\left(L = t \mid M, K_i\right). \tag{6.1}$$

The reliability is defined as the probability of meeting a latency bound ($\mathcal{L}_{\max}$). Let ϵ_r be the application-specific reliability criterion, a network provides desired QoS as long as $\mathcal{P}_{\text{out}}\left(M, K_i\right) \leq \epsilon_r$. Thus a smaller value of ϵ_r corresponds to a higher level of reliability. All active devices are assumed to have common values of $\mathcal{L}_{\max}$ and ϵ_r. The maximum number of active devices that BS-i can support under the given

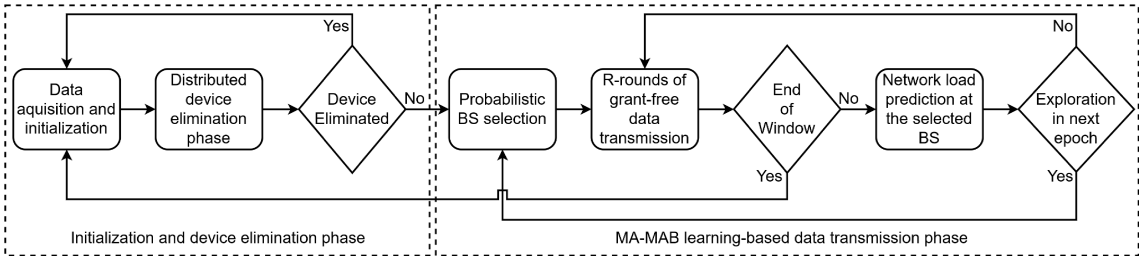

Figure 6.3: Flow chart of the proposed the MAB-GFA mechanism, each device executes independently.

latency-reliability criteria is denote by ζ_i. We define $\Gamma = \{\zeta_1, \zeta_2, ..., \zeta_B\}$, and the maximum network load support $\zeta_{\max} := \sum_{i=1}^{B} \zeta_i$.

In this chapter, our objective of designing an the MAB-GFA mechanism has two folds: first, we aim to design a DDE phase that limits the number of active devices according to a given $\zeta_{\max}$. Second, we aim to the enable end devices to perform an adaptive BS selection strategy in which the devices from the delay-sensitive class are prioritized to select a BS with a higher number of resources, resulting in lower average latency. Figure 6.3 demonstrates the overall flow of the proposed MAB-GFA mechanism to be executed by the active devices. At the same time, Algorithm-4 explains the execution of each step of the MAB-GFA protocol. In the following sections, we present analytical details of stages involved in the proposed the MAB-GFA mechanism.

6.3 Initialization Phase

The initialization phase is composed of B slots. Each BS uses a shared channel to broadcast ω_i and ζ_i in a dedicated time slot. Under a given latency-reliability criterion, the maximum number of devices supported by BS-i is

$$\zeta_i := \sup_{M} \{M \geq 1;\ \mathcal{P}_{\text{out}}(M, K_i) \leq \epsilon_r\}. \tag{6.2}$$

To compute ζ_i, we first need to obtain the PMF of random variable L. As explained in the transmission model, the grant-free scheme considered in this chapter allows each active device to have only one successful transmission per round. Therefore, the number of transmitting devices in each slot of a round is random. Let M_i be

Algorithm 4 MAB Learning-based Network Access

Require: $\mathcal{B}$, Φ, N, $T_{\max}$

for Initialization Slots: $i = 1 : B$ **do**
  Get ω_i and ζ_i from BS-i in the respective slot
end for
Exploration-Flag := 1, $t := 1$
Select a BS from $\mathcal{B}$ following uniform distribution
Perform R transmission rounds over the selected BS
Compute $\widehat{D}$ using (6.23)
if $\widehat{D} > 0$ **then**
  Compute $\widehat{\beta}_0$ using (6.26)
  Generate a Bernoulli random variable $X_{i,0}^{(d)}$
else
  $X_{i,0}^{(d)} := 0$
end if
if $X_{i,0}^{(d)} == 0$ **then**
  while $t \leq T_{\max}$ **do**
    if Exploration-Flag == 1 **then**
      Select a BS from $\mathcal{B}$ following PMF given in (6.5)
    else
      Keep the BS selected in epoch-$t-1$
    end if
    Perform R transmission rounds over the selected BS
    Predict $\widehat{M}_{i,t}$ using (6.6)
    if $\widehat{M}_{i,t} > \zeta_i$ **then**
      Compute $\widehat{\beta}_{i,t}$ using (6.9)
      Generate a Bernoulli random variable $X_{i,t}^{(d)}$
      Exploration-Flag := $X_{i,t}^{(d)}$
    else
      Exploration-Flag := 0
    end if
    $t := t + 1$
  end while
else
  Wait for the next window
end if

the number of devices connected with BS-i in a given epoch. The average probability that an intended device's transmission remains unsuccessful in the n^{th} slot is computed as [111]:

$$\alpha_n := \frac{1}{R} \sum_{m=1}^{R} \left\{ 1 - \left(1 - \frac{1}{K_i} \right)^{M_{m,n}-1} \right\}, \tag{6.3}$$

where $n = 1, 2, ..., N$ and $M_{m,n}$ is the number of transmitting devices in the n^{th} slot of

the m^{th} round with $M_{m,1} = M_i \ \forall m = 1, 2, ..., R$. We define $\Theta = [M, \alpha_n, \alpha_2, ..., \alpha_N]$. For a given Θ, the probability that an intended device performs L retransmissions for a successful transmission is

$$\Pr\left(L = t \mid M, K_i\right) = \begin{cases} \left(1-\alpha_1\right)\left(\prod_{n=1}^{N}\alpha_n\right)^{\lfloor\frac{t}{N}\rfloor} \\ \qquad t = 1, N+1, 2N+1, ... \\ \left(1-\alpha_{t \bmod N}\right)\left(\prod_{n=1}^{(t \bmod N)-1}\alpha_n\right)\left(\prod_{n=1}^{N}\alpha_n\right)^{\lfloor\frac{t}{N}\rfloor} \\ \qquad t = 2, 3, ... \left(N-1\right), \left(N+2\right), ... \left(2N-1\right), ... \\ \left(1-\alpha_N\right)\left(\prod_{n=1}^{N-1}\alpha_n\right)\left(\prod_{n=1}^{N}\alpha_n\right)^{\frac{t}{N}-1} \\ \qquad t = N, 2N, ... \end{cases} \tag{6.4}$$

Please see Subsection-6.6.1 for the detailed derivation of (6.4).

The parameter $\zeta_i, \ \forall i = 1, 2, ..., B$ can be computed offline, and each BS knows its network load support in prior. To compute ζ_i, we use MATLAB to generate R independent samples of $M_{m,n}, \ \forall n = 1, 2, ..., N$ against a range of M, and compute α_n using (6.3). Thus for each value of M, we compute $\Pr\left(L = t \mid M, K_i\right)$ by substituting (6.3) in (6.4). The outage probability under a given M is computed by applying the resultant PMF in (6.1). Finally, ζ_i is obtained using $\mathcal{P}_{\text{out}}\left(M, K_i\right)$ in (6.2).

6.4 MAB Learning-based Data Transmission

The number of active devices at the beginning of each window is random. However, the maximum number of devices that can meet a given latency-reliability criterion bound is limited, denoted by $\zeta_{\max}$. Therefore, as explained in subsection-6.4-6.4.3, active devices first undergo the DDE phase. When $M > \zeta_{\max}$, the DDE phase probabilistically allows $M^* \leq \zeta_{\max}$ devices to join the multi-agent MAB learning-based data transmission phase.

During the MAB learning-based data Transmission phase, devices perform uplink data transmission over the selected base stations, where BS selection in each epoch follows an adaptive exploration and exploitation strategy. Let $M_{i,t}$ show the number of devices connected with BS-i in epoch-t, we have $M^* = \sum_{i=1}^{B} M_{i,t}$. We define the set $\phi_{i,t} \in \mathcal{M}$ which contains the devices' labels connected with BS-i in epoch-t,

where $|\phi_{i,t}| = M_{i,t}$.

As shown in 6.3, for a given number of active devices, the average probability that an intended device's transmission remains unsuccessful decreases as the number of channels increases resulting in lower latency. Since the number of active delay-sensitive and delay-tolerant devices is random, we propose a random BS selection mechanism for the exploration action that enables the active devices to select a BS randomly following a device-specific distribution. Under this BS selection approach, if a device belongs to a delay-sensitive class, the probability of selecting a particular BS is proportional to the number of channels allocated to that BS. On the other hand, if the device comes from a delay-tolerant class, the probability of selecting a particular BS is inversely proportional to the number of channels allocated to that BS. Thus the probability that an intended device selects BS-i in an exploration phase is given by

$$\phi_i := \begin{cases} \frac{K_i}{\sum_{n=1}^{B} K_n}, & \text{Delay-sensitive device;} \\ \\ \frac{1}{B-1}\left(1 - \frac{K_i}{\sum_{n=1}^{B} K_n}\right), & \text{Delay-tolerant device.} \end{cases} \tag{6.5}$$

We define $\Phi = \{\phi_1, \phi_2, ..., \phi_B\}$, and can readily show that $\sum_{i=1}^{B} \Pr\left[a_t^{(d)} = i\right] = 1$ for both classes. Moreover, it is also evident from (6.5) that the BS-selection becomes uniform when all BSs have the same number of channels.

After performing the BS selection step, the devices execute R rounds of data transmission employing the grant-free access of [111], and build their transmission history of epoch-t in a vector $\mathbf{h}_t = [A_{i,t,1,1}, A_{i,t,2,1}, ..., A_{i,t,R,1}]$. The random variable $A_{i,t,m,1} = 0$ if the transmission from an intended device is successful over BS-i in slot-1 of the m^{th} round, while $A_{i,t,m,1} = 1$ if the device faces a collision. The devices predict the current network load at the selected BS as follows [111]:

$$\widehat{M}_{i,t} = \left\lceil 1 + \frac{\ln\left(1 - \frac{1}{R}\sum_{m=1}^{R} A_{i,t,m,1}\right)}{\ln\left(\frac{K_i - 1}{Ki}\right)} \right\rceil. \tag{6.6}$$

At the end of each epoch, if the devices connected to BS-i observe that $\widehat{M}_{i,t} \leq \zeta_i$,

they keep BS-i for the next epoch (exploitation). However, in the case when the devices find that $\widehat{M}_{i,t} > \zeta_i$, the devices are enabled to use a probabilistic approach to perform the BS selection step (exploration) or keep the current BS (exploitation) in the next epoch. Let $X_{i,t}^{(d)}$ denote the decision taken by the d^{th} device from the i^{th} overloaded BS, defined as

$$X_{i,t}^{(d)} := \begin{cases} 1, & \text{Exploration in epoch-}t \quad \text{when } M_{i,t-1} > \zeta_i; \\ 0, & \text{Keep the current BS in epoch-}t \quad \text{when } M_{i,t-1} > \zeta_i. \end{cases} \tag{6.7}$$

We define $\gamma_{i,t} := \Pr\left[M_{i,t} \leq \zeta_i\right]$. We also let $\beta_{i,t-1}$ denote the probability that a device of interest from an overloaded BS decides to perform exploration in epoch-t. Thus the PMF of $X_{i,t}^{(d)}$ is defined as

$$\Pr\left[X_{i,t}^{(d)} = x \mid M_{i,t-1} > \zeta_i\right] := \begin{cases} \beta_{i,t-1}\ , & x = 1; \\ 1 - \beta_{i,t-1}\ , & x = 0. \end{cases} \tag{6.8}$$

In order to perform the adaptive exploration/exploitation strategy, active devices need to predict $\beta_{i,t-1}$. Network load prediction by using (6.6) at the selected BS enables end devices to predict $\beta_{i,t-1}$. Let $\widehat{\beta}_{i,t-1}$ be a prediction of $\beta_{i,t-1}$. End devices compute $\widehat{\beta}_{i,t-1}$ as follows:

$$\widehat{\beta}_{i,t-1} := 1 - \frac{\zeta_i}{\widehat{M}_{i,t-1}}. \tag{6.9}$$

Please see Subsection-6.6.2 for the derivation of (6.9).

Figure 6.4 shows the different states that an intended device can achieve in each epoch, and the associated state transition probabilities. The state transition probabilities of the d^{th} device are computed by

$$\Pr\left[a_t^{(d)} = i\right]_{\substack{i=1,2,\ldots,B \\ t=1}} := \phi_i, \tag{6.10}$$

$$\Pr\left[a_t^{(d)} = j \mid a_{t-1}^{(d)} = i\right]_{\substack{i=1,2,\ldots,B \\ j=1,2,\ldots,B \\ 1<t\leq T_{\text{con}}}} := \begin{cases} (1 - \beta_{i,t-1}) + \beta_{i,t-1}\phi_i\ , & i = j; \\ \beta_{i,t-1}\phi_j\ , & i \neq j. \end{cases} \tag{6.11}$$

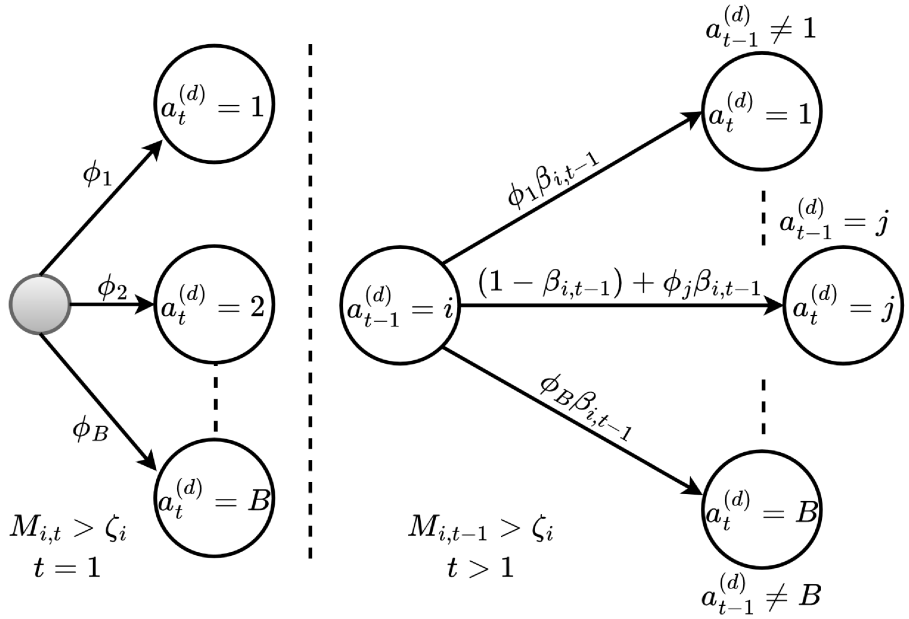

Figure 6.4: Possible states of the d^{th} device in each epoch along with the corresponding state transition probabilities.

We define a stable state when the number of devices performing exploration becomes zeros. From (6.11), we can see that to achieve convergence, the transition probability must approach zero as t increases. In the following subsection we present a statistical analysis of the convergence time.

6.4.1 Convergence Analysis

In this subsection, we analyze the convergence of the proposed MAB-GFA mechanism. In particular, we analyze network load distribution across all BSs, as the number of epochs increases. There are M^* devices performing BS selection in epoch-1. While, for $t > 1$, the number of devices that decide to perform BS selection in epoch-t is computed by using (6.7), which comes out to be $\sum_{i=1}^{B} \sum_{\substack{d \in \phi_{i,t} \\ |\phi_{i,t}| = M_{i,t}}} X_{i,t}^{(d)}$. Thus the number of devices performing exploration in each epoch is given by

$$\Delta_t := \begin{cases} M^*, & t = 1; \\ \sum_{i=1}^{B} \sum_{\substack{d \in \phi_{i,t} \\ |\phi_{i,t}| = M_{i,t}}} X_{i,t}^{(d)}, & t > 1. \end{cases} \tag{6.12}$$

On the other hand, the number of devices performing exploitation action in epoch-t is: $M^* - \Delta_t$. Thus the network converges to a stable state when Δ_t approaches zero as t increases; i.e., it is required that $\lim_{t \to \infty} \Delta_t = 0$.

We let random variable T_{con} denote the number of epochs to reach the stable state. Thus under the stable state network load at each BS does not change, and we have $M_{i,t} \leq \zeta_i, \forall i = 1, 2, ..., B$ for $t \geq T_{\text{con}}$. Since the number of epochs required to reach the stable state is random, a statistical analysis of the convergence time is necessary, which requires the computation of PMF associated with T_{con}. The PMF of T_{con} is given by

$$\Pr\left(T_{\text{con}} = t\right) := \begin{cases} \prod_{i=1}^{B} \gamma_{i,t} \ , & t = 1; \\ \prod_{y=1}^{t-1} \left(1 - \prod_{i=1}^{B} \gamma_{i,y}\right) \prod_{i=1}^{B} \gamma_{i,t} \ , & t > 1. \end{cases} \tag{6.13}$$

Please see Subsection-6.6.3 for the derivation of (6.13).

The expected number of epochs required to reach the stable state, denoted by $\mu_{T_{\text{con}}}$, is defined as

$$\mu_{T_{\text{con}}} := \mathrm{E}\left(T_{\text{con}}\right) = \sum_{t=1}^{\infty} t \Pr\left(T_{\text{con}} = t\right). \tag{6.14}$$

Finally, $\mu_{T_{\text{con}}}$ is computed by substituting (6.13) in (6.14), as follows:

$$\mu_{T_{\text{con}}} = \prod_{i=1}^{B} \gamma_{i,t} + \sum_{t=2}^{\infty} t \prod_{y=1}^{t-1} \left(1 - \prod_{i=1}^{B} \gamma_{i,y}\right) \prod_{i=1}^{B} \gamma_{i,t}. \tag{6.15}$$

We let $M_t^{*(\text{ds})}$ and $M_t^{*(\text{dt})}$ be the numbers of delay-sensitive and delay-tolerant devices, respectively, meeting the prescribed latency bound in epoch-t. Thus, $Z_t = M_t^{*(\text{ds})} + M_t^{*(\text{dt})}$. When the system reaches the stable state, the number of devices meeting the prescribed latency bound is M^*. Therefore, we define normalized average load meeting the prescribed latency-reliability criterion as: $\eta_t := \frac{Z_t}{M^*}$ and accordingly define $\eta_t^{(\text{ds})} := \frac{M_t^{*(\text{ds})}}{M^{(\text{ds})}}$ and $\eta_t^{(\text{dt})} := \frac{M_t^{*(\text{dt})}}{M^{(\text{dt})}}$. As a result of this normalization we have $0 \leq \eta_t \leq 1$, $0 \leq \eta_t^{(\text{ds})} \leq 1$, and $0 \leq \eta_t^{(\text{dt})} \leq 1$. In Section-6.5, through simulations we analyze $\eta_t^{(\text{ds})}$, $\eta_t^{(\text{ds})}$, η_t, and expected time to reach the stable state.

6.4.2 Computation of Regret

In epoch-t, a given BS can meet the desired latency-reliability criteria if the number of devices connected with that BS does not exceed the corresponding maximum supported load, i.e., $M_{i,t} \leq \zeta_i$. It is noteworthy that under this condition, the transmission of an intended device can still face a collision. However, the probability of such an event follows the desired reliability criterion. Therefore, the devices connected with BS-i receive a reward equal to 1 when $M_{i,t} \leq \zeta_i$; otherwise, devices get zero rewards. Thus the reward for the d^{th} device connected with BS-i in epoch-t, denoted by $Y_{i,t}^{(d)}$, is drawn from a Bernoulli distribution and given as

$$\Pr\left[Y_{i,t}^{(d)} = y \mid M_{i,t}\right] := \begin{cases} \gamma_{i,t}\ , & y = 1; \\ 1 - \gamma_{i,t}\ , & y = 0. \end{cases} \tag{6.16}$$

The expected reward for the d^{th} device is given by

$$\mathrm{E}\left(Y_{i,t}^{(d)} \mid M_{i,t}\right) = \gamma_{i,t}. \tag{6.17}$$

The reward generated by BS-i in epoch-t is computed by

$$Z_{i,t} := \sum_{\substack{d \in \phi_{i,t} \\ |\phi_{i,t}| = M_{i,t}}} Y_{i,t}^{(d)}. \tag{6.18}$$

Since all devices perform BS selection independently, the expected reward generated by BS-i for the given $M_{i,t}$ is computed by

$$\mathrm{E}\left(Z_{i,t} \mid M_{i,t}\right) = \gamma_{i,t} M_{i,t}. \tag{6.19}$$

where expectation in (6.19) is taken over $Z_{i,t}$. Moreover, $M_{i,t}$ $\forall i = 1, 2, ..., B$ is random, the expected reward in (6.19) is also random. The system-level reward generated in epoch-t is computed by: $Z_t := \sum_{i=1}^{B} Z_{i,t}$. Consequently. the system-level expected reward is computed by

$$\mathrm{E}\left(Z_t\right) = \sum_{i=1}^{B} \mathrm{E}\left(\gamma_{i,t} M_{i,t}\right), \tag{6.20}$$

where expectation in (6.20) is taken over $M_{i,t}$.

Let μ_i^* denote the optimal expected reward generated BS-i, then under the conditon that Given that $M^* \leq \zeta_{\max}$, the optimal system-level reward comes out to be $M^* = \sum_{i=1}^{B} \mu_i^*$. Thus the system-level expected regret over the time horizon of $T_{\max}$-epochs is computed as follows:

$$\mathrm{E}\left[R(T)\right] := \mathrm{E}\left[TM^* - \sum_{t=1}^{T} Z_t\right],$$

$$= TM^* - \sum_{t=1}^{T}\sum_{i=1}^{B} \mathrm{E}\left(\gamma_{i,t} M_{i,t}\right). \tag{6.21}$$

Due to the time-varying nature of Δ_t and different distributions used by delay-sensitive and delay-tolerant devices for BS selection, it becomes cumbersome to compute the distribution of $M_{i,t}$ in a closed form. Therefore, as explained in Section-6.5, we use the Monte-Carlo simulation method to estimate the expected regret. It is observed that under the condition $M^* \leq \zeta_{\max}$, system-level expected reward varies in a sub-linear manner against t.

6.4.3 Distributed Device Elimination

The number of active devices at the start of each window is random. Suppose the current network load is higher than the maximum network load support. We define the excessive network load as: $D := M - \zeta_{\max}$. In this case, we enable the end devices to use a probabilistic approach to choose between joining the multi-agent MAB learning-based data transmission phase and waiting for the next window. When $M > \zeta_{\max}$, the phase probabilistically allows $M^* \leq \zeta_{\max}$ devices to join the multi-agent MAB learning-based data transmission phase.

In epoch-0, each device selects a BS randomly such that the selection is uniform across all BSs. The active devices perform R rounds of grant-free data transmission over the selected BS and keep their transmission history in a vector $\mathbf{h}_0 = [A_{i,1,1}, A_{i,2,1}, ..., A_{i,R,1}]$. The random variable $A_{i,m,1} = 0$ if the transmission from an intended device is successful over BS-i in slot-1 of the m^{th} round, where $m =$

$1, 2, ..., R$. On the other hand, $A_{i,m,1} = 1$ if the device faces a collision. The devices are enabled to predict the current network load based on their transmission history as follows:

$$\widehat{M} = B \left\{ 1 + \frac{\ln\left(1 - \frac{1}{R}\sum_{m=1}^{R} A_{i,m,1}\right)}{\ln\left(\frac{K_i - 1}{Ki}\right)} \right\}. \tag{6.22}$$

Please see Subsection-6.6.4 for the derivation of (6.22).

Let $\widehat{D}$ denote a prediction of D defined as: $\widehat{D} := \widehat{M} - \zeta_{\max}$. Thus after predicting the number of active devices in the network, end devices can predict the excessive network load as follows:

$$\widehat{D} := B \left[1 + \frac{\ln\left(1 - \frac{1}{R}\sum_{m=1}^{R} A_{i,m,1}\right)}{\ln\left(\frac{K_i - 1}{Ki}\right)} \right] - \sum_{i=1}^{B} \zeta_i. \tag{6.23}$$

If $\widehat{D} \leq 0$, all devices proceed to perform the MAB-GFA mechanism phase. On the other hand, if $\widehat{D} > 0$, active devices undergo a probabilistic elimination process. To this end, the d^{th} active device generates a Bernoulli random variable $X_{i,0}^{(d)}$ defined as

$$X_{i,0}^{(d)} := \begin{cases} 1\ , & \text{Wait for the next window;} \\ 0\ , & \text{Join the multi-agent MAB learning-based data transmission phase.} \end{cases} \tag{6.24}$$

Each active device decides to wait for the next window with probability β_0 and joins the multi-agent MAB learning-based data transmission phase with probability $(1 - \beta_0)$. Thus the PMF of $X_{i,0}^{(d)}$ is defined as

$$\Pr\left(X_{i,0}^{(d)} = a\right) := \begin{cases} \beta_0\ , & a = 1; \\ 1 - \beta_0\ , & a = 0. \end{cases} \tag{6.25}$$

Let M^* denote the number of devices joining the multi-agent MAB learning-based data transmission phase. Since M^* is also random, it can still exceed $\zeta_{\max}$. Therefore, we aim to find the optimal value of β_0, denoted by β_0^*, so that the probability of occurrence of an event when $M^* > \zeta_{\max}$ does not exceed a given threshold δ,

where $0 < \delta \ll 1$.

Let $\widehat{\beta_0^*}$ denote a prediction of β_0^*. The active devices are enabled to predict β_0^*, as follows:

$$\widehat{\beta_0^*} = \begin{cases} \frac{-\widehat{C}_1 + \sqrt{\widehat{C}_1^2 - 4\widehat{C}_2\widehat{C}_0}}{2\widehat{C}_2}, & 0 < \delta < 0.5; \\ \\ \frac{-\widehat{C}_1 - \sqrt{\widehat{C}_1^2 - 4\widehat{C}_2\widehat{C}_0}}{2\widehat{C}_2}, & 0.5 \leq \delta < 1. \end{cases} \tag{6.26}$$

where

$$\widehat{C}_0 = \left(B\widehat{M}_{i,0} - \zeta_{\max} - 0.5\right)^2, \tag{6.27}$$

$$\widehat{C}_1 = -B\widehat{M}_{i,0}\left[2\left(B\widehat{M}_{i,0} - \zeta_{\max} - 0.5\right) + \left\{\Phi^{-1}(\delta)\right\}^2\right], \tag{6.28}$$

$$\widehat{C}_2 := \left(B\widehat{M}_{i,0}\right)^2 + B\widehat{M}_{i,0}\left\{\Phi^{-1}(\delta)\right\}^2. \tag{6.29}$$

Pleas see Subsection-6.6.5 for the derivations of (6.26)-(6.29).

6.5 Simulation Results

We perform extensive simulations to evaluate the performance of the proposed MAB-GFA mechanism. We take $B = 5$, $K_1 = 20$, $K_2 = 40$, $K_3 = 60$, $K_4 = 80$, $K_5 = 100$, $N = 5$, $\mathcal{L}_{\max} = 5$, and $\epsilon_r = 10^{-4}$. Using $R = 10000$ rounds, simulations are performed to obtain the network load support of each BS resulting $\zeta_1 = 22$, $\zeta_2 = 44$, $\zeta_3 = 66$, $\zeta_4 = 87$, and $\zeta_5 = 109$, and consequently $\zeta_{\max} = 328$.

We begin by analyzing the DDE phase. In epoch-0, if the number of active devices does not exceed the maximum network support, all devices proceed to perform the multi-agent MAB learning-based data transmission. When the number of active devices exceeds $\zeta_{\max}$, the devices undergo a DDE step. To analyze the performance of DDE phase, we evaluate optimal elimination probability under different values of M where $M > \zeta_{\max}$. For different values of δ, Figure 6.5 plots the optimal value of elimination probability defined in (6.65) against a range of M where $M > \zeta_{\max}$. It is observed that, for the given network load, smaller values of δ require higher values of β_0^* causing more devices to eliminate, as compared to the larger values of δ.

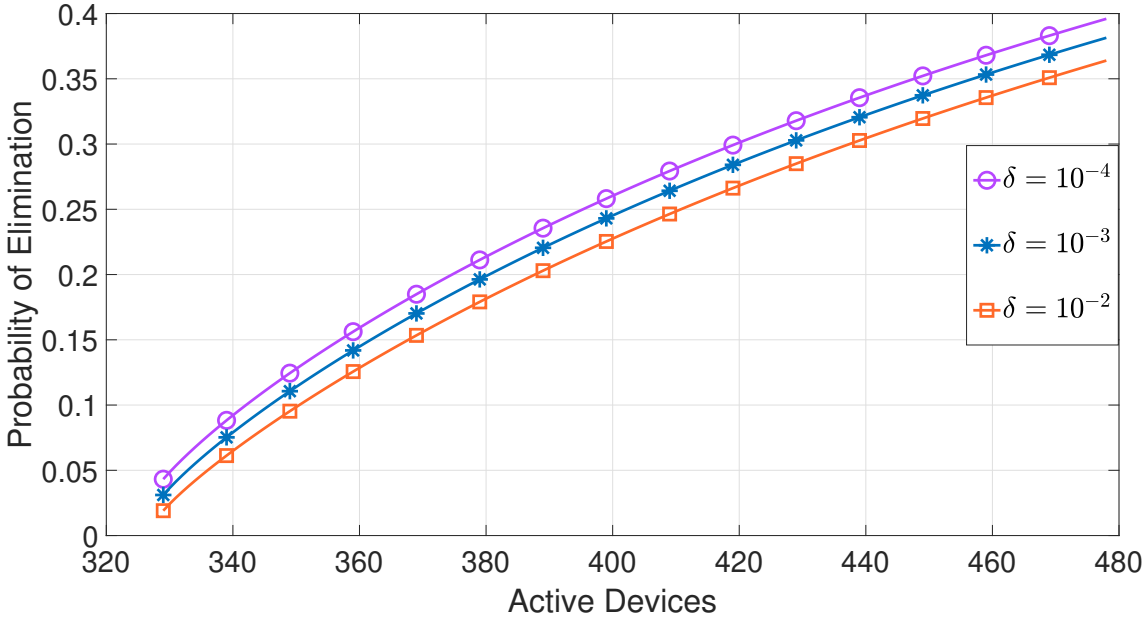

Figure 6.5: Probability of elimination against number of active devices when $M > \zeta_{\max}$ for different values of δ.

We analyze different aspects of the MA-MAB learning-based data transmission phase using $M \leq \zeta_{\max}$ and various settings of delay-sensitive and tolerant devices against a range of t. We first keep $M = 320$ and use different values of M_{ds} and M_{ds} and name it *Case-1*. Moreover, *Case-1a*, *Case-1b* and *Case-1c* correspond to the settings $M_{\text{ds}} = 150$, $M_{\text{dt}} = 170$; $M_{\text{ds}} = 200$, $M_{\text{dt}} = 120$; and $M_{\text{ds}} = 250$, $M_{\text{dt}} = 70$, respectively. Later, for various values of M, we use the same number of delay-sensitive and delay-tolerant devices, i.e., $M_{\text{ds}} = M_{\text{dt}} = \frac{M}{2}$ and name it *Case-2*. In this scenario *Case-2a*, *Case-2b* and *Case-2c* correspond to the settings $M_{\text{ds}} = M_{\text{dt}} = 110$, $M_{\text{ds}} = M_{\text{dt}} = 135$ and $M_{\text{ds}} = M_{\text{dt}} = 150$, respectively.

Figure 6.6 and Figure 6.7 plot $\eta_t^{(\text{ds})}$ and $\eta_t^{(\text{dt})}$ for *Case-1* and *Case-2*, respectively. In both cases, it is observed that $\eta_t^{(\text{ds})} > \eta_t^{(\text{dt})}$ for low to moderate values of t. Moreover, $\eta_t^{(\text{ds})}$ and $\eta_t^{(\text{dt})}$ approach to 1 when t gets large. This behavior of $\eta_t^{(\text{ds})}$ and $\eta_t^{(\text{dt})}$ indicates that the number of delay-sensitive devices meeting the latency-reliability criteria is no smaller than the number of delay-tolerant devices following the latency-reliability criteria. Thus the significance of using different distributions for delay-sensitive and delay-tolerant devices to select a BS during the exploration phase becomes apparent.

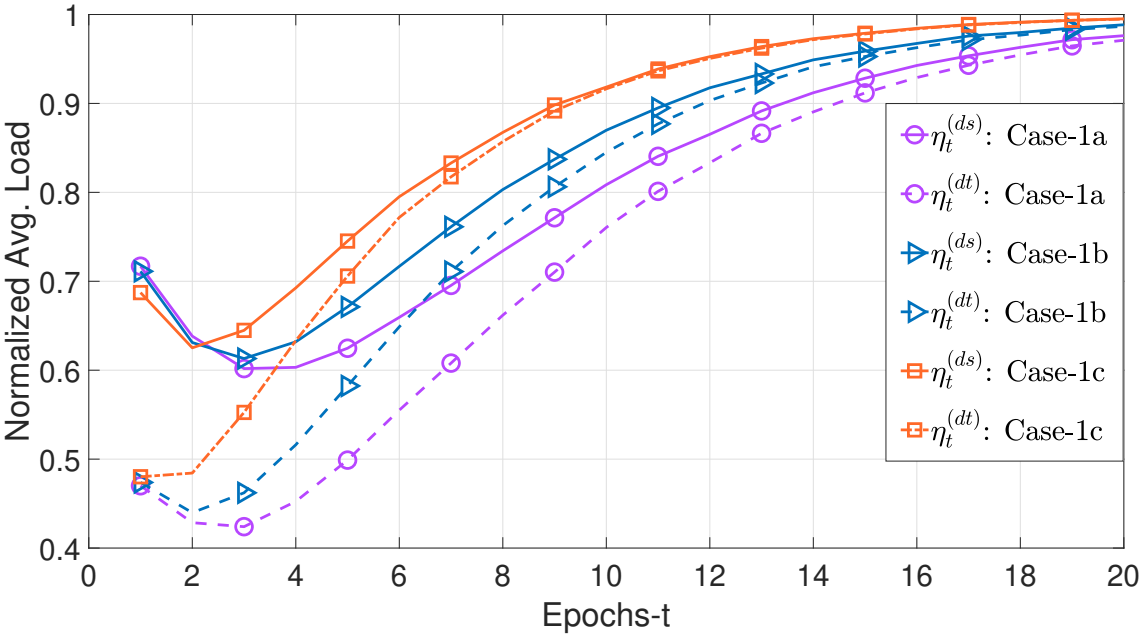

Figure 6.6: *Case-1*: Variation of $\eta_t^{(\mathrm{ds})}$ and $\eta_t^{(\mathrm{dt})}$ against t with $N = 5$, $\mathcal{L}_{\max} = 5$ and $\epsilon_r = 10^{-4}$.

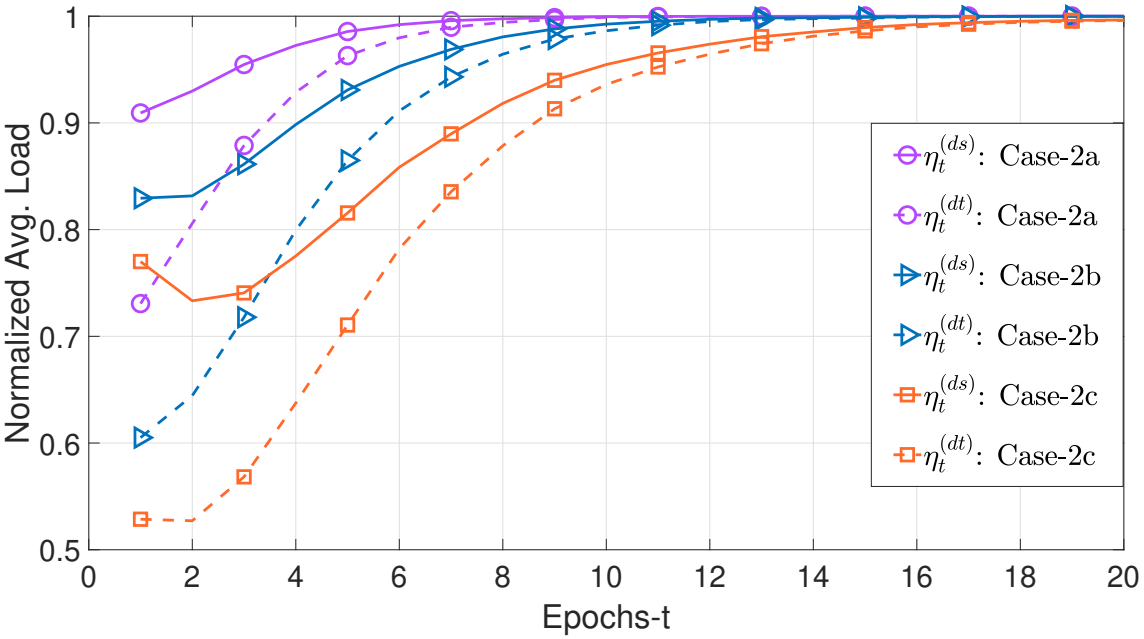

Figure 6.7: *Case-2*: Variation of $\eta_t^{(\mathrm{ds})}$ and $\eta_t^{(\mathrm{dt})}$ against t with $N = 5$, $\mathcal{L}_{\max} = 5$ and $\epsilon_r = 10^{-4}$.

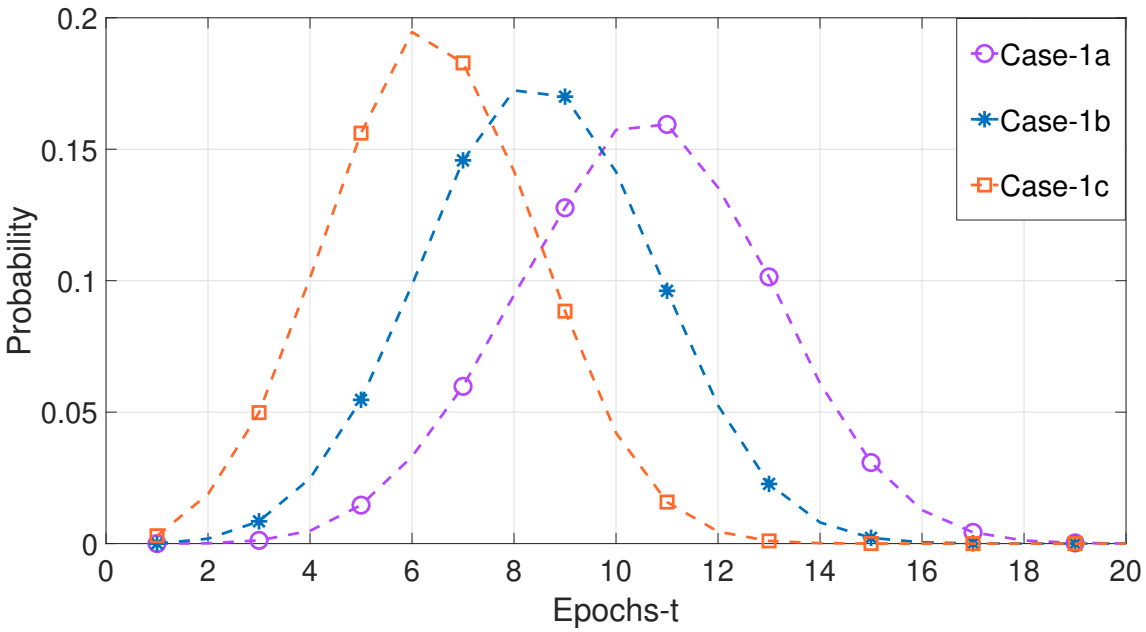

Figure 6.8: *Case-1*: PMF associated with the number of epochs required to reach the stable state under $N = 5$, $\mathcal{L}_{\max} = 5$ and $\epsilon_r = 10^{-4}$.

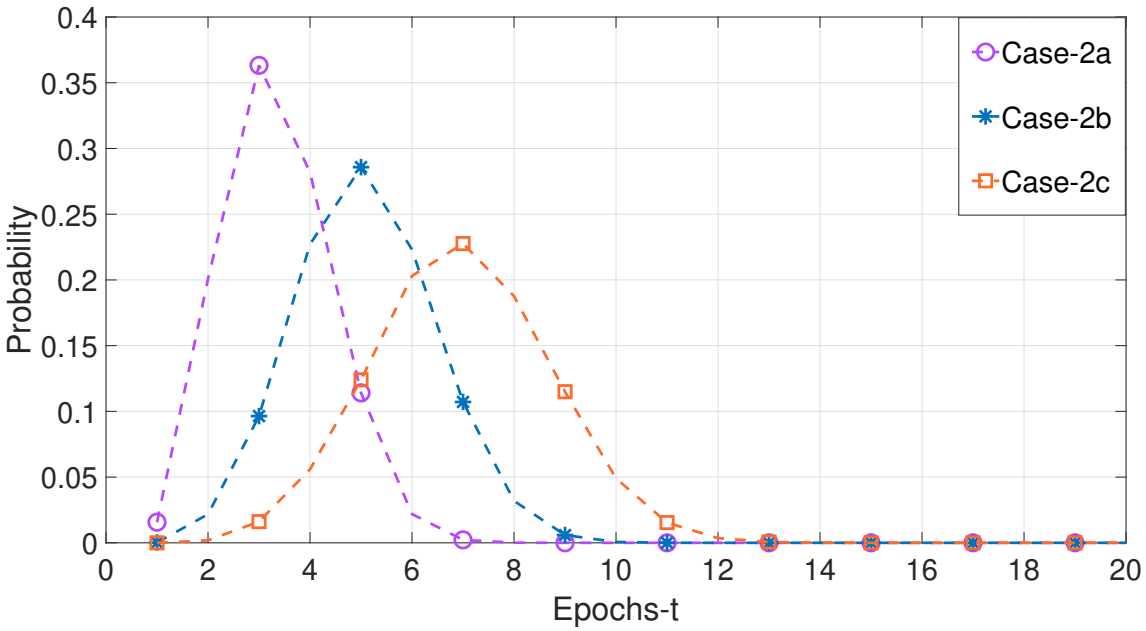

Figure 6.9: *Case-2*: PMF associated with the number of epochs required to reach the stable state under $N = 5$, $\mathcal{L}_{\max} = 5$ and $\epsilon_r = 10^{-4}$.

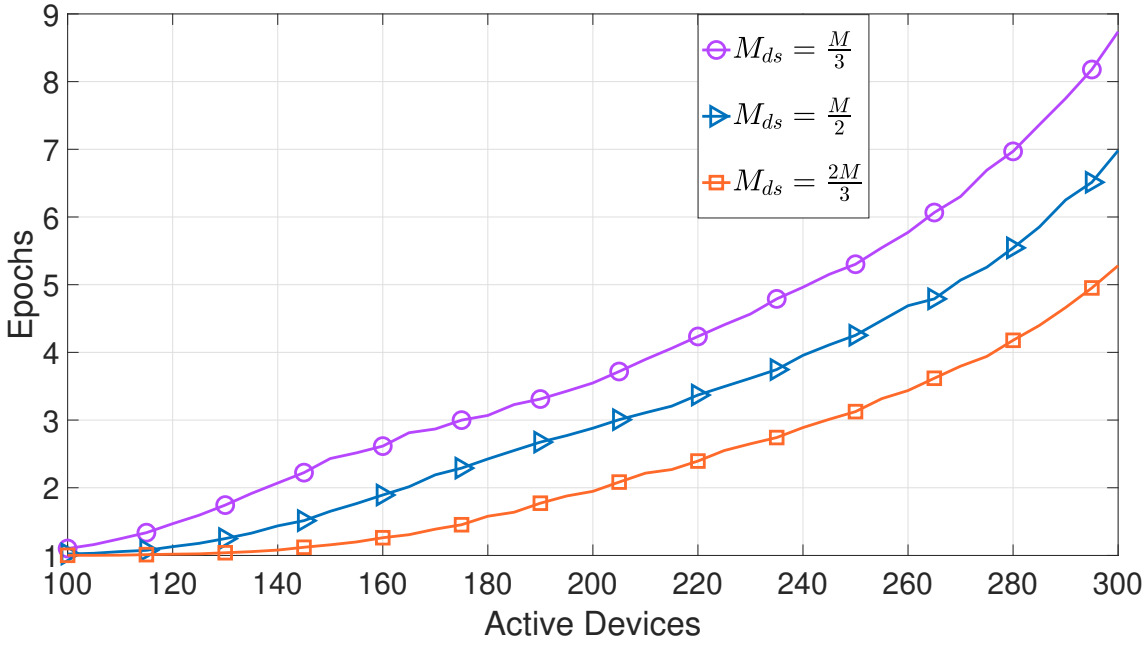

Figure 6.10: Average epochs to reach the stable state under different proportions of delay-sensitive devices with $N = 5$, $\mathcal{L}_{\max} = 5$ and $\epsilon_r = 10^{-4}$.

To demonstrate the convergence of the proposed mechanism, Figure 6.8 and Figure 6.9 plot the PMF for the number of epochs to reach a stable state under *Case-1* and *Case-2*, respectively. When the number of delay-sensitive devices decreases in *Case-1*, peak of the corresponding PMF is shifted at the higher values of t, and it becomes wider, resulting in larger values of the mean time to reach the stable state. On the other hand, when the number of delay-sensitive devices increases in *Case-2*, peak of the corresponding PMF is shifted at higher values of t and becomes wider, resulting in larger values of the mean time to reach the stable state.

Figure 6.10 plots the average number of epochs to reach the stable state in the MAB-GFA mechanism against a range of active devices. It is observed that, $\mu_{T_{\text{con}}}$ increases as the number of active devices increases. Moreover, for a given value of M, $\mu_{T_{\text{con}}}$ decreases as the proportion of delay-sensitive devices increases. Figure 6.11 and Figure 6.12 show the system-level average regret for *Case-1* and *Case-2*, respectively. It is observed that for both cases, the proposed the MAB-GFA mechanism achieves a sub-linear regret as t increases.

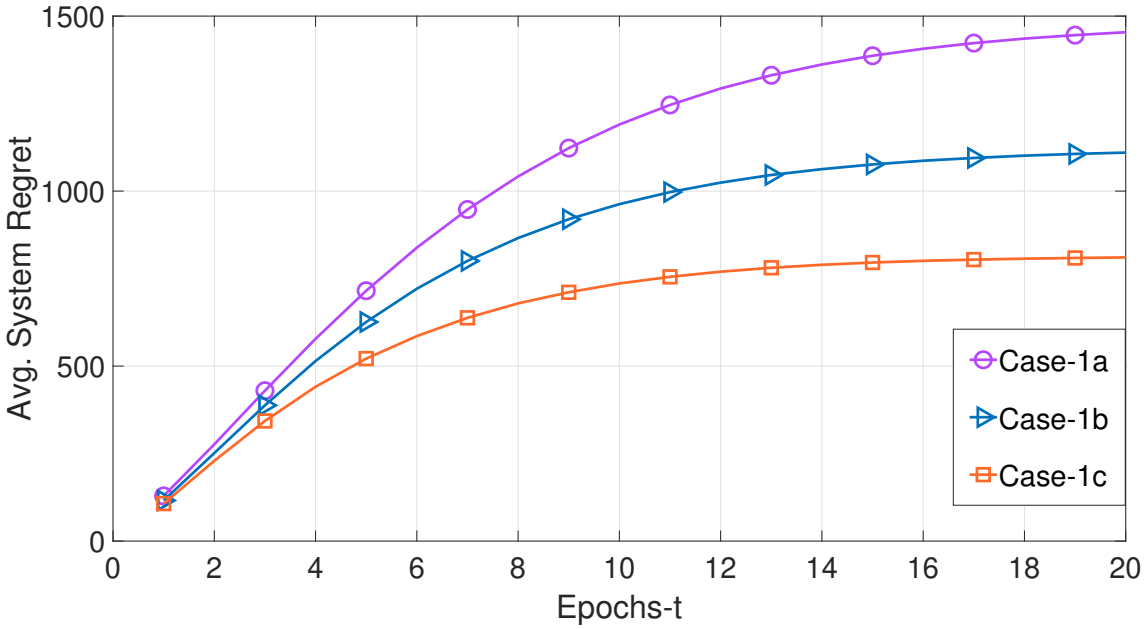

Figure 6.11: *Case-1*: System-level average regret against t with $N = 5$, $\mathcal{L}_{\max} = 5$ and $\epsilon_r = 10^{-4}$.

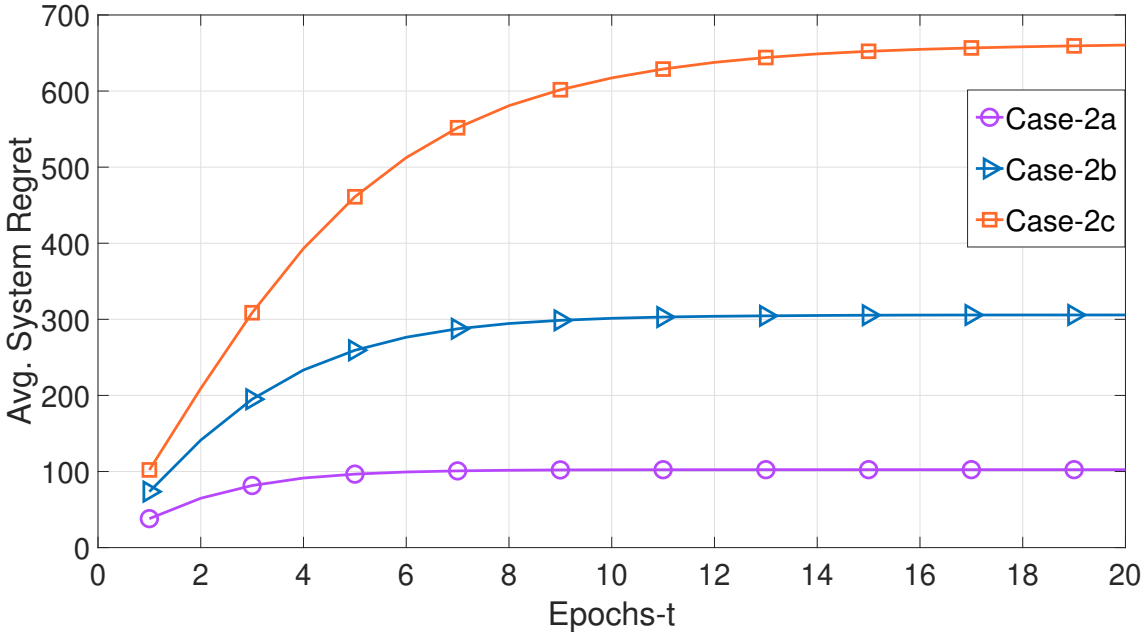

Figure 6.12: *Case-2*: System-level average regret against t with $N = 5$, $\mathcal{L}_{\max} = 5$ and $\epsilon_r = 10^{-4}$.

6.5.1 Performance Comparison

This subsection presents a performance comparison of the proposed MAB-GFA mechanism and the random BS selection (RBSS) policy. Under the RBSS approach, every active device selects a BS randomly and independently from other devices, following a uniform distribution in each epoch. Thus delay-sensitive and delay-tolerant devices observe the same probability of selecting a BS-i which is defined as $\phi_i^{(\text{RBSS})} := \frac{1}{B}\ \forall i = 1, 2, ..., B$. Moreover, devices do not employ any algorithm to learn different network parameters. It is noteworthy that during the DDE phase, active devices also follow the uniform distribution for BS selection. However, in contrast to the RBSS approach, active devices use their transmission history of the DDE phase to predict the current network load. Furthermore, active devices following the RBSS approach do not require additional control information to select a BS in each epoch. Therefore, the amount of control signaling overheads in the RBSS scheme remains the same as in the proposed MAB-GFA mechanism. Thus considering PHY-layer abstraction, the RBSS policy is an appropriate benchmark to compare the performance of the proposed MAB-GFA mechanism.

We compare the normalized average load following a given latency-reliability criterion offered by the MAB-GFA and RBSS mechanisms in each epoch using $M \leq \zeta_{\max}$. We define $\eta_t^{(\text{RBSS})} := \frac{M_t^{(\text{RBSS})}}{M}$, where $M_t^{(\text{RBSS})}$ shows the number of devices following a given latency-reliability criterion in epoch-t under the RBSS scheme. Figure 6.13 compares η_t and $\eta_t^{(\text{RBSS})}$ under *Case-1*, while Figure 6.14 compares η_t and $\eta_t^{(\text{RBSS})}$ under *Case-2*. Since the number of active devices is fixed in different settings of *Case-1*, and all devices follow the same probability distribution under the RBSS approach, $\eta_t^{(\text{RBSS})}$ curve in Figure 6.13 corresponds to *Case-1a*, *Case-1b* and *Case-1c*. However, there is a separate curve against each setting of *Case-1* for the proposed MAB-GFA mechanism. On the other hand, the number of active devices varies in different settings of *Case-2*. Therefore, along with the MAB-GFA mechanism, there are separate curves for the RBSS approach under each setting of *Case-2*.

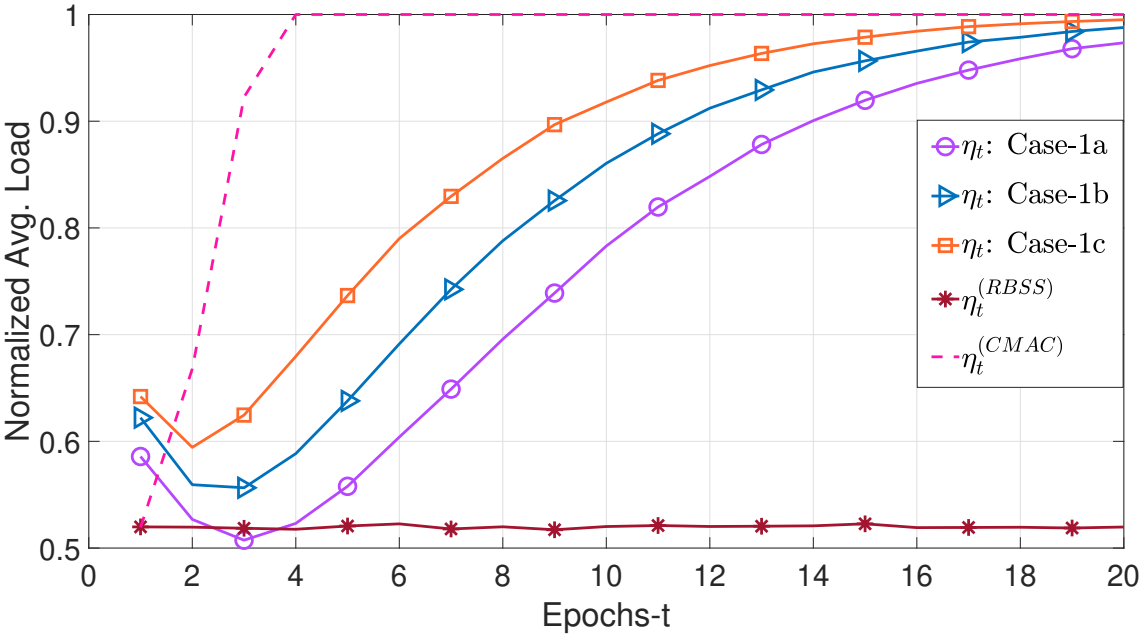

Figure 6.13: *Case-1*: Comparison of η_t, $\eta_t^{(\text{RBSS})}$ and $\eta_t^{(\text{CMAC})}$against t with $N = 5$, $\mathcal{L}_{\max} = 5$ and $\epsilon_r = 10^{-4}$.

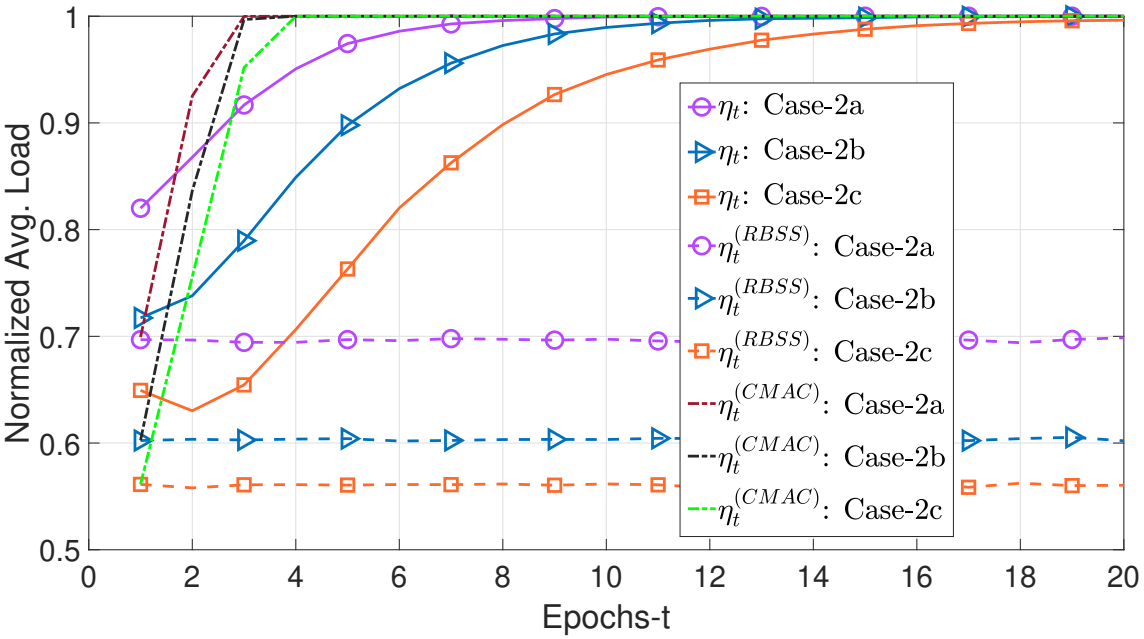

Figure 6.14: *Case-2*: Comparison of η_t, $\eta_t^{(\text{RBSS})}$ and $\eta_t^{(\text{CMAC})}$against t with $N = 5$, $\mathcal{L}_{\max} = 5$ and $\epsilon_r = 10^{-4}$.

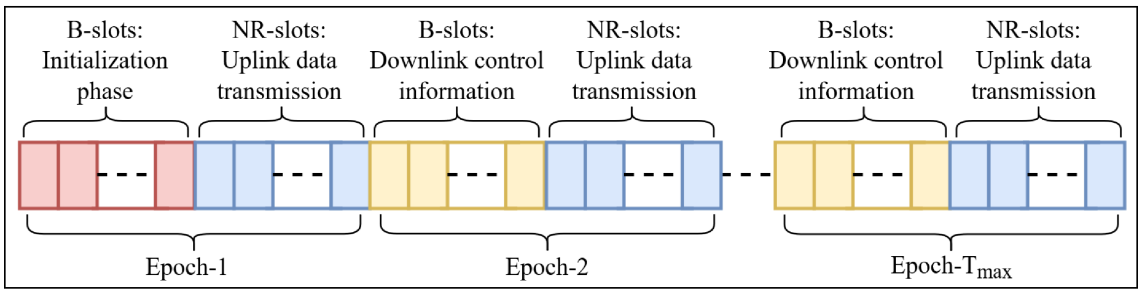

Figure 6.15: Structure of a window in the CMAC mechanism.

As shown in Figure 6.13 and Figure 6.14, η_t approaches 1 as t increases in both cases. Although the closed-form expression of η_t for both cases is not available, a possible explanation for the initial variation of η_t is that all active devices perform exploration in epoch-1. However, for $t > 1$, devices follow an adaptive exploration-exploitation strategy, enabling the devices to improve their BS selection over time. On the contrary, $\eta_t^{(\text{RBSS})}$ remains almost constant against t. Consequently, devices' BS selection is not improved in successive epochs under the RBSS approach. Moreover, $\eta_t^{(\text{RBSS})}$ decreases as the number of active devices increases. Thus considering the normalized average load that follows a given latency-reliability criterion, the proposed MAB-GFA mechanism outperforms the RBSS approach without requiring additional control information. Moreover, the proposed mechanism relies only on the devices' transmission history to explore the network. Therefore, it is a promising dynamic network access mechanism for IoT networks where devices have limited computation power.

6.5.2 Centralized Medium Access Control

We also compare the performance of the proposed distributed network access mechanism with the best possible centralized alternative, named centralized medium access control (CMAC) mechanism. Algorithm-5 describes the steps of the CMAC approach. Figure 6.15 shows the structure of a window in the CMAC mechanism composed of $T_{\max}$ epochs. Each epoch begins with B slots reserved for the transmission of control and feedback information in the downlink. Every BS is assigned a specific time slot to broadcast the required information. In the first epoch, the control slots are used to broadcast resource information of each BS. After this initialization phase, each active device selects a BS randomly and independently from

Algorithm 5 Centralized Medium Access Control

Require: $\mathcal{B}$, R, N

for Initialization Slots: $i = 1 : B$ **do**
  Get ω_i and ζ_i from BS-i
end for
$\mathcal{B}_{\text{avl}} := \mathcal{B}$
Exploration-Flag := 1
while Epochs: $t \leq T_{\max}$ **do**
  if Exploration-Flag == 1 **then**
    Select a BS from $\mathcal{B}_{\text{avl}}$ following uniform distribution
  end if
  Perform R transmission rounds over the selected BS
  for Control Slots: $i = 1$ to B **do**
    Get estimate of $M_{i,t}$ from BS-i
    Get feedback from the selected BS only
  end for
  if BS-Signal == 1 **then**
    Exploration-Flag := 0
  else
    Exploration-Flag := 1
  end if
  Update $\mathcal{B}_{\text{avl}}$ by keeping BSs where $M_{i,t} < \zeta_i$
end while

the other devices. In contrast to the MAB-GFA approach, the selection is uniform across all BSs under the CMAC mechanism. The active devices perform R rounds of uplink data transmission to the selected BS. At the end of each epoch, every BS estimates the number of devices communicating with it. Several BS-centered techniques have been proposed to estimate the current network load in the existing literature. e.g., [71, 72]. To compare the performance of the MAB-GFA mechanism, we assume that each BS has perfect knowledge regarding the number of devices connected with that BS under the CMAC approach.

Each BS broadcasts its current network load in the dedicated control slot of the following epoch. Moreover, each overloaded BS randomly selects the excessive devices and provides feedback (BS-Signal = 0), indicating to perform BS selection in the next epoch. Simultaneously, the rest of the devices from the overloaded BS get feedback (BS-Signal = 1), indicating to keep this BS for the remaining epochs of the current window. Consequently, each overloaded BS from epoch-t carries the maximum number of active devices during epoch-$t+1$ to epoch-$T_{\max}$. At the same time,

the BS for which the number of connected devices does not exceed the maximum network load support provides feedback (BS-Signal = 1) indicating them to keep the respective BSs in the next epoch. For epoch-$t+1$ to epoch-T, the devices performing exploration first need to update the set $\mathcal{B}$ by using the control information broadcasted by each BS in the respective slots. Thus at the end of each epoch, the active devices eliminate BSs from the set of available BSs for which the number of connected devices equals their respective maximum network load support.

Under the CMAC approach, along with the feedback signals, each BS needs to estimate the number of devices performing uplink data transmission to that BS and broadcast this information at the start of each epoch. The periodic broadcast of the required information introduces significant control signaling overheads. Moreover, the network load estimation step increases the computation burden at each BS.

Now we compute the expected time to reach the stable state under the CMAC approach for the case $M^* \leq \zeta_{\max}$. Let $M_{i,t}^{(\mathrm{CMAC})}$ be the number of devices connected with BS-i in epoch-t. The excessive network load at each BS follows

$$\Delta_{i,t}^{(\mathrm{CMAC})} := \begin{cases} 0, & M_{i,t}^{(\mathrm{CMAC})} \leq \zeta_i; \\ M_{i,t}^{(\mathrm{CMAC})} - \zeta_i & M_{i,t}^{(\mathrm{CMAC})} > \zeta_i. \end{cases} \tag{6.30}$$

Thus the number of devices performing exploration in epoch-t is defined as

$$Y_t^{(\mathrm{CMAC})} := \begin{cases} M^*, & t = 1; \\ \sum_{i=1}^{B} \Delta_{i,t-1}^{(\mathrm{CMAC})} & 1 < t \leq T_{\max}, \end{cases} \tag{6.31}$$

We define $\eta_t^{(\mathrm{CMAC})} := \frac{M_t^{*(\mathrm{CMAC})}}{M^*}$, where $M_t^{*(\mathrm{CMAC})}$ is the number of devices meeting the required latency-reliability criteria in epoch-t. Moreover, we define $\gamma_{i,t}^{(\mathrm{CMAC})} := \Pr\left[M_{i,t}^{(\mathrm{CMAC})} \leq \zeta_i\right]$. Let $T_{\mathrm{con}}^{(\mathrm{CMAC})}$ denote the time to reach the stable state under CMAC approach. By following the method used to compute the PMF of T_{con} for

the MAB-GFA mechanism, the PMF of $T_{\text{con}}^{(\text{CMAC})}$ is given by

$$\Pr\left(T_{\text{con}}^{(\text{CMAC})}=t\right):=\begin{cases}\prod_{i=1}^{B}\gamma_{i,t}^{(\text{CMAC})}, & t=1;\\ \\ \prod_{y=1}^{t-1}\left(1-\prod_{i=1}^{B}\gamma_{i,y}^{(\text{CMAC})}\right)\prod_{i=1}^{B}\gamma_{i,t}^{(\text{CMAC})}, & t>1.\end{cases} \tag{6.32}$$

Consequently, by using (6.32), the expected time to reach the stable state under the CMAC approach is

$$\mu_{T_{\text{con}}}^{(\text{CMAC})}=\prod_{i=1}^{B}\gamma_{i,t}^{(\text{CMAC})}+\sum_{t=2}^{\infty}t\prod_{y=1}^{t-1}\left(1-\prod_{i=1}^{B}\gamma_{i,y}^{(\text{CMAC})}\right)\prod_{i=1}^{B}\gamma_{i,t}^{(\text{CMAC})}. \tag{6.33}$$

Figure 6.13 compares η_t and $\eta_t^{(\text{CMAC})}$ under Case-1, while Figure 6.14 compares η_t and $\eta_t^{(\text{CMAC})}$ under Case-2. It is observed that, for both cases, η_t approaches $\eta_t^{(\text{CMAC})}$. At the same time, both η_t and $\eta_t^{(\text{CMAC})}$ approach 1 as t increases. Thus the performance of the proposed distributed network access converges to the centralized network access when t increases while avoiding excessive control signaling and feedback communication overheads caused by the centralized system.

6.6 Derivations

6.6.1 Derivation of (6.4)

The random variable L is represented as a function of the number of failed rounds ($\mathcal{Y}_M$) and the number of (re)transmissions ($\mathcal{Z}_M$) performed in the successful round, i.e, $L = N\mathcal{Y}_M + \mathcal{Z}_M$, where $\mathcal{Y}_M$ and $\mathcal{Z}_M$ are two independent random variables. The random variable $\mathcal{Y}_M$ follows the geometric distribution and the PMF of $\mathcal{Y}_M$ is computed by

$$\Pr\left(\mathcal{Y}_M=y\right):=\left(1-\prod_{n=1}^{N}\alpha_n\right)\left(\prod_{n=1}^{N}\alpha_n\right)^{y}, \qquad y=0,1,2,... \tag{6.34}$$

On the other hand, the PMF of $\mathcal{Z}_M$ is derived in [111], and it gets the following form

$$\Pr\left(\mathcal{Z}_M = z\right) \quad = \begin{cases} \dfrac{1}{1-\prod_{n=1}^{N}\alpha_n}\left(1-\alpha_z\right)\prod\limits_{\substack{j=1\\ z>1}}^{z-1}\alpha_j\ , & z=1,2,...,N; \\ 0, & \text{Otherwise} \end{cases} \tag{6.35}$$

Since $\mathcal{Y}_M$ and $\mathcal{Z}_M$ are independent random variables, the PMF of L is computed as

$$\Pr\left(L=t\right) := \begin{cases} \Pr\left(\mathcal{Z}_M = 1\right)\Pr\left(\mathcal{Y}_M = \left\lfloor \frac{t}{N} \right\rfloor\right) \\ \qquad\qquad t = 1, N+1, 2N+1, ... \\ \Pr\left(\mathcal{Z}_M = t \bmod N\right)\Pr\left(\mathcal{Y}_M = \left\lfloor \frac{t}{N} \right\rfloor\right) \\ \qquad t = 2, 3, ... \left(N-1\right), \left(N+2\right), ... \left(2N-1\right), ... \\ \Pr\left(\mathcal{Z}_M = N\right)\Pr\left(\mathcal{Y}_M = \frac{t}{N} - 1\right) \\ \qquad\qquad t = N, 2N, ... \end{cases} \tag{6.36}$$

Thus the PMF of L is obtained by applying (6.34) and (6.35) in (6.36) resulting in (6.4).

6.6.2 Derivation of (6.9)

The number of devices performing exploration in epoch-t comes out be

$$\Delta_{i,t} := \sum_{\substack{d\in\phi_{i,t}\\ |\phi_{i,t}|=M_{i,t}}} X_{i,t}^{(d)}, \qquad\qquad t>1. \tag{6.37}$$

The random variable $\Delta_{i,t}$ follows the Binomial distribution with parameters $M_{i,t-1}$ and $\beta_{i,t-1}$. Therefore, we have

$$\Pr\left(\Delta_{i,t}=x\right) := \binom{M_{i,t}}{x}\beta_{i,t-1}^{x}\left(1-\beta_{i,t-1}\right)^{M_{i,t}-x}, \tag{6.38}$$

where $x = 0, 1, 2, ..., M_{i,t}$, and

$$\mathrm{E}\left[\Delta_{i,t}\right] = \beta_{i,t-1}M_{i,t-1}, \qquad\qquad t>1. \tag{6.39}$$

The parameter $\beta_{i,t-1}$ is determined such that the expected number of devices leaving the BS-i becomes $M_{i,t-1} - \zeta_i$. Thus $\beta_{i,t-1}$ is computed as follows

$$\beta_{i,t-1} := 1 - \frac{\zeta_i}{M_{i,t-1}}, \qquad M_{i,t-1} > \zeta_i,\ t > 1. \tag{6.40}$$

6.6.3 Derivation of (6.13)

To obtain PMF of T_{con}, we analyse the status of every BS in each epoch. Let random variable $W_{i,t}$ show the status of BS-i in epoch-t defined as

$$W_{i,t} = \begin{cases} 1, & M_{i,t} > \zeta_i; \\ 0, & M_{i,t} \leq \zeta_i. \end{cases} \tag{6.41}$$

Thus PMF of $W_{i,t}$ is written as

$$\Pr\left(W_{i,t} = w\right) := \begin{cases} 1 - \gamma_{i,t}\ , & w = 1; \\ \gamma_{i,t}\ , & w = 0. \end{cases} \tag{6.42}$$

The number of overloaded BSs in epoch-t is computed by

$$W_t := \sum_{i=1}^{B} W_{i,t}, \tag{6.43}$$

where $0 \geq W_t \leq B$. The PMF of T_{con} is computed by

$$\Pr\left(T_{\text{con}} = t\right) := \begin{cases} \Pr\left(W_t = 0\right), & t = 1; \\ \prod_{y=1}^{t-1} \Pr\left(W_y > 0\right) \Pr\left(W_t = 0\right), & t > 1. \end{cases} \tag{6.44}$$

The probability that non of the BSs is overloaded in epoch-t is given by

$$\Pr\left(W_t = 0\right) = \prod_{i=1}^{B} \gamma_{i,t}, \tag{6.45}$$

On the other hand, probability that there is at least one overloaded BS in epoch-t is computed by

$$\Pr\left(W_y > 0\right) = 1 - \Pr\left(W_y = 0\right). \tag{6.46}$$

By substituting (6.45) in (6.46), $\Pr(W_y > 0)$ get the following form

$$\Pr(W_y > 0) = 1 - \prod_{i=1}^{B} \gamma_{i,y}. \tag{6.47}$$

Finally, the PMF of T_{con} is obtained by substituting (6.45) and (6.47) in (6.44).

6.6.4 Derivation of (6.22)

The probability that an intended device's transmission remains unsuccessful in slot-1 of the m^{th} round is defined as

$$\Pr(A_{i,m,1} = 1) := 1 - \left(\frac{K_i - 1}{K_i}\right)^{M_{0,i}-1}. \tag{6.48}$$

By using (6.48), active devices predict the number of devices connected with the respective BS as follows [111]:

$$\widehat{M}_{i,0} = 1 + \frac{\ln\left(1 - \frac{1}{R}\sum_{m=1}^{R} A_{i,m,1}\right)}{\ln\left(\frac{K_i - 1}{Ki}\right)}. \tag{6.49}$$

The number of devices connected with BS-i during epoch-0, denoted by $M_{i,0}$, follows the following PMF

$$\Pr[M_{i,0} = x \mid M, K_i] = \binom{M}{x}\left(\frac{1}{B}\right)^{x}\left(1 - \frac{1}{B}\right)^{M-x}, \tag{6.50}$$

where $x = 0, 1, ..., M$. Thus the expected number of devices connected with BS-i in epoch-0 is given by

$$\mathrm{E}[M_{i,0} \mid M, K_i] = \frac{M}{B}. \tag{6.51}$$

As shown in (6.51), each BS has the same expected number of devices in the device elimination phase. Therefore, each device predicts the total number of actives devices by: $\widehat{M} = B\widehat{M}_{i,0}$, where $\widehat{M}$ is the prediction of M. Finally, each active device

computes $\widehat{M}$ as follows:

$$\widehat{M} = B\left\{1 + \frac{\ln\left(1 - \frac{1}{R}\sum_{m=1}^{R} A_{i,m,1}\right)}{\ln\left(\frac{K_i - 1}{Ki}\right)}\right\}. \tag{6.52}$$

6.6.5 Derivation of (6.26)-(6.29)

From (6.24), we obtain the number of eliminated devices in the DDE phase as

$$Y := \sum_{i=1}^{B} \sum_{d \in \phi_{i,0}} X_{i,0}^{(d)}\ , \tag{6.53}$$

where the set $\phi_{i,0} \in \mathcal{M}$ contains the devices' labels connected with BS-i in epoch-0, and $|\phi_{i,0}| = M_{i,0}$. Thus, Y follows the Binomial distribution with parameters M and β_0. The PMF of Y is given by

$$\Pr\left[Y = y \mid M, K_i > \zeta_{\max}\right] = \binom{M}{y} \beta_0^y \left(1 - \beta_0\right)^{M-y}. \tag{6.54}$$

Finally, the number of devices joining the multi-agent MAB learning-based data transmission phase is

$$M^* := \begin{cases} M, & M \leq \zeta_{\max}; \\ M - Y, & M > \zeta_{\max}. \end{cases} \tag{6.55}$$

The optimal value of β_0 is computed by

$$\beta_0^* = \inf_{\beta_0} \left\{0 < \beta_0 < 1;\ \Pr\left(Y \leq M - \zeta_{\max} - 1\right) \leq \delta\right\}, \tag{6.56}$$

where $\Pr\left[Y \leq M - \zeta_{\max} - 1\right]$ is the cumulative distribution function (CDF) of Y evaluated at point $M - \zeta_{\max} - 1$. Since, M can be very large compared to $\zeta_{\max}$, the computation of $\Pr\left[Y \leq M - \zeta_{\max} - 1\right]$ by definition may not be feasible due to the involvement of large Binomial coefficient. Therefore, we use the Normal approximation for Binomial distribution to compute the CDF of Y as follows

$$\Pr\left[Y \leq M - \zeta_{\max} - 1\right] \simeq \Phi\left(\frac{M - \zeta_{\max} - 0.5 - M\beta_0}{\sqrt{M\beta_0\left(1 - \beta_0\right)}}\right), \tag{6.57}$$

where $-\infty < z < +\infty$, and $\Phi(z)$ is the CDF of a standard normal random variable computed at point z. A lookup table is used to obtain $\Phi(z)$ against different values of z. By substituting (6.57) in (6.56), it follows

$$\beta_0^* := \inf_{\beta_0} \left\{ 0 < \beta_0 < 1;\ \Phi\left(\frac{M - \zeta_{\max} - 0.5 - M\beta_0}{\sqrt{M\beta_0\left(1-\beta_0\right)}} \right) \leq \delta \right\}. \tag{6.58}$$

Thus, β_0^* is computed by solving the following:

$$\Phi^{-1}(\delta) := \frac{M - \zeta_{\max} - 0.5 - M\beta_0^*}{\sqrt{M\beta_0^*\left(1-\beta_0^*\right)}}, \tag{6.59}$$

where $\Phi^{-1}(\delta)$ is the inverse of the CDF of a standard normal random variable evaluated at point ϵ. We simplify (6.59) as

$$\left[M^2 + M\left\{\Phi^{-1}(\delta)\right\}^2\right](\beta_0^*)^2 + \left[-2M\left(M - \zeta_{\max} - 0.5\right) - M\left\{\Phi^{-1}(\delta)\right\}^2\right]\beta_0 + M - \zeta_{\max} - 0.5 = 0. \tag{6.60}$$

Here, (6.60) can be further rewritten as

$$C_2(\beta_0^*)^2 + C_1\beta_0^* + C_0 = 0, \tag{6.61}$$

where

$$C_0 := \left(M - \zeta_{\max} - 0.5\right)^2, \tag{6.62}$$

$$C_1 := -2M\left(M - \zeta_{\max} - 0.5\right) - M\left\{\Phi^{-1}(\delta)\right\}^2, \tag{6.63}$$

$$C_2 := M^2 + M\left\{\Phi^{-1}(\delta)\right\}^2. \tag{6.64}$$

Thus for a given δ, β_0^* is computed by solving (6.61) as

$$\beta_0^* = \begin{cases} \frac{-C_1 + \sqrt{C_1^2 - 4C_2C_0}}{2C_2}, & 0 < \delta < 0.5; \\ \\ \frac{-C_1 - \sqrt{C_1^2 - 4C_2C_0}}{2C_2}, & 0.5 \leq \delta < 1. \end{cases} \tag{6.65}$$

The computation of β_0^* through (6.65) requires the availability of knowledge regard-

ing the total number of active devices. On the other hand, every active device can predict the current network load using (6.52). Consequently, the end devices are enabled to predict C_0, C_1, and C_2 by substituting (6.52) in (6.62), (6.63), and (6.64), respectively, resulting in (6.27), (6.28), and (6.29). Finally, devices predict β_0^* by substituting (6.27), (6.28), and (6.29) in (6.65) resulting in (6.26). After performing the DDE phase, M^* successful devices join the multi-agent MAB learning-based data transmission phase spanned over epoch-1 to epoch-$T_{\max}$.

6.7 Conclusion

Distributed network access protocols can potentially address the problem of meeting diverse latency and reliability requirements in dense heterogeneous IoT networks, and MAB learning is a promising tool in this regard. This chapter proposed a multi-agent MAB learning-based distributed network access mechanism for IoT networks, where multiple BSs serve delay-sensitive and delay-tolerant devices. The proposed mechanism enables the end devices to improve their BS selection over time, thus maximizing the number of devices meeting prescribed latency-reliability criteria. Simulation results revealed that when comparing the average number of devices meeting the desired latency-reliability criterion, the MAB-GFA mechanism outperforms the random BS selection approach where IoT devices do not employ any learning strategy. The distributed network access enables end devices to adapt to network dynamics while avoiding additional feedback and control signaling overheads. Therefore, it is greatly suitable for uplink-dominant heterogeneous IoT networks with massive devices operating in a dynamic environment. The radio channel fading plays a crucial role in meeting the desired QoS in wireless networks. Moreover, radio channel conditions between end devices and different BSs can vary significantly. Therefore, extending the proposed mechanism by considering the channel's behavior can lead to an interesting future research direction.

Chapter 7

Conclusions and Future Work

The growing number of devices in the IoT networks generate data in varying amounts and with diverse QoS requirements in terms of application-specific latency and reliability requirements. The MC-IoT applications require ultra-reliability and low-latency communication interfaces. Fulfilling the diverse QoS requirements becomes challenging when devices communicate over shared radio resources and network parameters change dynamically. Therefore, efficient network access mechanisms are crucial in the design of IoT networks supporting MC-IoT applications. The grant-based centralized network access schemes allow devices to transmit data over dedicated resources after successfully going through a random access channel phase. These mechanisms result in significant latency due to their inherent feedback and control signaling overheads.

On the other hand, under the grant-free network access mechanism, the active devices transmit data over shared radio resources without going through a request grant phase. This approach avoids the control signaling overheads resulting in lower latency. However, simultaneous transmissions from multiple devices over the same channel impact reliability. Moreover, due to the random nature of the number of active devices at a given time, the static resource allocation can result in lower utilization of the available shared radio resources. Therefore, network load-aware dynamic resource allocation-based network access schemes can improve the utilization of shared radio resources. Moreover, device-level network exploration-based distributed grant-free access can play a significant role in designing the wireless

networks which can MC-IoT applications.

This research identifies that device-level learning-assisted distributed network access protocols are essential for IoT networks operating under dynamic network load. To this end, statistical learning and multi-agent MAB learning are promising tools for addressing decision-making problems in a dynamic environment and designing distributed network access protocols. Statistical learning is the theoretical foundation of machine learning algorithms. Under the incomplete knowledge of probability distributions associated with different network parameters, this tool enables the end devices to predict them using their transmission history. At the same time, the MAB learning framework is an online learning strategy and is considered suitable for addressing the network access design problems for ultra-dense IoT networks where multiple BSs serve a large number of devices. This learning paradigm avoids excessive control signaling overheads by allowing the devices to perform exploration and exploitation actions independently without any coordination among them.

7.1 Summary of Outcomes

This thesis considers uplink dominant IoT networks in which massive devices generate delay-sensitive and delay-tolerant data and communicate over shared radio resources. Considering PHY layer abstraction, this thesis aims to design distributed network access mechanisms for the IoT networks supporting mission-critical applications. In this regard, we first propose a statistical learning-based dynamic transmission mechanism for the MC-IoT networks employing the multi-channel slotted ALOHA protocol. The proposed mechanism enables the end devices to use their transmissions history to predict retransmissions limit against a given latency-reliability criterion.

Secondly, we design a statistical learning-based grant-free network access mechanism for delay-sensitive IoT applications. The proposed enables end devices to use their transmission history to predict the current network load, the average probability of success per round, the average number of successful devices per round, and the average latency offered by the network. We use the probability of exception criterion to evaluate the robustness of the proposed mechanism for device-level network load

prediction. We demonstrate that the proposed device-level network load prediction mechanism is more robust than the BS-centered approach.

Thirdly, we propose a novel statistical learning-based grant-free access scheme for the IIoT networks where devices generate delay-sensitive and delay-tolerant data. Under this mechanism, for each slot of a round, active devices are enabled to partition the available channels into two disjoint subsets. One subset is used for delay-sensitive transmissions, while the other subset is used for delay-tolerant transmissions. Active devices execute a network exploration phase to predict the average latency and the parameters related to resource partitioning for this scheme. During this phase, devices transmit delay-sensitive data only using the grant-free access scheme with static resource allocation. Since the grant-free schemes with dynamic and static resource allocations depict different behaviors against different ranges of the number of active devices, we design an adaptive network access mechanism that enables the devices to select an optimal scheme under variable network load. Consequently, this mechanism offers better channel utilization while meeting the application-specific latency bound in IIoT networks operating under a dynamic environment.

Finally, we propose a multi-agent MAB learning-based grant-free access, named MAB-GF, mechanism for dense IoT networks, where multiple base stations serve delay-sensitive and delay-tolerant devices. The proposed mechanism enables the devices to improve their BS selection over time to accommodate the maximum number of devices that can meet a prescribed latency-reliability criterion. Through simulation, we show that the proposed MAB learning-based network access mechanism outperforms the random base station selection strategy in which end devices do not employ any learning scheme to adapt to the network dynamics. Moreover, a centralized network access scheme, CMAC, is also presented as an alternative to the proposed distributed network access mechanism. The CMAC protocol enables each BS to control the number of devices connected with that BS at the cost of significant control signaling overheads and feedback information. We demonstrate that the performance of the proposed MAB-GF mechanism approaches the CMAC as time increases.

7.2 Future Work

This thesis leads to interesting future research directions in designing distributed network access protocols for heterogeneous IoT networks supporting MC-IoT applications. Some of these directions are highlighted as follows:

- In Chapter-5 and Chapter-6, we classified the data generated by end devices into delay-sensitive and delay-tolerant data. The delay-sensitive devices share the same latency bound. As a future research work, we aim to design a network access mechanism for the heterogeneous network in which different IoT applications can have different latency bounds.
- Furthermore, in many IoT applications, devices are battery-powered and have limited energy, while battery replacement may not always be a simple process. Therefore, energy consumption is a critical network design parameter for IoT networks. Since this thesis enables end devices to explore the network by learning different network parameters based on their transmission history, this can lead to designing energy-efficient MAC schemes for IoT networks.
- Last but not least, by enabling the BS to utilize the network knowledge learned by end devices, the BS can optimize the resource allocation strategy. Such device-assisted resource optimization can result in higher resource utilization and is also part of our future research work.

7.3 Concluding Remarks

In summary this thesis demonstrates that the device-level learning-assisted distributed grant-free network access approach can efficiently manage delay-sensitive and delay-tolerant transmissions over shared radio resources in a dynamic environment. Moreover, this thesis opens new research venues for designing future wireless networks that are empowered by on-device intelligence to support heterogeneous IoT applications.

Bibliography

[1] M. S. Elbamby, C. Perfecto, C. Liu, J. Park, S. Samarakoon, X. Chen, and M. Bennis, "Wireless edge computing with latency and reliability guarantees," *Proceedings of the IEEE*, vol. 107, no. 8, pp. 1717–1737, 2019.

[2] M. Bennis, M. Debbah, and H. V. Poor, "Ultrareliable and low-latency wireless communication: Tail, risk, and scale," *Proceedings of the IEEE*, vol. 106, no. 10, pp. 1834–1853, 2018.

[3] E. Sisinni, A. Saifullah, S. Han, U. Jennehag, and M. Gidlund, "Industrial Internet of Things: Challenges, opportunities, and directions," *IEEE Transactions on Industrial Informatics*, vol. 14, no. 11, pp. 4724–4734, 2018.

[4] *5G; Service requirements for next generation new services and markets*, 3GPP Std. TS 22.261, Jun. 2018.

[5] G. Durisi, T. Koch, and P. Popovski, "Toward massive, ultrareliable, and low-latency wireless communication with short packets," *Proceedings of the IEEE*, vol. 104, no. 9, pp. 1711–1726, 2016.

[6] C. She, Z. Chen, C. Yang, T. Q. S. Quek, Y. Li, and B. Vucetic, "Improving network availability of ultra-reliable and low-latency communications with multi-connectivity," *IEEE Transactions on Communications*, vol. 66, no. 11, pp. 5482–5496, 2018.

[7] A. Weinand, M. Karrenbauer, J. Lianghai, and H. D. Schotten, "Physical layer authentication for mission critical machine type communication using gaussian mixture model based clustering," in *2017 IEEE 85th Vehicular Technology Conference (VTC Spring)*, 2017, pp. 1–5.

[8] H. Forssell, R. Thobaben, H. Al-Zubaidy, and J. Gross, "Physical layer authentication in mission-critical MTC networks: A security and delay performance analysis," *IEEE Journal on Selected Areas in Communications*, vol. 37, no. 4, pp. 795–808, 2019.

[9] H. Wang, Q. Yang, Z. Ding, and H. V. Poor, "Secure short-packet communications for mission-critical IoT applications," *IEEE Transactions on Wireless Communications*, vol. 18, no. 5, pp. 2565–2578, 2019.

[10] H. Thomsen, N. K. Pratas, C. Stefanovic, and P. Popovski, "Analysis of the LTE access reservation protocol for real-time traffic," *IEEE Communications Letters*, vol. 17, no. 8, pp. 1616–1619, 2013.

[11] M. Deghel, P. Brown, S. E. Elayoubi, and A. Galindo-Serrano, "Uplink contention-based transmission schemes for URLLC services," in *Proceedings of the 12th EAI International Conference on Performance Evaluation Methodologies and Tools*, ser. VALUETOOLS 2019. New York, NY, USA: Association for Computing Machinery, 2019, p. 87–94. [Online]. Available: https://doi.org/10.1145/3306309.3306323

[12] B. Singh, O. Tirkkonen, Z. Li, and M. A. Uusitalo, "Contention-based access for ultra-reliable low latency uplink transmissions," *IEEE Wireless Communications Letters*, vol. 7, no. 2, pp. 182–185, 2018.

[13] G. Choudhury and S. Rappaport, "Diversity aloha - A random access scheme for satellite communications," *IEEE Transactions on Communications*, vol. 31, no. 3, pp. 450–457, 1983.

[14] R. Abreu, P. Mogensen, and K. I. Pedersen, "Pre-scheduled resources for retransmissions in ultra-reliable and low latency communications," in *2017 IEEE Wireless Communications and Networking Conference (WCNC)*, 2017, pp. 1–5.

[15] R. Abreu, G. Berardinelli, T. Jacobsen, K. Pedersen, and P. Mogensen, "A blind retransmission scheme for ultra-reliable and low latency communications," in *2018 IEEE 87th Vehicular Technology Conference (VTC Spring)*, 2018, pp. 1–5.

[16] T.-W. Chiang, H.-H. Liang, S.-S. Wang, and S.-T. Sheu, "On parallel retransmission for uplink ultra-reliable and low latency communications," in *2019 IEEE 90th Vehicular Technology Conference (VTC2019-Fall)*, 2019, pp. 1–5.

[17] O. Galinina, A. Turlikov, S. Andreev, and Y. Koucheryavy, "Multi-channel random access with replications," in *2017 IEEE International Symposium on Information Theory (ISIT)*, 2017, pp. 2538–2542.

[18] C. Boyd, R. Kotaba, O. Tirkkonen, and P. Popovski, "Non-orthogonal contention-based access for URLLC devices with frequency diversity," in *2019 IEEE 20th International Workshop on Signal Processing Advances in Wireless Communications (SPAWC)*, 2019, pp. 1–5.

[19] C. A. Astudillo, F. H. S. Pereira, and N. L. S. da Fonseca, "Probabilistic retransmissions for the random access procedure in cellular IoT networks," in *ICC 2019 - 2019 IEEE International Conference on Communications (ICC)*, 2019, pp. 1–7.

[20] E. Dosti, U. L. Wijewardhana, H. Alves, and M. Latva-aho, "Ultra reliable communication via optimum power allocation for type-i arq in finite blocklength," in *2017 IEEE International Conference on Communications (ICC)*, 2017, pp. 1–6.

[21] M. B. Shahab, R. Abbas, M. Shirvanimoghaddam, and S. J. Johnson, "Grant-free non-orthogonal multiple access for IoT: A survey," *IEEE Communications Surveys Tutorials*, pp. 1–1, 2020.

[22] X. Foukas, G. Patounas, A. Elmokashfi, and M. K. Marina, "Network slicing in 5G: Survey and challenges," *IEEE Communications Magazine*, vol. 55, no. 5, pp. 94–100, 2017.

[23] H. Zhang, N. Liu, X. Chu, K. Long, A. Aghvami, and V. C. M. Leung, "Network slicing based 5G and future mobile networks: Mobility, resource management, and challenges," *IEEE Communications Magazine*, vol. 55, no. 8, pp. 138–145, 2017.

[24] W. Guan, X. Wen, L. Wang, Z. Lu, and Y. Shen, "A service-oriented deployment policy of end-to-end network slicing based on complex network theory,"

IEEE Access, vol. 6, pp. 19 691–19 701, 2018.

[25] C. Campolo, A. Molinaro, A. Iera, and F. Menichella, "5G network slicing for vehicle-to-everything services," *IEEE Wireless Communications*, vol. 24, no. 6, pp. 38–45, 2017.

[26] P. Popovski, K. F. Trillingsgaard, O. Simeone, and G. Durisi, "5G wireless network slicing for embb, URLLC, and mmtc: A communication-theoretic view," *IEEE Access*, vol. 6, pp. 55 765–55 779, 2018.

[27] F. Kurtz, C. Bektas, N. Dorsch, and C. Wietfeld, "Network slicing for critical communications in shared 5G infrastructures - An empirical evaluation," in *2018 4th IEEE Conference on Network Softwarization and Workshops (NetSoft)*, 2018, pp. 393–399.

[28] V. Petrov, M. A. Lema, M. Gapeyenko, K. Antonakoglou, D. Moltchanov, F. Sardis, A. Samuylov, S. Andreev, Y. Koucheryavy, and M. Dohler, "Achieving end-to-end reliability of mission-critical traffic in softwarized 5G networks," *IEEE Journal on Selected Areas in Communications*, vol. 36, no. 3, pp. 485–501, 2018.

[29] F. Kurtz, N. Dorsch, and C. Wietfeld, "Empirical comparison of virtualized and bare-metal switching for SDN-based 5G communication in critical infrastructures," in *2016 IEEE NetSoft Conference and Workshops (NetSoft)*, 2016, pp. 453–458.

[30] N. T. Hai and D. Kim, "Efficient load balancing for multi-controller in SDN-based mission-critical networks," in *2016 IEEE 14th International Conference on Industrial Informatics (INDIN)*, 2016, pp. 420–425.

[31] M. H. Rehmani, A. Davy, B. Jennings, and C. Assi, "Software defined networks-based smart grid communication: A comprehensive survey," *IEEE Communications Surveys Tutorials*, vol. 21, no. 3, pp. 2637–2670, 2019.

[32] J. Choi and S. R. Pokhrel, "Federated learning with multichannel ALOHA," *IEEE Wireless Communications Letters*, vol. 9, no. 4, pp. 499–502, 2020.

[33] Z. Yang, M. Chen, W. Saad, C. S. Hong, and M. Shikh-Bahaei, "Energy efficient federated learning over wireless communication networks," 2019.

[34] H. H. Yang, Z. Liu, T. Q. S. Quek, and H. V. Poor, "Scheduling policies for federated learning in wireless networks," *IEEE Transactions on Communications*, vol. 68, no. 1, pp. 317–333, 2020.

[35] M. Chen, Z. Yang, W. Saad, C. Yin, H. V. Poor, and S. Cui, "A joint learning and communications framework for federated learning over wireless networks," 2019.

[36] S. Samarakoon, M. Bennis, W. Saad, and M. Debbah, "Distributed federated learning for ultra-reliable low-latency vehicular communications," *IEEE Transactions on Communications*, vol. 68, no. 2, pp. 1146–1159, 2020.

[37] A. Azari, M. Ozger, and C. Cavdar, "Risk-aware resource allocation for URLLC: Challenges and strategies with machine learning," *IEEE Communications Magazine*, vol. 57, no. 3, pp. 42–48, 2019.

[38] M. Angjelichinoski, K. F. Trillingsgaard, and P. Popovski, "A Statistical Learning Approach to Ultra-Reliable Low Latency Communication," *IEEE Transactions on Communications*, vol. 67, no. 7, pp. 5153–5166, 2019.

[39] F. Li, D. Yu, H. Yang, J. Yu, H. Karl, and X. Cheng, "Multi-armed-bandit-based spectrum scheduling algorithms in wireless networks: A survey," *IEEE Wireless Communications*, vol. 27, no. 1, pp. 24–30, 2020.

[40] S. Liu, P. Cheng, Z. Chen, B. Vucetic, and Y. Li, "A tutorial on bandit learning and its applications in 5G mobile edge computing (Invited paper)," *Frontiers in Signal Processing*, vol. 2, 2022. [Online]. Available: https://www.frontiersin.org/articles/10.3389/frsip.2022.864392

[41] S. Hu, X. Chen, W. Ni, E. Hossain, and X. Wang, "Distributed machine learning for wireless communication networks: Techniques, architectures, and applications," *IEEE Communications Surveys Tutorials*, vol. 23, no. 3, pp. 1458–1493, 2021.

[42] C. She, C. Yang, and T. Q. S. Quek, "Radio resource management for ultra-reliable and low-latency communications," *IEEE Communications Magazine*, vol. 55, no. 6, pp. 72–78, 2017.

[43] G. Baldini, S. Karanasios, D. Allen, and F. Vergari, "Survey of wireless communication technologies for public safety," *IEEE Communications Surveys Tutorials*, vol. 16, no. 2, pp. 619–641, 2014.

[44] A. Kumbhar, F. Koohifar, I. Guvenc, and B. Mueller, "A survey on legacy and emerging technologies for public safety communications," *IEEE Communications Surveys Tutorials*, vol. 19, no. 1, pp. 97–124, 2017.

[45] T. Doumi, M. F. Dolan, S. Tatesh, A. Casati, G. Tsirtsis, K. Anchan, and D. Flore, "Lte for public safety networks," *IEEE Communications Magazine*, vol. 51, no. 2, pp. 106–112, 2013.

[46] A. Al-Hourani, S. Chandrasekharan, S. Kandeepan, and A. Jamalipour, "7 - Aerial platforms for public safety networks and performance optimization," in *Wireless Public Safety Networks 3*, D. Câmara and N. Nikaein, Eds. Elsevier, 2017, pp. 133–153. [Online]. Available: https://www.sciencedirect.com/science/article/pii/B978178548053950007X

[47] K. Gomez, L. Goratti, T. Rasheed, and L. Reynaud, "Enabling disaster-resilient 4g mobile communication networks," *IEEE Communications Magazine*, vol. 52, no. 12, pp. 66–73, 2014.

[48] L. G. U. Garcia, E. P. L. Almeida, V. S. B. Barbosa, G. Caldwell, I. Rodriguez, H. Lima, T. B. Sørensen, and P. Mogensen, "Mission-critical mobile broadband communications in open-pit mines," *IEEE Communications Magazine*, vol. 54, no. 4, pp. 62–69, 2016.

[49] A. Orsino, A. Ometov, G. Fodor, D. Moltchanov, L. Militano, S. Andreev, O. N. C. Yilmaz, T. Tirronen, J. Torsner, G. Araniti, A. Iera, M. Dohler, and Y. Koucheryavy, "Effects of heterogeneous mobility on D2D- and drone-assisted mission-critical MTC in 5G," *IEEE Communications Magazine*, vol. 55, no. 2, pp. 79–87, 2017.

[50] M. Mozaffari, W. Saad, M. Bennis, Y. Nam, and M. Debbah, "A tutorial on uavs for wireless networks: Applications, challenges, and open problems," *IEEE Communications Surveys Tutorials*, vol. 21, no. 3, pp. 2334–2360, 2019.

[51] A. Fotouhi, H. Qiang, M. Ding, M. Hassan, L. G. Giordano, A. Garcia-Rodriguez, and J. Yuan, "Survey on UAV cellular communications: Practical aspects, standardization advancements, regulation, and security challenges," *IEEE Communications Surveys Tutorials*, vol. 21, no. 4, pp. 3417–3442, 2019.

[52] Y. Yan, Y. Qian, H. Sharif, and D. Tipper, "A survey on smart grid communication infrastructures: Motivations, requirements and challenges," *IEEE Communications Surveys Tutorials*, vol. 15, no. 1, pp. 5–20, 2013.

[53] D. Feng, C. She, K. Ying, L. Lai, Z. Hou, T. Q. S. Quek, Y. Li, and B. Vucetic, "Toward ultrareliable low-latency communications: Typical scenarios, possible solutions, and open issues," *IEEE Vehicular Technology Magazine*, vol. 14, no. 2, pp. 94–102, 2019.

[54] P. Popovski, C. Stefanovic, J. J. Nielsen, E. de Carvalho, M. Angjelichinoski, K. F. Trillingsgaard, and A. Bana, "Wireless access in ultra-reliable low-latency communication (URLLC)," *IEEE Transactions on Communications*, vol. 67, no. 8, pp. 5783–5801, 2019.

[55] G. J. Sutton, J. Zeng, R. P. Liu, W. Ni, D. N. Nguyen, B. A. Jayawickrama, X. Huang, M. Abolhasan, Z. Zhang, E. Dutkiewicz, and T. Lv, "Enabling technologies for ultra-reliable and low latency communications: From PHY and MAC layer perspectives," *IEEE Communications Surveys Tutorials*, vol. 21, no. 3, pp. 2488–2524, 2019.

[56] C. Li, N. Yang, and S. Yan, "Optimal transmission of short-packet communications in multiple-input single-output systems," *IEEE Transactions on Vehicular Technology*, vol. 68, no. 7, pp. 7199–7203, 2019.

[57] D. Huang, A. Al-Hourani, K. Sithamparanathan, W. S. T. Rowe, L. Bulot, and A. Thompson, "Deep learning methods for device authentication using RF fingerprinting," in *2021 15th International Conference on Signal Processing and Communication Systems (ICSPCS)*, 2021, pp. 1–7.

[58] C. Li, C. She, N. Yang, and T. Q. S. Quek, "Secure transmission rate of short packets with queueing delay requirement," *IEEE Transactions on Wireless Communications*, vol. 21, no. 1, pp. 203–218, 2022.

[59] S. Kaul, M. Gruteser, V. Rai, and J. Kenney, "Minimizing age of information in vehicular networks," in *2011 8th Annual IEEE Communications Society Conference on Sensor, Mesh and Ad Hoc Communications and Networks*, 2011, pp. 350–358.

[60] W. Yang, X. Lu, S. Yan, F. Shu, and Z. Li, "Age of information for short-packet covert communication," *IEEE Wireless Communications Letters*, vol. 10, no. 9, pp. 1890–1894, 2021.

[61] S. Vitturi, C. Zunino, and T. Sauter, "Industrial communication systems and their future challenges: Next-generation ethernet, IIoT, and 5G," *Proceedings of the IEEE*, vol. 107, no. 6, pp. 944–961, 2019.

[62] F. Liang, W. Yu, X. Liu, D. Griffith, and N. Golmie, "Toward computing resource reservation scheduling in Industrial Internet of Things," *IEEE Internet of Things Journal*, vol. 8, no. 10, pp. 8210–8222, 2021.

[63] H. He, P. Ren, Q. Du, L. Sun, and Y. Wang, "Traffic-aware overload control scheme in 5G ultra-dense M2M networks," *Transactions on Emerging Telecommunications Technologies*, vol. 28, no. 9, p. e3146, 2017, e3146 ett.3146. [Online]. Available: https://onlinelibrary.wiley.com/doi/abs/10.1002/ett.3146

[64] M. S. Ali, E. Hossain, and D. I. Kim, "LTE/LTE-A random access for massive machine-type communications in smart cities," *IEEE Communications Magazine*, vol. 55, no. 1, pp. 76–83, 2017.

[65] Y. Liu, Y. Deng, M. Elkashlan, A. Nallanathan, and G. K. Karagiannidis, "Analyzing grant-free access for URLLC service," *IEEE Journal on Selected Areas in Communications*, vol. 39, no. 3, pp. 741–755, 2021.

[66] J. Gao, W. Zhuang, M. Li, X. Shen, and X. Li, "MAC for machine-type communications in industrial IoT—part i: Protocol design and analysis," *IEEE Internet of Things Journal*, vol. 8, no. 12, pp. 9945–9957, 2021.

[67] J. Gao, M. Li, W. Zhuang, X. Shen, and X. Li, "MAC for machine-type communications in industrial IoT—part ii: Scheduling and numerical results," *IEEE Internet of Things Journal*, vol. 8, no. 12, pp. 9958–9969, 2021.

[68] N. Xia, H.-H. Chen, and C.-S. Yang, "Radio resource management in machine-to-machine communications—a survey," *IEEE Communications Surveys Tutorials*, vol. 20, no. 1, pp. 791–828, 2018.

[69] C. She, R. Dong, W. Hardjawana, Y. Li, and B. Vucetic, "Optimizing resource allocation for 5G services with diverse quality-of-service requirements," in *2019 IEEE Global Communications Conference (GLOBECOM)*, 2019, pp. 1–6.

[70] J. Brown and J. Y. Khan, "Predictive allocation of resources in the LTE uplink based on maximum likelihood estimation of event propagation characteristics for M2M applications," in *2014 IEEE Global Communications Conference*, 2014, pp. 4965–4970.

[71] C. Oh, D. Hwang, and T. Lee, "Joint access control and resource allocation for concurrent and massive access of M2M devices," *IEEE Transactions on Wireless Communications*, vol. 14, no. 8, pp. 4182–4192, 2015.

[72] S. Duan, V. Shah-Mansouri, Z. Wang, and V. W. S. Wong, "D-ACB: Adaptive congestion control algorithm for bursty M2M traffic in LTE networks," *IEEE Transactions on Vehicular Technology*, vol. 65, no. 12, pp. 9847–9861, 2016.

[73] H. He, P. Ren, Q. Du, L. Sun, and Y. Wang, "Traffic-aware overload control scheme in 5G ultra-dense M2M networks," *Trans. Emerging Telecommun. Technol.*, vol. 28, no. 9, Art. no. e3146, 2017.

[74] N. Jiang, Y. Deng, O. Simeone, and A. Nallanathan, "Online supervised learning for traffic load prediction in framed-ALOHA networks," *IEEE Communications Letters*, vol. 23, no. 10, pp. 1778–1782, 2019.

[75] G. Miao, A. Azari, and T. Hwang, "E^2 -MAC: Energy efficient medium access for massive M2M communications," *IEEE Transactions on Communications*, vol. 64, no. 11, pp. 4720–4735, 2016.

[76] A. Azari, C. Stefanovic, P. Popovski, and C. Cavdar, "Energy-efficient and reliable IoT access without radio resource reservation," *IEEE Transactions on Green Communications and Networking*, vol. 5, no. 2, pp. 908–920, 2021.

[77] B. Al Homssi, A. Al-Hourani, S. Chandrasekharan, K. M. Gomez, and S. Kandeepan, "On the bound of energy consumption in cellular iot networks," *IEEE Transactions on Green Communications and Networking*, vol. 4, no. 2, pp. 355–364, 2020.

[78] J. Choi, "Re-transmission diversity multiple access based on SIC and HARQ-IR," *IEEE Transactions on Communications*, vol. 64, no. 11, pp. 4695–4705, 2016.

[79] S. A. Tegos, P. D. Diamantoulakis, A. S. Lioumpas, P. G. Sarigiannidis, and G. K. Karagiannidis, "Slotted ALOHA with NOMA for the next generation IoT," *IEEE Transactions on Communications*, vol. 68, no. 10, pp. 6289–6301, 2020.

[80] M. Gharbieh, H. ElSawy, M. Emara, H.-C. Yang, and M.-S. Alouini, "Grant-free opportunistic uplink transmission in wireless-powered IoT: A spatio-temporal model," *IEEE Transactions on Communications*, vol. 69, no. 2, pp. 991–1006, 2021.

[81] J. Choi, "On improving throughput of multichannel aloha using preamble-based exploration," *Journal of Communications and Networks*, vol. 22, no. 5, pp. 380–389, 2020.

[82] M.-J. Youssef, V. V. Veeravalli, J. Farah, and C. A. Nour, "Stochastic multi-player multi-armed bandits with multiple plays for uncoordinated spectrum access," in *2020 IEEE 31st Annual International Symposium on Personal, Indoor and Mobile Radio Communications*, 2020, pp. 1–7.

[83] R. Bonnefoi, L. Besson, C. Moy, E. Kaufmann, and J. Palicot, "Multi-armed bandit learning in IoT networks: Learning helps even in non-stationary settings," in *Cognitive Radio Oriented Wireless Networks*. Cham: Springer International Publishing, 2018, pp. 173–185.

[84] J. Choi, "Two-sided learning for NOMA-based random access in IoT networks," *IEEE Access*, vol. 9, pp. 66 208–66 217, 2021.

[85] O. Avner and S. Mannor, "Multi-user lax communications: A multi-armed bandit approach," in *IEEE INFOCOM 2016 - The 35th Annual IEEE International Conference on Computer Communications*, 2016, pp. 1–9.

[86] T. Gafni and K. Cohen, "A distributed stable strategy learning algorithm for multi-user dynamic spectrum access," in *2019 57th Annual Allerton Conference on Communication, Control, and Computing (Allerton)*, 2019, pp. 347–351.

[87] ——, "Distributed learning over markovian fading channels for stable spectrum access," *IEEE Access*, vol. 10, pp. 46 652–46 669, 2022.

[88] A. Magesh and V. V. Veeravalli, "Multi-user MABs with user dependent rewards for uncoordinated spectrum access," in *2019 53rd Asilomar Conference on Signals, Systems, and Computers*, 2019, pp. 969–972.

[89] C. Shi and C. Shen, "Multi-player multi-armed bandits with collision-dependent reward distributions," *IEEE Transactions on Signal Processing*, vol. 69, pp. 4385–4402, 2021.

[90] M. Bande, A. Magesh, and V. V. Veeravalli, "Dynamic spectrum access using stochastic multi-user bandits," *IEEE Wireless Communications Letters*, vol. 10, no. 5, pp. 953–956, 2021.

[91] A. Magesh and V. V. Veeravalli, "Decentralized heterogeneous multi-player multi-armed bandits with non-zero rewards on collisions," *IEEE Transactions on Information Theory*, vol. 68, no. 4, pp. 2622–2634, 2022.

[92] M.-J. Youssef, V. V. Veeravalli, J. Farah, C. A. Nour, and C. Douillard, "Resource allocation in NOMA-based self-organizing networks using stochastic multi-armed bandits," *IEEE Transactions on Communications*, vol. 69, no. 9, pp. 6003–6017, 2021.

[93] M. Mukherjee, L. Shu, and D. Wang, "Survey of fog computing: Fundamental, network applications, and research challenges," *IEEE Communications*

Surveys Tutorials, vol. 20, no. 3, pp. 1826–1857, 2018.

[94] C. Mouradian, D. Naboulsi, S. Yangui, R. H. Glitho, M. J. Morrow, and P. A. Polakos, "A comprehensive survey on fog computing: State-of-the-art and research challenges," *IEEE Communications Surveys Tutorials*, vol. 20, no. 1, pp. 416–464, 2018.

[95] L. M. Vaquero and L. Rodero-Merino, "Finding your way in the fog: Towards a comprehensive definition of fog computing," *SIGCOMM Comput. Commun. Rev.*, vol. 44, no. 5, p. 27–32, Oct. 2014. [Online]. Available: https://doi.org/10.1145/2677046.2677052

[96] X. Hou, Y. Li, M. Chen, D. Wu, D. Jin, and S. Chen, "Vehicular fog computing: A viewpoint of vehicles as the infrastructures," *IEEE Transactions on Vehicular Technology*, vol. 65, no. 6, pp. 3860–3873, 2016.

[97] M. Peng, S. Yan, K. Zhang, and C. Wang, "Fog-computing-based radio access networks: Issues and challenges," *IEEE Network*, vol. 30, no. 4, pp. 46–53, 2016.

[98] B. McMahan, E. Moore, D. Ramage, S. Hampson, and B. A. y Arcas, "Communication-efficient learning of deep networks from decentralized data," in *Proceedings of the 20th International Conference on Artificial Intelligence and Statistics*, ser. Proceedings of Machine Learning Research, A. Singh and J. Zhu, Eds., vol. 54. Fort Lauderdale, FL, USA: PMLR, 20–22 Apr 2017, pp. 1273–1282. [Online]. Available: http://proceedings.mlr.press/v54/mcmahan17a.html

[99] H. B. McMahan, E. Moore, D. Ramage, and B. A. y Arcas, "Federated learning of deep networks using model averaging," *CoRR*, vol. abs/1602.05629, 2016. [Online]. Available: http://arxiv.org/abs/1602.05629

[100] T. Li, A. K. Sahu, A. Talwalkar, and V. Smith, "Federated learning: Challenges, methods, and future directions," *IEEE Signal Processing Magazine*, vol. 37, no. 3, pp. 50–60, 2020.

[101] I. Zhou, I. Makhdoom, N. Shariati, M. A. Raza, R. Keshavarz, J. Lipman, M. Abolhasan, and A. Jamalipour, "Internet of things 2.0: Concepts, appli-

cations, and future directions," *IEEE Access*, vol. 9, pp. 70 961–71 012, 2021.

[102] J. Ding, D. Qu, H. Jiang, and T. Jiang, "Success probability of grant-free random access with massive MIMO," *IEEE Internet of Things Journal*, vol. 6, no. 1, pp. 506–516, 2019.

[103] N. Jiang, Y. Deng, A. Nallanathan, and J. A. Chambers, "Reinforcement learning for real-time optimization in NB-IoT networks," *IEEE Journal on Selected Areas in Communications*, vol. 37, no. 6, pp. 1424–1440, 2019.

[104] M. A. Raza, M. Abolhasan, J. Lipman, N. Shariati, and W. Ni, "Statistical learning-based dynamic retransmission mechanism for mission critical communication: An edge-computing approach," in *2020 IEEE 45th Conference on Local Computer Networks (LCN)*, 2020, pp. 393–396.

[105] S. Chattopadhyay, C. Murthy, and S. K. Pal, "Fitting truncated geometric distributions in large scale real world networks," *Theoretical Computer Science*, vol. 551, pp. 22–38, 2014. [Online]. Available: https://www.sciencedirect.com/science/article/pii/S0304397514003521

[106] Q. Wang and J. Jiang, "Comparative examination on architecture and protocol of industrial wireless sensor network standards," *IEEE Communications Surveys Tutorials*, vol. 18, no. 3, pp. 2197–2219, 2016.

[107] A. Aijaz, "Private 5G: The future of industrial wireless," *IEEE Industrial Electronics Magazine*, vol. 14, no. 4, pp. 136–145, 2020.

[108] M. Saki, M. Abolhasan, and J. Lipman, "A novel approach for big data classification and transportation in rail networks," *IEEE Transactions on Intelligent Transportation Systems*, vol. 21, no. 3, pp. 1239–1249, 2020.

[109] F. Guo, F. R. Yu, H. Zhang, X. Li, H. Ji, and V. C. M. Leung, "Enabling massive IoT toward 6G: A comprehensive survey," *IEEE Internet of Things Journal*, vol. 8, no. 15, pp. 11 891–11 915, 2021.

[110] N. Jiang, Y. Deng, A. Nallanathan, X. Kang, and T. Q. S. Quek, "Analyzing random access collisions in massive IoT networks," *IEEE Transactions on Wireless Communications*, vol. 17, no. 10, pp. 6853–6870, 2018.

[111] M. A. Raza, M. Abolhasan, J. Lipman, N. Shariati, W. Ni, and A. Jamalipour, "Statistical learning-based grant-free access for delay-sensitive Internet of Things applications," *IEEE Transactions on Vehicular Technology*, vol. 71, no. 5, pp. 5492–5506, 2022.

[112] M. Makhanbet, T. Lv, W. Ni, and M. Orynbet, "Energy-delay-aware power control for reliable transmission of dynamic cell-free massive MIMO," *IEEE Transactions on Communications*, vol. 70, no. 1, pp. 276–290, 2022.

[113] A. Ghaderi and Z. Movahedi, "Joint latency and energy-aware data management layer for industrial IoT," in *2022 8th International Conference on Web Research (ICWR)*, 2022, pp. 70–75.

[114] K. Wang, Y. Wang, Y. Sun, S. Guo, and J. Wu, "Green Industrial Internet of Things architecture: An energy-efficient perspective," *IEEE Communications Magazine*, vol. 54, no. 12, pp. 48–54, 2016.

[115] J. Choi, "NOMA-based random access with multichannel ALOHA," *IEEE Journal on Selected Areas in Communications*, vol. 35, no. 12, pp. 2736–2743, 2017.

[116] W. Zhang, M. Derakhshani, and S. Lambotharan, "Non-parametric statistical learning for URLLC transmission rate control," in *ICC 2021 - IEEE International Conference on Communications*, 2021, pp. 1–6.

[117] M. S. Allahham, A. A. Abdellatif, N. Mhaisen, A. Mohamed, A. Erbad, and M. Guizani, "Multi-agent reinforcement learning for network selection and resource allocation in heterogeneous multi-RAT networks," *IEEE Transactions on Cognitive Communications and Networking*, vol. 8, no. 2, pp. 1287–1300, 2022.